Scholars' Mine

Doctoral Dissertations

Student Theses and Dissertations

Summer 2017

# The effect of testing conditions on lost circulation materials' performance in simulated fractures

Montri Jeennakorn

Follow this and additional works at: https://scholarsmine.mst.edu/doctoral_dissertations

Part of the Petroleum Engineering Commons

Department: Geosciences and Geological and Petroleum Engineering

Recommended Citation

Jeennakorn, Montri, "The effect of testing conditions on lost circulation materials' performance in simulated fractures" (2017). *Doctoral Dissertations*. 2599.
https://scholarsmine.mst.edu/doctoral_dissertations/2599

This thesis is brought to you by Scholars' Mine, a service of the Missouri S&T Library and Learning Resources. This work is protected by U. S. Copyright Law. Unauthorized use including reproduction for redistribution requires the permission of the copyright holder. For more information, please contact scholarsmine@mst.edu.

# THE EFFECT OF TESTING CONDITIONS ON LOST CIRCULATION MATERIALS' PERFORMANCE IN SIMULATED FRACTURES

by

MONTRI JEENNAKORN

A DISSERTATION

Presented to the Faculty of the Graduate School of the

MISSOURI UNIVERSITY OF SCIENCE AND TECHNOLOGY

In Partial Fulfillment of the Requirements for the Degree

DOCTOR OF PHILOSOPHY

in

PETROLEUM ENGINEERING

2017

Approved

Runar Nygaard, Advisor
Ralph Flori
Shari Dunn-Norman
Peyman Heidari
Leslie Gertsch

© 2017

Montri Jeennakorn

All Rights Reserved

## PUBLICATION DISSERTATION OPTION

This dissertation consists of the following four articles which have been published, submitted, or will be submitted for publication as follows:

Paper I: Pages 23 to 50 have been submitted to Journal of Natural Gas Science and Engineering.

Paper II: Pages 51 to 74 have been submitted to Journal of Petroleum Exploration and Production Technology.

Paper III: Pages 75 to 92 have been published to American Association of Drilling Engineer.

Paper IV: Pages 93 to 107 are intended for submission to Society of Petroleum Engineers.

## ABSTRACT

Lost circulation (LOC) problems increase costs of drilling significantly. It is not only the cost of the drilling fluid that is lost into the formation but also the costs of subsequent problems that can be higher than the cost of the drilling fluids. LOC also possibly leads to a serious risk of blowout incident.

Lost circulation materials (LCM) are regularly added to the drilling fluids with an expectation of plugging the flow path. Due to the difficulties of testing and monitoring LCM sealing processes in the field, LCM evaluation in the laboratory is often used to prove and assure successful treatment. Investigating LCM behavior and the causation of obtaining different results would expand the reliability of the laboratory evaluation methods.

In this study, a steel cylindrical cell was used to simulate downhole high-pressure conditions. Steel discs with precisely sized slots (simulating wellbore fractures) were used to study the effect of testing conditions on the particulate LCM sealing performance. Results show that the fracture wall angles, the disc thickness, the base fluids, the drilling fluid density, the particle size of weighting materials related to the LCM grain sizes, and the dynamic aging conditions all affect the testing results significantly. LCM that performed well in the slow injection rate tests also exhibited sealing behavior effectively in the instantaneous flow conditions. The experiments provided an understanding of the fracture sealing mechanism to be applied in improving the laboratory evaluation methods and field treatment design. This knowledge is useful for both the preventive and corrective LOC mitigating approaches.

## ACKNOWLEDGEMENT

I would like to express my great appreciation to my advisor, Dr. Runar Nygaard, for giving me the educational opportunity joining his research group as a PhD student. Tremendously, it is the most valuable chance allowing my academic development to occur. Without his kindheartedness, my dream of higher education would not come true. Being his student has provided so much profit to me and my beloved family. Also, I would like to appreciate the advisory committee members, Dr. Ralph Flori, Dr. Shari Dunn-Norman, Dr. Peyman Heidari and Dr. Leslie Gertsch for their nice help and comments from the study proposal to the accomplishment of the dissertation.

I would like to express thanks to my research group members, Dr. Mortadha Alsaba, Dr. Mohammed Al Dushaishi, Dr. Reza Rahimi, Dr. Yurong Li, Mr. Farqad Hadi and Mr. Ahmed Alsubaih for their help during my study, the experiments, the results analysis, and the technical writing. Some of them still helped me even though they were extremely busying with their early stage of the careers.

I appreciate the Defense Energy Department (Thailand) for supporting the valuable scholarship that made my chance of education possible. I also would like to acknowledge Aker BP ASA (former Det Norske Oljeselskap ASA) for the financial support through the research group. The experimental study could not be conducted without the apparatus, materials and the administrative fund.

Finally, I would like to thank my parents, my wife, and my two dear daughters for their endless love, help, and encouragement.

# TABLE OF CONTENTS

Page

PUBLICATION DISSERTATION OPTION ..... iii

ABSTRACT ..... iv

ACKNOWLEDGEMENT ..... v

LIST OF ILLUSTRATIONS ..... ix

LIST OF TABLES ..... xi

NOMENCLATURE ..... xii

SECTION

1. INTRODUCTION ..... 1

1.1 THE LOST CIRCULATION PROBLEM ..... 1

1.2 EVALUATION AND MITIGATION ..... 2

2. LITERATURE REVIEW ..... 4

2.1 LOST CIRCULATION OCCURRENCE ..... 4

2.2 FLUID FLOW THROUGH FRACTURES ..... 10

2.3 TYPE AND USAGE OF SEALING MATERIALS ..... 15

2.4 TESTING APPARATUS PREVIOUSLY USED ..... 18

2.5 LITERATURE REVIEW DISCUSSION ..... 20

2.6 OBJECTIVE ..... 21

PAPER

I. TESTING CONDITIONS MAKE A DIFFERENCE WHEN TESTING LCM ..... 23

ABSTRACT ..... 23

1. INTRODUCTION ..... 23

2. EXPERIMENTAL SETUP ..... 25

2.1 TESTING APPARATUS ..... 25

2.2 LOST CIRCULATION MATERIALS ..... 26

2.3 SLOT DISCS ..... 27

3. TESTING METHODOLOGY ..... 28

4. TESTING RESULTS ..... 29

5. DISCUSSIONS ..... 34

5.1 IMPLICATIONS FROM THE EXPERIMENT ..... 34
5.2 SEALING MECHANISM APPLIED TO LCM TREATMENT ..... 46
6. CONCLUSIONS ..... 48
ACKNOWLEDGEMENT ..... 48
REFERENCE ..... 49
II. EFFECT OF TESTING CONDITIONS ON THE PERFORMANCE OF LOST CIRCULATION MATERIAL: UNDERSTANDABLE SEALING MECHANISM……...……51
ABSTRACT ..... 51
1. BACKGROUND ..... 52
2. EXPERIMENTAL METHODOLOGY ..... 54
2.1 TESTING APPARATUS ..... 54
2.2 DRILLING FLUID AND ADDITIVES ..... 55
2.3 LCM FORMULATIONS ..... 58
3. RESULTS AND DISCUSSIONS ..... 59
3.1 THE EFFECT OF THE BASE FLUIDS ..... 62
3.2 THE EFFECT OF DENSITY ..... 64
3.3 THE EFFECT OF WEIGHTING MATERIALS: BARITE VS. HEMATITE ..... 66
3.4 THE EFFECT OF DYNAMIC AGING CONDITIONS ..... 68
4. CONCLUSIONS ..... 70
ACKNOWLEDGEMENT ..... 71
REFERENCE ..... 71
III. SEALING PRESSURE PREDICTION MODEL FOR LOST CIRCULATION TREATMENTS BASED ON EXPERIMENTAL INVESTIGATIONS……...……75
ABSTRACT ..... 75
1. INTRODUCTION ..... 76
2. PREVIOUS EXPERIMENTAL INVESTIGATION ..... 77
3. STATISTICAL METHODS ..... 78
4. STATISTICAL ANALYSIS RESULTS ..... 82
5. SEALING PRESSURE PREDICTION MODEL ..... 88
6. CONCLUSIONS ..... 89

ACKNOWLEDGEMENT ..... 90
NOMENCLATURE ..... 90
REFERENCE ..... 91
IV. EFFECT OF EPERIMENTAL SETUP
ON LOST CURCULATION MATERIALS EVALUATION RESULTS……..……..93
ABSTRACT ..... 93
1. INTRODUCTION ..... 93
2. EXPERIMENTAL SETUP ..... 94
3. TESTING METHODOLOGY ..... 99
4. TESTING RESULTS ..... 101
5. DISCUSSION ..... 104
6. CONCLUSIONS ..... 105
NOMENCLATURE ..... 105
REFERENCE ..... 105
SECTION
3. DISCUSSION AND CONCLUSIONS……..…….…….108
3.1 DISCUSSION ..... 108
3.2 CONCLUSIONS ..... 115
BIBLIOGRAPHY ..... 119
VITA ..... 123

# LIST OF ILLUSTRATIONS

Figure Page

Section

2.1. The plot of filtrate vs. time yields a straight line.....6

2.2. The numerical study presents fracture plane induced by the wellbore pressure propagating in the direction of the maximum principal stress.....8

Paper I

1. Schematics of the HPA apparatus. .....25

2. A plot of injecting pressure over time obtained from an HPA test.....29

3. The plot between maximum sealing pressure vs. time obtained from 0°, 7°, 9° and 13° wall angle tests.....29

4. Sealing pressure in tapered discs with 6.35 and 25.4 mm thickness.....33

5. The plot displays fluid losses obtained from the instantaneous flow tests.....33

6. Seals from the straight slot and tapered slot.....35

7. Seals formed on a straight slot (G & SCC 105 ppb formulation).....37

8. Bridging mechanism of LCM in straight slots at the slot entrance.....38

9. Possible changing in load magnitudes and orientations acts on the same front line of the bridging particles in different wall angle.....40

10. Comparison of seals on 6.35 mm and 25.4 mm thick discs.....42

11. Comparison of the plot from the instantaneous flow tests and a slow injection test....43

12. A cross-section view of a seal.....45

13. The plot shows the instantaneous flow test (small broken circle) and the response pressure from a seal integrity test (big broken circle) after the pressure stabilized.....47

Paper II

1. High-pressure LCM testing apparatus (Alsaba et al. 2014b).....54

2. Pressure vs. time plot obtained from a test using 30 ppb G & SCC mixed with 14.5 ppg OBF using 1000 microns fracture width.....55

3. Base fluid effects on sealing pressure for each LCM formulation.....62

4. Effect of increasing the drilling fluid density on the sealing pressure.....64

5. The effect of weighting materials between barite and hematite.....67

6. Effect of adding three ranges of sieved barite particles on the sealing pressures of 12.5 ppg OBF treated with G & SCC # 1 at 30 ppb.....68

7. Sealing pressure of the drilling fluids treated with different LCM after subjected to different aging conditions.....69

Paper III

1. Schematic of the High-Pressure Testing Apparatus.....78

2. Leverage Plot Showing the Effect of Fracture Width on Sealing Pressure.....82

3. Leverage Plot Showing the Effect of Density on Sealing Pressure.....83

4. Leverage Plot Showing the Effect of D90 on Sealing Pressure.....83

5. Leverage Plot Showing the Effect of LCM Blend on Sealing Pressure.....84

6. Leverage Plot Showing the Effect of D75 on Sealing Pressure.....84

7. Leverage Plot Showing the Effect of Base Fluid on Sealing Pressure.....85

8. Leverage Plot Showing the Effect of D25 on Sealing Pressure.....85

9. Leverage Plot Showing the Effect of D50 on Sealing Pressure.....86

10. Leverage Plot Showing the Effect of D10 on Sealing Pressure.....86

11. Leverage Plot Showing the Actual Sealing Pressure vs. the Predicted Sealing Pressure using the fit model.....87

12. Residual Plot of Sealing Pressure vs. the Predicted Sealing Pressure.....87

Paper IV

1. Schematic of the first testing apparatus.....95

2. Schematics of the second apparatus.....96

3. The testing cell of the second apparatus.....97

4. A plot of injecting pressure over time from a test showing the peak pressure (circled), recorded as the maximum sealing pressure.....99

5. The plot of monitored pressure over time obtained from three tests of the second testing condition.....101

6. Graph comparing the averaged sealing pressure from condition#1, condition#3, and condition#4.....103

7. Graph comparing the averaged initial fluid loss from condition#1, condition#3, and condition#4.....103

8. Graph comparing the averaged fluid loss per cycle (seal formed and breaking) from condition#1, condition#3, and condition#4.....103

# LIST OF TABLES

Table Page

Section

2.1. Testing apparatus used in previous studies.....19

Paper I

1. LCM formulation used for all the tests in this paper.....27

2. Name and dimension of the discs used in the effect of wall angle experiment.....28

3. Testing results from the sealing under wall angle and thickness variation tests.....30

4. Testing results from the instantaneous flow tests.....31

Paper II

1. Tapered slots specifications.....54

2. LCM Treatment formulations.....58

3. LCM particle size distribution obtained from blending the formulations in Table 2.....59

4. Summary of the results from previous studies (Alsaba et al. 2014a, 2014b) and this study.....60

5. Aging condition testing results.....61

Paper III

1. Summary of the Particle Size Distribution Analysis for the Different LCM Blends.....79

2. Effect of Different Parameters on the Sealing Pressure and Model Fit.....88

3. Empirical Coefficients for the Fluid Type and the Different LCM Blends.....89

Paper IV

1. LCM formulation used in the tests.....98

2. PSD of used LCM using sieve analysis method.....98

3. Fracture disc dimensions.....99

4. Testing results from the first, third, and fourth testing conditions.....102

5. The results from the second testing conditions.....102

# NOMENCLATURE

| Symbol | Description |
|---|---|
| API | American Petroleum Institute |
| NPT | None-productive time |
| LCM | Lost circulation material |
| LOC | Lost circulation |
| PSD | Particle size distribution |
| PPA | Particle plugging apparatus |
| HPA | High pressure plugging apparatus |
| HPHT | High pressure high temperature |
| IPT | Ideal packing theory |
| WBF | Water-based fluid (the same as water-based mud) |
| WBM | Water-based mud |
| OBF | Oil-based fluid (the same as oil-based mud) |
| OBM | Oil-based mud |
| G | Graphite |
| SCC | Sized calcium carbonate |
| NS | Nut shells |
| CF | Cellulosic fiber |
| lb/bbl | Adding in lb (mass) of solid per one barrel of liquid |
| ppb | Concentration of mixing in lb/bbl |
| ppg | Density in lbm/gal |
| Conc. | Concentration (in lb/bbl) |
| gal/min | Flow rate in gallon per minute |
| bbl/min | Flow rate in barrel per minute |

# 1. INTRODUCTION

## 1.1 THE LOST CIRCULATION PROBLEM

Lost Circulation (LOC) is defined as the loss of drilling fluids into rock formation voids during well drilling or completion (Howard and Scott 1951). It has been experienced since the early days of rotary drilling (Gockel et al. 1987) and is one of the most difficult problems in drilling. The cost of the problem was approximated to be US$800 million per year. Of the total cost, the LOC curing product was as much as US$200 million per year (Ivan et al. 2003). An SPE workshop on lost circulation in Dubai, UAE (2014) provided the amount of drilling fluid lost into the formation estimated to be 1.8 million barrels in one year (Alsaba et al. 2014a). If one well consumes 3,000 bbl of drilling fluid in the overall drilling operation, the lost volume could be used for drilling as many as 600 wells only in one year. These numbers confirm that LOC is an important problem in the petroleum industry.

Drilling fluid provides essential functions supporting the drilling operation (Bourgoyne et al. 1986); for example, it removes the rock cuttings from underneath the drill bit and transports the cuttings out of the hole, supports the newly drilled borehole keeping it stable until the casing is set and cemented in place, and cools and lubricates the drill bit and the drill string to prolong the equipment life. Having an insufficient amount of the drilling fluid in the active system allows more serious subsequent problems to occur. For instance, formation damage decreasing the well's productivity, the loss of downhole tools and bottomhole assembly in pipe sticking incidents (Ghalambor et al. 2014; Howard and Scott 1951), loss of the well section or complete loss of the entire well (Deeg 2004; Alsaba et al. 2014a; Vajargah and Van Oort 2016). Every introduced problem always involves delays of the drilling process known as the non-productive time (NPT). Cost from NPT is often 10% to 20% of the drilling budget (Baggini Almagro et al. 2014). Mixing, transporting and reconditioning the drilling fluid and additives are also time-consuming and tend to slow down the overall processes.

In addition to the loss of the expenses, LOC creates a serious risk to the lives of the rig crew due to an increase chance of blowouts. One vital function of drilling fluids is to provide a hydrostatic pressure sufficient to hold back the formation pore pressure,

preventing the flow of undesired formation fluids into the well (Bourgoyne et al. 1986). Trying to control the formation pressure might encourage LOC and worsen the situation.

Under the current oil economy, most high-investment projects might be deferred, but oil demand in the future will essentially force the industry to drill into LOC problematic zones. The LOC problems will challenge and threaten the modern drilling industry no matter how much technology is improved. There is no question that LOC problem mitigation is important to be studied.

## 1.2 EVALUATION AND MITIGATION

Lost circulation materials (LCM) are substances added to drilling fluids to increase the maximum particle size presented in the mixture, in order to plug or seal the formation openings, to slow down and finally stopping the flow (White 1956). Routinely, LCM are added to drilling fluids. It may be dispersed in the active system or mixed in a high concentration placed against the losing zones referred as LCM pills (Kefi et al. 2010; Baggini Almagro et al. 2014). Recently, LCM was classified into seven main categories (Alsaba et al., 2014a). This dissertation focuses on only the widely used conventional granular LCM.

The loss of fluid through subsurface fractures is one of the loss mechanisms, either lost through natural fractures or induced fractures (Canson 1985; Ghalambor et al. 2014; Kumar and Savari 2011; Savari and Whitfill 2016). It usually consumes a relatively high rate of flow through the long propagating and complicated network of fractures.

The rock matrix can be permeable or impermeable. The difference is that the fluid can flow through both the fracture channels and the rock pores in the case of fractured permeable formations, but can only flow through the fracture system in impermeable formations. Sealing fractures in impermeable rock was found to be harder to cure compared to permeable rock (Onyla 1994; Sanders et al. 2008). In permeable formations, some drilling fluid will be filtered through the porous fracture wall, leaving behind the solid particles accumulated in the channel which tend to restrict the flow as screenout (Alberty and McLean 2001; van Oort, et al. 2011). These particles help develop a bridging structure inside the flow channel and plug the flow, making it easier to form a seal in fractured porous rock. The sealing mechanism will be reviewed in Section 2.

Comprehensive studies have verified LCM sealing ability and the treatment effectiveness in simulated fracture slots. Different experimental setups have been used to evaluate LCM formulation and performance (White 1956; Hettema et al. 2007; Whitfill and Miller 2008; Wang and Soliman 2009; Sanders et al. 2010; Alsaba et al. 2014a). Most of the experiments investigated the effect of LCM physical properties on sealing performance (Scott and Lummus 1955; Loeppke et al. 1990; Hettema et al., 2007; Alsaba et al. 2014b, 2014c). After the laboratory testing, results were applied for LCM selection and some field experiments were conducted (Fuh et al. 2007; Savari and Whitfill 2016). Logically, the apparatuses used in those experiments were designed to meet some specific downhole conditions; however, few studies have been performed to investigate the change of the results if the testing environment was changed.

The majority of the experiments were performed using single or mixed granular materials, such as ground marble or sized calcium carbonate, graphite and walnut shell. Some studies used fibrous materials to form bridging structures (Canson 1985; Kefi et al., 2010; Baggini Almagro et al. 2014; Xu et al. 2014). Special and unconventional LCM included long-chain fiber and crosslink polymer (Growcock et al. 2009; Kumar et al. 2011), thermoset rubber and expanded aggregate (Loeppke et al. 1990), or foam wedge combined with particulate LCM (Alsaba et al. 2014c). The application of nanoparticle technology improving fracture gradient (Contreras et al. 2014; Cedola et al. 2016) was also conducted in the experiments. This study focused on the blending of widely used granular materials: nutshell, cellulosic fiber, graphite, and sized (sorted) calcium carbonate. Their sealing performance was evaluated using different testing apparatus and environments, and the difference of the evaluation results was observed and compared.

# 2. LITERATURE REVIEW

## 2.1 LOST CIRCULATION OCCURRENCE

Like every flow that needs pressure differential, LOC can occur when the wellbore pressure is higher than the penetrated formation's pressure (Gockel et al. 1987). The formations that receive the fluids from the wellbore can be divided into four categories; porous, cavernous, naturally fractured and induced fractured formations (Howard and Scott 1951). The categorized formation openings have different flow path geometry which required different curing mechanism of LOC (Ghalambor et al. 2014). These types of loss mechanisms need to be understood to evaluate how drilling fluids flow into the formation and how to handle it.

In porous rocks, filtration loss generally occurs during the development of a protective membrane forming against the newly drilled formation, while the drilling fluid pressure is higher than the formation pore pressure. Relatively clear drilling fluid filtrate is filtered out by the porous rock leaving behind the solid phase, forming a thin sealing skin of the filter cake on the wellbore. Once the filter cake is fully developed, ideally it has a very low permeability which will temporarily secure the wellbore's stability (Opedal et al. 2013; Alsaba et al., 2014a) until the well is cased with steel pipes and cemented to the rock formation (Bourgoyne et al. 1986).

American Petroleum Institute (API) has a standardized test to determine the filtration properties of drilling fluid using standard filter paper called "the API filter press" (Bourgoyne et al. 1986). The flow of filtrate is measured and recorded with time with a measurement of the thickness of the filter cake at the end of the test. The volume of filtrate, the relationship of filtrate volume with time, and the filter cake thickness indicate how the drilling performed in terms of filtration properties. A testing apparatus for high pressure-high temperature drilling operation is also available.

Bourgoyne et al. (1986) presented that at any time during the filtration process, Darcy's law can be applied to the process. The rate of filtration is given by

$$\frac{d\,V_f}{dt} = \frac{k\,A\,\Delta p}{\mu\,h_{fc}} \tag{1}$$

where

$\frac{d\,V_f}{dt}$ = the filtration rate, cm$^3$ / s,

$k$ = the permeability of the filter cake, darcies,

$A$ = the area of the paper (cross-sectional area of the flow), cm$^2$,

$\Delta p$ = the pressure drop across the filter cake, atm,

$\mu$ = the fluid viscosity, cp, and

$h_{fc}$ = the thickness of the filter cake, cm.

The solids volume in the drilling fluid that has been filtered is equal to the volume of solids deposited in the filter cake,

$$f_s\, V_{df} = f_{sc}\, h_{fc}\, A. \tag{2}$$

$f_s$ is the volume fraction of solids in the drilling fluid, $V_{df}$ is the volume of the filtered drilling fluid, cm$^3$, $f_{sc}$ is the volume fraction of solids in the filter cake. Equation 2 can also be written as:

$$f_s\left(h_{fc}\, A + V_f\right) = f_{sc}\, h_{fc}\, A. \tag{3}$$

Therefore,

$$h_{fc} = \frac{f_s\, V_f}{A(f_{sc} - f_s)} = \frac{V_f}{A\left(\frac{f_{sc}}{f_s}\right) - 1}. \tag{4}$$

Inserting this expression for $h_{fc}$ into Eq. 1, integrating and rearranging yields

$$V_f = \sqrt{2\, k\, \Delta p \left(\frac{f_{sc}}{f_s} - 1\right)}\; A\, \frac{\sqrt{t}}{\sqrt{\mu}}. \tag{5}$$

When the parameters on the right-hand side other than $\sqrt{t}$ are held constant, plotting of $V_f$ with $\sqrt{t}$ results in a straight-line relationship as shown in Figure 2.1. A spurt loss can be determined from the y-intercept. Ideally, the spurt loss is the volume of filtrate flow through the filter at time zero, before the filter cake structure can form any flow resistance on the surface.

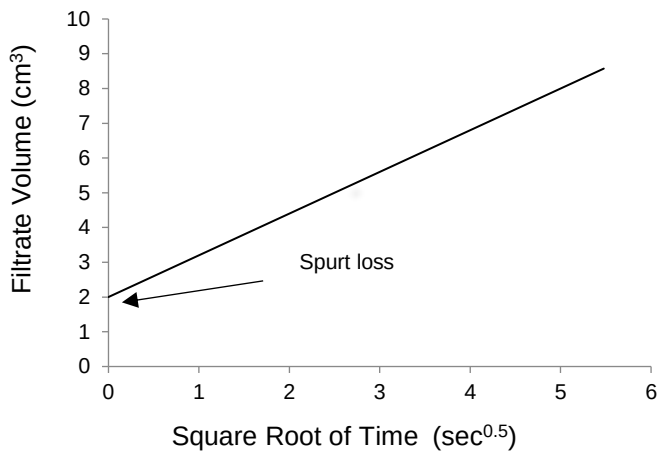


Figure 2.1. The plot of filtrate vs. time yields a straight line.

In the filtration process, the filter cake is still porous and wet, some small amount of the fluid phase is trapped inside the tiny pore spaces. Assuming no air is allowed in the system, the volume of filtered solid plus the trapped liquid volume equals the filter cake volume. The volume of filtered drilling fluid is the combined volume of filter cake and filtrate. Volume and mass conservation can be applied to any filtration process, including the screening of LCM. This idea can be applied to understand the LCM sealing process where the solid phase is separated from the liquid phase. The liquid-solid separation from the mixture during the seal forming follows the same concept. If a solid structure is forming in the fracture, the volume fraction of liquid needs some space to occupy. The more volume of the solid structure, the more volume of liquid is needed to flow away from the structure. This process is sometimes referred in the industry as “defluidization” (Kaageson-Loe et al. 2009; Sanders et al. 2010).

Since the filter cake formation is essential for the drilling process and the drilling fluid is not significantly consumed during the filter cake formation, the drilling fluid lost during filter cake formation is not considered as an LOC problem (Howard and Scott 1951); however, the concept of filtration loss helps understand how solids in the fluid mixture develop the bridging and sealing structures.

Even though a well drilled with an overbalance condition between the wellbore pressure and the formation pressure is going to lose the drilling fluid through the same mechanism as the filtration, the flowing mechanism of LOC must occur at a larger scale compared to filter cake forming process. Typically, loss in a porous formation happens when the permeability exceeds 100 darcys, where the intergranular pore sizes are sufficient size (Howard and Scott 1951). In this case, the whole drilling fluid mixture, both liquid and solid phases, can be forced to flow into the rock pore at any pressure higher than the formation pressure without forming a filter cake (Canson 1985). The non-development of filtration can be eliminated if the pore spaces are plugged by LCM (Chaney 1949).

Decreasing the flow area so the filtration control can take place, as in the trouble-free porous formations, seems to be the fundamental concept of the LOC mitigation mechanism in any type of formation. The difference is the variation of the opening area geometry and size that needs to be plugged before the filtration control process can perform a good seal.

In a cavern or vugular formation, the opening pattern is not consistent and is usually larger in size compared to the intergranular pores of a porous formation. The reduced flow restriction allows the fluid to flow out of the well at a much higher rate. The fluid can flow suddenly and severely after the drill bit penetrates and drops through the lost zone, even if only a few inches (Howard and Scott 1951). Since the openings are so large, special treatment such as cement gunk or a thickened polymer is required (Canson 1985; Loeppke et al. 1990; Scott and Lummus 1955). Cavity formation solving have been published by many researchers; however, the vugular LOC mechanism is not included in this dissertation. The main idea obtained after reviewing this problem is that the plugging procedure in any formation is to seal off the opening areas. They may be

sealed by chemical processes (cement or polymers), or by physical processes as the filter cake development.

In the case of drilling-induced fracture, the wellbore pressure can hydraulically fracture the formation if the pressure is sufficiently high. Theoretically, under the stress concentration around the wellbore, the intact rock fails when and where the wellbore pressure exceeding the tensile strength of the rock considering its confining stress (Canson 1985). Because the tensile strength of the rock is relatively low, the wellbore can fracture when the wellbore pressure slightly exceeds the least principle stress (Zoback 2007). Induced fracturing can happen in any type of rock but expectedly occurs in weak plane rock like a shale formation (Howard and Scott 1951).

Figure 2.2 shows how drilling induced fractures occur on the wellbore wall. In this example, the plane of the fracture is perpendicular to the direction of the minimum horizontal stress ($\sigma_h$), while the fracture propagates in the direction of the maximum horizontal stress ($\sigma_H$) (the broken arrow). The magnitude of the stress shown in the figure varied from compression (cross-sectional view of the well) to tension (across the fracture plane).

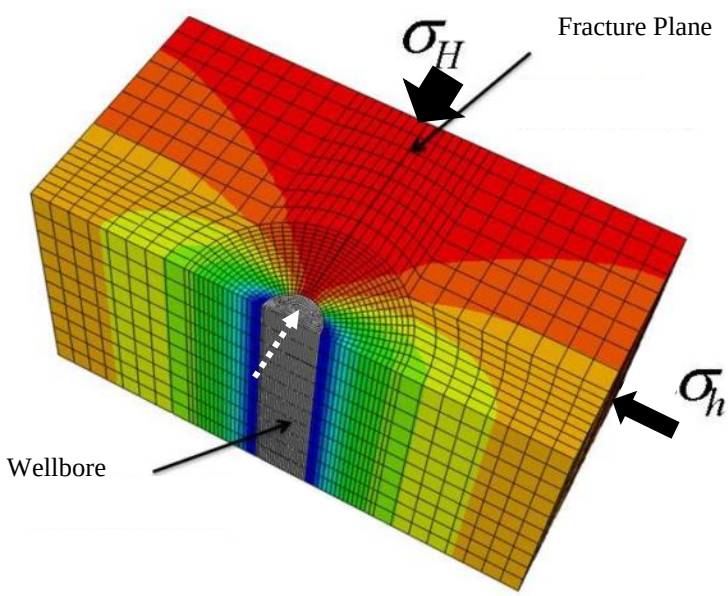


Figure 2.2. The numerical study presents fracture plane induced by the wellbore pressure propagating in the direction of the maximum principal stress (Salehi and Nygaard 2011).

The fracturing pressure might be only the hydrostatic pressure governed by the drilling fluid density or combined with an additional surging pressure resulting from a sudden drop of the drill stem into the hole or the frictional pressure while circulating. The excessive drilling fluid density can be the result of an inaccurate operating window prediction, while the surging pressure is caused by inappropriate drilling practice (Ghalambor et al. 2014). After the fracture initiation, the propagation requires less wellbore pressure. The propagating pressure decreases dramatically with the increasing of the distance from the fracture mouth to the tip (Zoback 2007).

A problematic situation occurs when the induced fractures propagate out through a network of flow paths. The intersection of the passages provides an open flow system for drilling fluids to flow out of the well at a higher rate. Even without the induced fracture, the drilled well penetrates through a network of the natural fracture system, a sufficiently high wellbore pressure can suddenly drive the fluid into the formation causing severe loss (Canson 1985).

Zoback (2007) presented that over geologic time, the fracture systems were formed and developed by the tectonic activities of the earth crust. The fracture orientations between the older and the newer developed fracture systems tend to be complicated from the changing of the stress fields with time. The fractures did not occur only in Mode I (tensile failure opening mode) as in induced fracture (hydraulic fracturing), but also occur in Mode II and III (shear failure, sliding in the parallel or perpendicular direction to the fracture channels). In the subsurface formation, the shear mode fracture happened on a larger scale, combining to become the minor and major faulting systems. These faults can be more permeable compared to Mode I fractures. Other than being induced during the drilling operation, mode I fracture can happen naturally. The opening fracture might close after the fracture pressure is equilibrated, while Mode II and III fractures are more active with high permeability. It is known that drilling through an active fault zone, containing Mode II or Mode III fracture, is considered the risky with the high possibility of pipe sticking and severe LOC incidents. The LOC can simply occur after the wellbore penetrates through these faults, or a fracture network connecting to the faults; or after the wellbore pressure creates the induced fractures propagating through the fractures and faults zones.

Loss mechanism in induced fractures and natural fractures are similar in terms of the flow channels shape. Both contained long openings with a narrow width between the fracture walls. Mitigating LOC in the fractured formations needs LOC particles to plug the flow area between the fracture walls, the same as plugging the pore throat in the case of porous formations. Flowing of drilling fluids through fractures is reviewed in the following section.

## 2.2 FLUID FLOW THROUGH FRACTURES

The fracture openings on the wellbore wall provide the entrances for the drilling fluids to enter the formation around the borehole. The flow of drilling fluid through the fractures cannot be considered as an inviscid flow because the viscosity of the flow is important (Potter and Wiggert 1997). Flow regime of a fluid can be classified as a laminar flow or a turbulent flow. Combining three flow parameters in a single dimensionless parameter named Reynolds Number (Re) is a convenient way to identify the flow regime. Reynolds Number ($Re$) definition is given by

$$Re = \frac{\rho \, \bar{\nabla} \, b}{\mu} \tag{6}$$

where $\rho$ is the fluid density, $\bar{\nabla}$ is the averaged flow velocity, $b$ is the characteristic length (in this case, the fracture aperture), and $\mu$ is the fluid viscosity (Potter and Wigger 1997).

The Reynolds Number, both for Oil Base Fluid (OBF) and Water Base Fluid (WBF), is not a constant parameter. The drilling fluid is a Pseudo-plastic fluid, where the viscosity tends to decrease as the shear rate increases. The density can be considered constant assuming the drilling fluid is an incompressible fluid. The flow velocity can change as the flow area controlling by the characteristic length changes. At any point of interest along a flow path, the flow is starting to change from a laminar flow to a transitional state between laminar and turbulent flow (transition flow) if Reynolds Number changes to be higher than 2100. The flow becomes a turbulent flow when Reynolds Number reaches 4000 and beyond. With different flow parameters, the flow

can have different flow regimes along the flow path even though the flow rate is kept constant (Bourgoyne et al. 1986).

For a flow in fracture of a constant density fluid with a fixed flow rate, the Reynolds Number is directly proportional to the fracture width, where a smaller fracture width gives a smaller Reynolds Number. However, the narrower openings will have smaller flow area which increases the flow velocity and decreases the viscosity. This dominates the change of the Reynold Number to be increasing instead of decreasing as the fracture width decreases. Interestingly, at a high flow rate in LOC incident, it is likely that the Reynolds Number will fall into a turbulent range. The cross-sectional geometry (and area) of the flow area strongly affects the flow behavior of the fluids. At the same time, the cross-sectional flow area is also the target space for LCM particles to occupy in the sealing processes.

The fundamental of fluid mechanics (Potter and Wiggert 1997) offers an open flow approximation between two parallel horizontal plates derived from an elemental approach or the Navier-Stokes equation. Under a steady state, laminar flow with a very long open channel, a flow rate per unit width of an incompressible fluid $Q$ is given by

$$Q = \frac{[b]^3}{12\mu}\nabla P \tag{7}$$

where $\nabla P$ is the pressure gradient, usually assumed to be one dimensional flow in a long breadth or channel length. Equation 7 can be used widely in fluid mechanics calculation where the two planes are opened with no flow restriction. In LOC application, it is more applicable to the naturally occurring opened fractures than the drilling induced fractures.

Zoback (2007) introduced an analytical approximation in the case of the fluid flow through an elliptical cross-sectional area fracture under the confining stress acting on the fracture planes, the maximum fracture width ($b_{max}$ ) is given by

$$b_{max} = \frac{2\left(P_f - S_3\right)L(1 - \upsilon^2)}{E} \tag{8}$$

where $P_f$ is the fluid pressure inside the fracture, $S_3$ is the least principle stress, $L$ is the flow channel length or breadth, υ is Poisson's ratio, E is Young's modulus.
The flow rate $(Q)$ is then given by

$$Q = \frac{\pi}{8\mu}\left[\frac{b_{max}}{2}\right]^3 \nabla P \tag{9}$$

which yields

$$Q = \frac{\pi}{8\mu}\left[\frac{L(1-\upsilon^2)(P_f - S_3)}{E}\right]^3 \nabla P. \tag{10}$$

Equations 8, 9 and 10 can be used to find the maximum fracture width related to flow rate when other parameters are known or assumed. Many assumptions have been made along the derivation and may not meet the real physical flow phenomena of the drilling fluids.

Rahimi et al. (2016) summarized many other flow-in-fracture models analytically developed for the fracture width determination when the other parameters such as the least principal stress, wellbore or fracture pressure, pore pressure, and rock mechanical properties are known. The models were created with different assumptions and input parameters that can be used in LCM analysis for fracture sealing (Hillerborg et al. 1976; Carbonell and Detournay 1995; Alberty and McLean 2004; Wang et al. 2008; Morita and Fuh 2012). Different forms of relationships and parameters yield different results among those models. The simplification of the models causes most of the results to be significantly different from their hydraulic fracturing experiment results.

Ghalambor et al. (2014) introduced a fluid flow model of natural fractures using lubrication theory. The fundamental equation was given by

$$\frac{\partial\,(w\bar{v})}{\partial r} + \frac{1}{r}w\bar{v} + \frac{\partial w}{\partial t} = 0 \tag{11}$$

where $\frac{\partial w}{\partial t}$ is the time rate of change of the fracture width, $\bar{v}$ is the averaged fluid velocity, and r is the coordinate position in the flow direction.

The fluid flow velocity and the fracture width can be changed with the specified condition. The fracture width may be kept constant or changed using an appropriate constitutive law. The drilling fluid rheology was also considered using Bingham-Plastic, Power law or Yield Power law to take care of the change in viscosity respect to the shear rate and shear stress of the non-Newtonian drilling fluids. With the yield power law rheological model, the fluid velocity in terms of pressure drop is given by

$$\bar{v} = \left(\frac{m}{2m+1}\right)\left(\frac{w^{\frac{m+1}{m}}}{2^{\frac{m+1}{m}}k^{\frac{1}{m}}}\right)\left(-\frac{dP}{dr} - \left(\frac{2m+1}{m+1}\right)\left(\frac{2\tau_y}{w}\right)\right)^{\frac{1}{m}} \tag{12}$$

where $\frac{dP}{dr}$ is the pressure drop respect to the position in the flow direction, $m$ is the flow behavior index, $k$ is the consistency index, and $\tau_y$ is the yield stress. Substituting Equation 12 into Equation 11 and applying the proper deformation law yields

$$\begin{aligned}&\left(\frac{m}{2m+1}\right)\left(\frac{1}{2^{\frac{m+1}{m}}k^{\frac{1}{m}}}\right)\frac{\partial}{\partial r}\left(w^{\frac{2m+1}{m}}\left(-\frac{dp}{dr} - \left(\frac{2m+1}{m+1}\right)\left(\frac{2\tau_y}{w}\right)\right)^{\frac{1}{m}}\right)\\ &+\left(\frac{m}{2m+1}\right)\left(\frac{1}{2^{\frac{m+1}{m}}k^{\frac{1}{m}}}\right)\frac{1}{r}w^{\frac{2m+1}{m}}\left(-\frac{dp}{dr} - \left(\frac{2m+1}{m+1}\right)\left(\frac{2\tau_y}{w}\right)\right)^{\frac{1}{m}} + \frac{\partial w}{\partial t} = 0\end{aligned} \tag{13}$$

The partial differential equation above must be solved numerically, based on a group of complex variables. The solution suggests that the LOC can stop after a flow period due to frictional losses in the fractures, where an ultimate cumulative lost volume with the LOC time relationship can be determined if the fracture width is known, and vice-versa.

This model gives a quantitative idea of how significantly the fracture width affects the lost volume if the drilling fluid is infinitely available and the problem is ignored without mitigating the loss. Ghalambor et al. (2014) also provided an example of a drilling fluid loss through a fractured formation. A volume of 20,000 bbl of drilling fluid can flow through a 2000-microns width fracture under a differential pressure of 300 psi before the flow stop. Even though the drilling fluid available in the well site should not be as high as the mentioned volume, but the model's result gives a quantitative idea how severe the LOC can possibly be in fractured formations.

The difference between flow model equations implies that they were developed from different assumptions or laws, and the calculated results often do not agree with the others. Some models may not be realistic due to the assumptions and simplifications of the physical problems, while the more the realistic models are more complicated and difficult to obtain the parameters required to solve the model. The accuracy of the results is also questionable.

In LCM treatment design, the fracture width is an important parameter because it indicates the size of granular materials to be used both in corrective and preventive approach (Whithfill and Miller 2008). Field cases reporting flow rates may give a clearer picture about the LOC by knowing the loss severity and using history matching to obtain thickness (fracture length) and other parameter approximations (Ghalambor et al. 2014).

The rate of LOC varies significantly. Losses can be classified into seepage losses (1-10 bbl/hr), partial losses (10 to 500 bbl/hr), and severe losses (over 500 bbl/hr) (Nayberg 1986). Total loss occurs when the flow rate of the drilling fluid entering the formation exceeds the rig pumping capacity (Baggini Almagro et al. 2014). With this rate, all drilling fluid in the active system can be spent out in less than two hours, for example; a circulating rate of 420 gal/min or 10 bbl/min can empty the rig tanks with 900 bbl drilling fluid within 90 mins.

As reviewed above, the loss rate depends strongly on the fracture width, but the length of the channel on the wellbore is also important in terms of the total flow area of the incident. Understanding the effect of the fracture width and the fracture width approximation from flow rate should be useful and provide some ideas for the testing apparatus development.

Flow models were developed only for drilling fluid flow without LCM mixed with the fluid which will affect the flow behavior significantly. Moreover, during the seal structure development, the decreasing the flow area with time should occur as LCM sealing structure develops in the space between the fracture walls. The study in this area should expect complicated unsteady flow with time, the rate of change of the flow velocity, flow area, and the fluid viscosity.

## 2.3 TYPE AND USAGE OF SEALING MATERIALS

Various LCM types and formulations have been developed and used since the early days of rotary drilling. One of the US patents issued at the very beginning of rotary drilling method was to M T. Chapman (1890) describing the use of LCM in circulating fluid (White 1956). Since then, the application of LCM has been studied, revised and improved continuously (Robinson 1940).

Recently, LCM are classified in seven categories based on their appearance and application (Alsaba et al. 2014a). They are granular, flaky, fibrous, granular-flaky-fibrous combinations, acid/water soluble, high fluid loss squeeze, swellable/hydratable combinations, and nanoparticles (Alsaba et al. 2014a). However, granulate LCM is the type of material normally added to the drilling fluids. The LCM particles will bridge across opening areas so filter cake can be built and proper circulation is regained (Bourgoyne et al. 1986). Granular materials can form seals at the porous formation face or within the fracture to prevent the losses into the formation (Howard and Scott 1951, Nayberg 1986). The Materials with high crushing resistance (graphite) were found to be suitable for fracture sealing and wellbore strengthening applications where higher stress acts on the particles (Whitfill 2008; Kumar and Savari 2011).

Field observations and measurements can identify the type of formation where the loss occurs (Howard and Scott 1951). The mud logging unit continuously monitors the drilling fluid level in the rig tanks and alarms as soon as the drilling fluid level in the system drops down to a preset value. Cutting analysis gives the information of the penetrated formations. Wireline logs such as temperature logs and gamma ray logs are used to locate the lost zones if the drill string is pulled out of the hole (Canson 1985). If the drilling operation is in progress, the state-of-the-art measurement while drilling

(MWD) tool is available to measure downhole parameters that are used to detect and monitor the loss zones effectively. If the interval depth of the loss zones and the rate of LOC with time are known, fracture width estimation can be performed accurately in a short time.

The treatment applied after LOC detection is classified as a corrective approach. In some cases, if the loss is likely to happen in a known formation, the treatment might be done before the LOC incident happens to prevent it. This is referred as the preventive approach (Kumar and Savari 2011). Mixing LCM as a preventive treatment allows the LCM to cure LOC at an early time of the incident (Howard and Scott 1951).

The use of LCM to plug the fracture and widen the operating window increass the fracture gradient. This practice permits higher wellbore pressure known as the wellbore strengthening concept and has been studied broadly. Unfortunately, the strengthening mechanism is a subject of disagreement between groups of researchers. Alberty and McLean (2004) suggested that LCM props at the fracture entrance could increase the hoop stress around the wellbore. Dupriest (2005) believed that the fracture gradient of the formation would be increased by increasing the fracture closure stress (FCS), the normal stress on the fracture plane keeping the fracture face contacted. FCS increases by the use of LCM to keep the fracture wider and seal the fracture tip. Aadnoy and Belayneh (2004) introduced the elastic-plastic fracture model, where the fracture gradient could be increased more than the original hoop stress by the fracture healing effect of the filter cake plastic deformation at the fracture entrance. Van Oort et al. (2011) explained that the tip isolation by LCM could increase the fracture propagation pressure.

Salehi and Nygaard (2012) presented the results obtained from a three-dimensional finite-element model simulating the fracture initiation, propagation and sealing in the near wellbore region. His results showed that using LCM in wellbore strengthening approach could not enhance the hoop stresses to be higher than the intact (originally before strengthened) wellbore strength.

From previous studies stated above, the theory of wellbore strengthening is not clear and different from researcher to researcher; however, all of them agree that LCM treatment is the primary tool for plugging or sealing the fracture, providing the increased fracture propagating pressure (Mortadha 2016). Understanding the LCM placement and

sealing application is useful for both the healing or corrective approach and the strengthening or preventive approach.

From a known fracture width, different LCM size selection for LOC curing was recommended by researchers. The size solutions were usually given in the form of the particle size distribution (PSD) with respect to fracture width.

White (1956) presented that a mixture of the normal solid component of drilling fluids with LCM is adequate for sealing porous formations until the pore or crack size exceeds approximately three times the diameter of the largest particle present. The size of the LCM is limited by the mud pump. A few different rules developed specifically for plugging pore throats in porous rock have slightly different definitions about the PSD of LCM and the pore sizes.

Abrams (1977) suggested that the median particle size of the bridging particles should be equal to or slightly greater than one-third the median pore size of the formation, while the bridging size solids must be five percent or more by volume of the solid in the LCM treated drilling fluid. In a different way, Hands et al. (1998) proposed that the bridging properties of the fluid must be selected so the D90 (90% of the particles are smaller than the size) is equal to the pore size of the rock.

Dick et al. (2000) introduced the Ideal Packing Theory, applied previously in the painting industry, to be used for LCM application. The theory stated that the ideal packing occurs when the percent of cumulative volume vs. the square root of the particle diameter forms a straight-line relationship. Following the theory, the particles can obtain an ideal packed seal structure with the least possible porosity. Vickers et al. (2006) presented a more detailed bridging theory by adding the target fractions where D90 is equal to the largest pore throat, D75 is less than two-third of the largest pore throat, D50 is about one-third of the mean pore throat, D25 is one-seventh of the mean pore throat, and D10 is larger than the smallest pore throat. The volume percentage of each range of LCM grain sizes were developed.

Later, the bridging theory specifically for fracture sealing was presented. Whitfill (2008) recommended that for fracture bridging, the D50 size should be equal to the fracture width. This bridging idea implies that there must be particles larger in size, approximately 50% of the fracture width available for the bridging mechanism.

Mortadha et al. (2014c, 2016) observed LCM seals removed from the plugs formed in fracture discs. Digital microscope and electron scanning microscope images revealed that using LCM formulations with a wide range of PSD resulted in less seal pore space and higher seal integrity compared to a narrow range of particle sizes; the results agreed with the ideal packing theory. It was also found that the D90 value should be slightly larger than the expected fracture width to get the highest sealing efficiency, in contrast with the formerly investigated bridging idea. From the D90 rule, Mortadha et al. (2014c) concluded that conventional granular LCM has the capability to seal the fracture up to 2000 microns corresponding to the LCM sizes, and the attempt to use larger particle size to cover wider fracture width is limited by the risk of plugging downhole tools during the pill placement using the drill string.

The latest bridging theory of Alsaba et al. (2016) was developed from more than a hundred tests using a high-pressure test cell with steel slotted discs. Their experiment indicated to get an effective fracture sealing, D50 and D90 values should be equal to or greater than 3/10 and 6/5 the fracture width, respectively. This theory was then used for LCM selection in this experiment with confidence that the selected LCM would form a seal effectively, while only the effect of testing conditions on sealing performance could be concentrated.

## 2.4 TESTING APPARATUS PREVIOUSLY USED

The apparatuses previously used simulated a certain formation type of interest. The simulated fractures can be constructed from permeable materials to study LOC in a permeable formation (Hettama et al. 2007), or impermeable material such as steel or aluminum alloy to study LOC in an impermeable formation (Alsaba et al. 2014b, 2014c, Loeppke et al. 1990, Scott and Lummus 1955).

The testing method forced the drilling fluid treated with LCM sample through the simulated fracture, while parameters were recorded and the seal forming was observed at the end of the experiment. Table 2.1 lists the apparatus used in previous studies related to sealing performance evaluation.

The injection process falls into two categories, a constant injecting pressure with the fluid loss volume as the evaluation, or a constant injecting flow rate recording the

maximum sealing pressure (Howard and Scott 1951, Nayberg 1986, Loeppke et al., 1990, Kageson-Loe et al. 2009, Kefi et al. 2010, van Oort 2011, Alsaba et al. 2014).

Table 2.1 Testing apparatus used in previous studies.

| Publication | Measured Values | Max. Press. (psi) | Temp. ˚F | Simulated Fracture | Fracture Width (mm) |
|---|---|---|---|---|---|
| Howard and Scott (1951) | Fluid loss | 1,000 | N/A | Cast cement in steel pipe | 12.7 mm |
| Kelsey 1981, Hinkebein et al. 1983 | Sealing efficiency | 1,000 | 300 | API slots, tapered slots | 1 - 5 mm (straight) 2 – 12.7 (tapered) |
| Van Oort (2011) | Sealing pressure and fluid loss | 1,250 | N/A | Uneven aluminum platens | 0.3 – 1.0 mm (two circular plates) |
| Savari et al. 2011 (PPA) | Filtration/ bridging | 4,000-5,000 | 500 | API slot, tapered slots | 2 mm (tapered) 5 mm (straight) |
| Mostafavi et al. 2011 | Sealing pressure | 8,700 | N/A | Fabricated steel fractures | 0.3, 0.5 and 0.7 mm |
| Alsaba et al. (2014a) | Sealing pressure (and fluid losses) | 10,000 | 180 | Steel slot discs | 1–10 mm (tapered / straight) |

The constant pressure injection method intends to simulate a constant bottomhole pressure during an LOC treatment to observe how successfully and effectively the seals are formed. Fluid loss is used as the performance indicator where the smaller volume of fluid loss is considered a success in terms of sealing effectiveness.

The constant injecting flow rate method monitors both the buildup pressure to measure the seal integrity obtained from a specific LCM blending, as well as the fluid loss volume indicating the seal forming efficiency.

Hinkebein et al. (1983) presented a publication that was the only LCM aging test found in the technical paper database. They used the modified API slot tester as listed in Table 2.1 to conduct both the experiment measuring the sealing ability of LCM under the

room temperature and the higher temperature aging test. In the aging test, they used eight aging test cells and a rolling oven. The drilling fluid was a 5% to 8% Wyoming Bentonite with a density of 8.8 ppg. Five single LCM formulations available at that time with no detailed LCM specification (cottonseed hull; Kwik-Seal or fibers, flakes, and granular particles mixed; Ruf-Plug or ground corn cops; ground battery casing; and ground battery casing with Micatex) were used in the aging tests. The temperature selected were 250 and 400 °F with four-hours aging time in the rolling oven. The results showed that the cottonseed hulls formulation was adversely affected by the aging temperature at 250 °F, while the Ruf-Plug totally failed to seal at the 400 °F aging temperature.

## 2.5 LITERATURE REVIEW DISCUSSION

The literature review provided the occurrence and significance of the LOC problems, where all the attempts in the past have been made to overcome, mitigate and limit the consequential difficulties using LCM to control losses of drilling fluid into the formations. The design and application in the field essentially rely on laboratory testing and evaluation as the main suggestive approach.

The physical properties of the LCM were widely used as the key parameters needed to get the treatment effectiveness, while the testing condition that should significantly affect the testing results has been overlooked. The LCM aging experiment was conducted using old types of LCM that are not available at the present time.

If the effect of testing conditions can be found, it can be merged with the previous findings and applied to the laboratory evaluation improvement and the field treatment. The apparatuses can be modified or adjusted to get a more accurate simulation to the actual phenomenon. The treatment design and testing will increase the evaluation reliability and design confidence. The finding can be used to predict the treatment performance if the downhole conditions are varied from the expected condition as tested in the laboratory. The obtained information will be useful for further studies in this area.

For field applications, if possible, the parameters known to provide positive results in the laboratory might be applied to the field treatment to improve the LCM sealing ability and integrity. Improving the operational environment to be a better

permissive condition should increase the treatment effectiveness and the chance of success.

Furthermore, during the test, LCM behavior could be monitored along with the indicative parameters to gain the understanding of the fracture plugging and sealing processes. The knowledge can be applied to LCM selection and the treatment design to obtain the more effective LOC mitigation in impermeable rock fractures.

## 2.6 OBJECTIVE

This dissertation objective is to quantify how significant the indicative parameters used in LCM evaluation change as the results of varying the testing conditions, other than the LCM physical properties, that are known to govern the sealing capability. This overall objective will be addressed by studying the following questions.

a) If the injection flow rate is changed from a continuous slow rate to a sudden high rate, will the seal forming ability be disrupted, and will the sealing mechanism change?

b) What is the effect on seal integrity if the testing conditions related to the fracture simulated disc parameters (wall angles and thickness) are changed?

c) What is the effect on seal capability if the testing environment related to the base fluids, drilling fluid density, type of weighting materials, the availability of fine weighting particles, and the dynamic aging condition of higher pressure and temperature are changed?

d) When combining the fracture width, LCM properties and other testing conditions that are known, what is the relationship between those parameters and sealing pressure, i.e., can sealing integrity be estimated from those parameters?

e) If the testing apparatus moves a step closer to the actual dynamic downhole condition, what is the effect of dynamic circulating conditions on the sealing ability of LCM?

To reach the objective, the experiment was broken down into five tasks.

1) Modify loss circulation apparatus to test how sudden flow affects the LCM sealing ability.

2) Evaluate the effects of variation of simulated fracture slots i.e., wall angles, and simulated fracture slot thickness.

3) Evaluate the effects of changing base fluids, type of weighting materials used in base fluids, PSD of weighting agent, and aging condition of the LCM-treated drilling fluids affect the sealing capability.

4) Create a statistical model that can predict LCM sealing pressure based on the experimental results.

5) Conduct a set of experiments in a dynamic test cell to observe how circulating conditions affect the sealing ability of LCM.

The first paper "Testing Conditions Make a Difference While Testing LCM" addressed the first and the second tasks. The second paper "Effect of Testing Conditions on the Performance of Lost Circulation Materials: Understandable Sealing Mechanism" addresses the third task. The third paper "Pressure Prediction Model for Lost Circulation Treatments Based on Experimental Investigation" addressed the fourth task. The fifth task has been addressed in the fourth paper "Effect of Experimental setup on Lost Circulation Materials Evaluation Results".

# PAPER

# I. TESTING CONDITIONS MAKE A DIFFERENCE WHEN TESTING LCM


## ABSTRACT

Laboratory studies have been used extensively to evaluate loss circulation materials (LCM) treatments to solve or prevent lost circulation problems in fractured formations. Experiments with slotted disks simulating fractures have been performed with the amount of fluid loss and sealing pressure used as evaluation criteria. This study presents the investigation of LCM behavior with different slot designs and fluid flow patterns for water-based and oil-based drilling fluids. Experiments on tapered-slot discs that simulate fractures with different fracture wall angles and fracture lengths were conducted at high pressure. A bladder-type accumulator was added to the system to provide an instantaneous flow condition. Results showed that increasing the wall angle tended to decrease sealing efficiency. Increasing the fracture length (disc thickness) in tapered discs resulted in higher sealing pressure. In the instantaneous flow tests, LCM formulations used to perform a strong seal in HPA tests also sealed the slot under the sudden flow condition with a similar bridging and sealing profile. This set of experiments shows that the experimental setup can change the results, so caution should be taken when quantitatively comparing LCM tests on slot disks from different experimental setups.


## 1. INTRODUCTION

Lost circulation is defined as the loss of drilling fluid to formation void during drilling or completion (Howard & Scott, 1951). The drilling industry tries to solve fluid loss problems by adding lost circulation materials (LCM) to the drilling fluids to form a plug or seal in the open area to stop the flow. The cause of losses can be divided into four categories: highly permeable unconsolidated sand or gravels, cavity or cavernous, naturally fractured, and induced fractured formation (Howard & Scott, 1951). The rate of losses can be divided into seepage losses (1-10 bbl/hr), partial losses (10 to 500 bbl/hr), and severe losses (over 500 bbl/hr) which are controlled by the loss mechanisms (Nayberg, 1986). In wider fractures, the flow rate of the drilling fluid entering the

formation may exceed the rig pumping capacity because the area of the openings is sufficiently large and a high differential pressure is exerted by the drilling fluid column. In this case, special treatment is typically required (Canson, 1985).

Laboratory experiments have been conducted to investigate the lost circulation curing. Blends of selected LCM have been tested using different experimental setups to evaluate sealing performance. In the case of investigating LCM for losses into impermeable fractured formations, researchers use impermeable materials such as steel or aluminum alloy to construct the simulated fracture opening (Scott & Lummus, 1955; White, 1956; Loeppke et al., 1990; Hettama et al., 2007; Kageson-Loe et al., 2009; Kumar et al., 2011; Alsaba et al., 2014b, 2014c). A number of physical properties were studied for LCM treatment design, such as LCM type and formulations (Alsaba et al., 2014b, 2014c), LCM particles sizes (Alsaba et al., 2016; Kageson-Loe et al., 2009), shape, concentration, size distribution (PSD) respected to fracture width (Alsaba et al., 2016; Hettama et al., 2007; White, 1956), treatment concentration (Alsaba et al., 2014b), swelling and deformability under higher temperature (Alsaba et al., 2014a), density and mechanical properties (such as compressive strength, Young's Modulus, Poisson's ratio, and hardness) (Loeppke et al., 1990), and resiliency as deformable or flexible materials (Mostafavi et al., 2011; Xu et al., 2014). Most researchers used single or mixed granular materials such as ground marble or sized calcium carbonate (SCC), graphite (G), and walnut shells (NS). Some studies used fibrous materials to form a fiber network in the fractures (Baggini Almagro et al., 2014; Canson, 1985; Kefi et al., 2010; Xu et al., 2014). Typically, an injection rate of 10 – 25 ml/min was used (Alsaba et al., 2014b, 2014c; Mark et al., 2008; Mostafavi et al., 2011).

The objective of this paper is to address how the testing conditions affect the experimental LCM performance. To reach this objective, a specifically designed particle plugging apparatus was used (Alsaba et al., 2014b, 2014c). Inside the cylindrical testing cell, the simulated fracture disc can be replaced to observe different results corresponding to the difference of fracture wall angle and disc thickness. Lastly, different driving differential pressures were set to study the effect of high flow conditions. The geometry and LCM distribution of the formed seals were also observed to better understand LCM behavior and sealing mechanisms that affect the testing results. This study used stainless

steel discs to simulate fractures for lost circulation treatment in fractured impermeable formation.

## 2. EXPERIMENTAL SETUP

### 2.1 TESTING APPARATUS

The purpose of the experiment is to investigate the behavior of selected LCM formulations forming the seal on simulated fracture discs under different test conditions including wall angle, disc thicknesses, and flow conditions. Two slightly different experimental setups were used along with a set of stainless steel simulated fracture discs.

Figure 1 shows a schematic diagram of the HPA (Alsaba et al., 2014a).

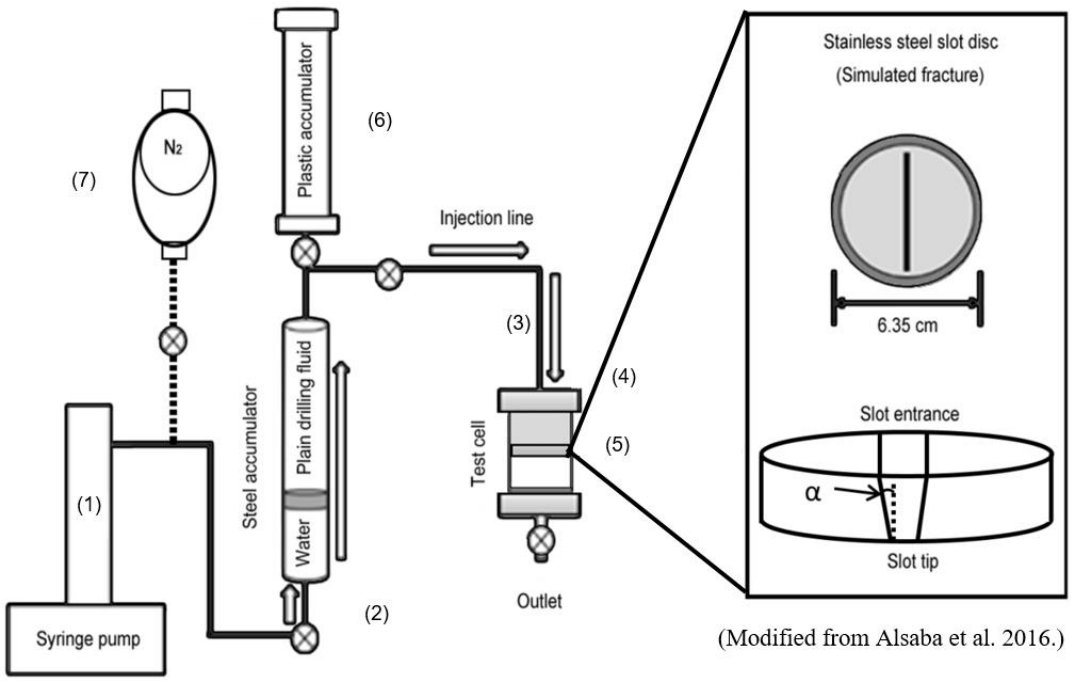


Figure 1. Schematics of the HPA apparatus. The syringe pumps water to pressurize the accumulator filled with drilling fluid without LCM. The test cell contains drilling fluid with LCM. The broken line was used for the second set of experiments where installation of the nitrogen gas accumulator to the injection line (7) provides pneumatic spring action driving the drilling fluid sample through the slot. The wall angle (α) is also displayed in the figure.

A slotted disc (5) is placed inside the testing cell on a spacer cylinder. The spacer provides a room for fluid LCM that passes through the slot during the test to prevent plugging or restriction of flow at the cell outlet. Above the slotted disc is drilling fluid filled with LCM. During the test, the cell cap (4) was closed, and drilling fluid from the plastic accumulator (6) was filled in the injecting line (3) and into the steel accumulator (2). The pressure buildup was created in two different ways. A syringe pump (1) could provide a continuous flow of water to displace drilling fluid from the steel accumulator to flow into the testing cell at 25 ml/min flow rate. In the instantaneous flow test, the bladder-type accumulator (7) connected to the discharge line of the syringe pump could also provide a sudden flow to form the pneumatic spring action of the compressed nitrogen gas in the bladder. The bladder was precharged with nitrogen gas at 33% or 66% of the targeted test pressure. Four differential pressures could be set from two different precharged pressures. A pre-charged pressure of 100 psi was set for 150 and 300 psi differential pressures, and a precharged pressure of 200 psi was set for 300 and 600 psi differential pressures.

A system flow test was run to estimate the possible flow rate without the presence of LCM in the system. The plain drilling fluid was forced to suddenly flow through the 7°-disc slot without LCM treatment. The test gave an average flow rate of 1.6 gpm (100 ml/sec) through the 2000 x 5000 microns opening tip. This flow rate is comparable to a lost circulation rate of 190 gpm (270 bbl/hr) flowing out of a well with a 20-foot-long fracture (2000-micron fracture width) along the borehole wall.

## 2.2 LOST CIRCULATION MATERIALS

For the tests, a formulation of graphite (G), sized calcium carbonate (SCC), and nutshell (NS) blends were used per recommended formulations from a previous study (Alsaba et al., 2014c). Table 1 shows the LCM formulations identified by the type of LCM with the fraction of particle size blend.

The formulations were also used in sealing with disc thickness variation and sealing with instantaneous flow conditions. Two types of drilling fluids were used. An 8.6 lb/gal density, simple 7% bentonite (by weight) water-based fluid (WBF), raised up to 11 lb/gal using barite; and an environmental-friendly oil-based drilling fluid (OBF),

11 ppg (ready-mixed), which was obtained from an oil company; were used. For the WBF, the tests were run three times to evaluate the repeatability of the tests.

Table 1. LCM formulation used for all the tests in this paper.

| Formulation and type | | D50 | % by weight | After Blended PSD | | | | |
|---|---|---|---|---|---|---|---|---|
| | | | | D10 | D25 | D50 | D75 | D90 |
| NS 50 ppb | Coarse NS | 2300 | 34 | 180 | 400 | 1000 | 1600 | 2400 |
| | Medium NS | 1450 | 33 | | | | | |
| | Fine NS | 620 | 33 | | | | | |
| G & SCC 105 ppb | Coarse SCC | 2500 | 33 | 170 | 650 | 1300 | 1900 | 2600 |
| | Medium SCC | 1400 | 33 | | | | | |
| | Fine G & SCC | 500-600 | 34 | | | | | |
| G &NS 40 ppb | Coarse G | 1000 | 15 | 80 | 180 | 580 | 1400 | 2000 |
| | Medium G | 400 | 15 | | | | | |
| | Fine G | 100 | 10 | | | | | |
| | Very fine G | 50 | 10 | | | | | |
| | Coarse NS | 2300 | 17 | | | | | |
| | Medium NS | 1450 | 17 | | | | | |
| | Fine NS | 620 | 16 | | | | | |

### 2.3 SLOT DISCS

A set of simulated fracture discs with different slot wall angles varied from 0 (straight slot), 7°, 9°, and 13° with the same thickness of 6.35 mm was manufactured (Table 2). The cross-sectional diagram of a tapered disc providing a slot wall angle measurement (α) is shown in Figure 1.

Two simulated fracture discs with 0° and 9° slot wall angles (25.4 mm thick) were also produced to investigate the variation of disc thickness. In the variation of wall angle and disc thickness experiments, the fracture outlet width was set to be constant at 2000 microns, but for the rapid flow tests, both 1500 and 2000-microns slot width were used corresponding with specified LCM formulations and concentrations. The first four discs in Table 2 were used in the wall angle experiment. The discs vary in wall angle while the tip width was kept constant at 2000 microns.

Table 2. Name and dimension of the discs used in the effect of wall angle experiment.

| Disc code | Slot entrance width (mm) | Wall angle (degree) |
|---|---|---|
| SS2-R | 2.0 | 0 |
| TS2-R7 | 3.5 | 7 |
| TS2-R9 | 4.0 | 9 |
| TS2-R13 | 5.0 | 13 |
| TS15-R7 | 3.0 | 7 |
| SS2-T | 2.0 | 0 |
| SS2-T9 | 10.0 | 9 |

*All discs are 63.5 mm diameter, slot outlet width 2000 microns, slot length 50 mm and disc thickness 6.35 mm, except the tip of TS 15-R7 is 1500 microns and the thickness of SS2-T and SS2-T9 is 25.4 mm

## 3. TESTING METHODOLOGY

Figure 2 shows an example of a plot of the injecting pressures vs. time of an HPA test at 25 ml/min. When starting the pump, the pressure increased to 50 psi due to the frictional losses in the system. Fluid losses from the drilling fluid sample containing LCM particles started to flow out of the cell's outlet, first at the injecting rate and decreasing as the seal was formed. Pressure increased when the LCM started to form a seal bridge across the slot. In this paper, bridging is defined as the first group of particles that were successfully set at rest in-between the opening area of the slot and performed a strong foundation for the other particles to develop a complete seal.

After the seal formed and pressure was rising, the seal was broken partially at a weak point, and the pressure dropped down. At this moment, some fluid loss could be observed at the outlet. The bridge redeveloped quickly, where pressure rebounded sharply. The seal was broken and reestablished many times as a cyclical process. Normally, higher peak pressures were detected while the injection continued. The pressure was built up until it reached a maximum pressure (the circled peak point on Figure 2). After that, the seal might develop with lower sealing pressures or might not be able to reform anymore due to insufficient LCM concentration left in the cell. In this case, the test was stopped when no seal or only weak seals were observed. If the pressure went above 3,000 psi (rarely happened in 0° and 7° slot discs), the test was also stopped

due to test limitations. After the testing, the seal was visually observed under a microscope and photographed.

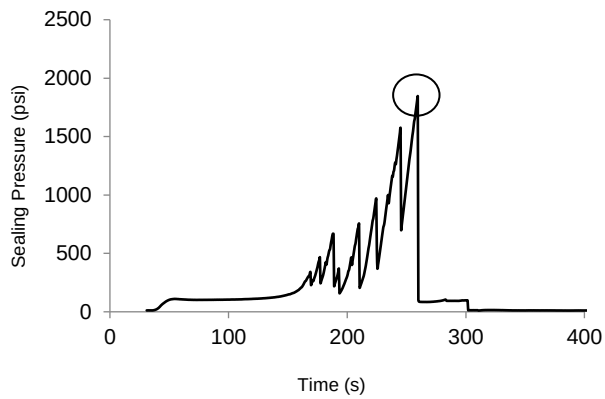


Figure 2. A plot of injecting pressure over time obtained from an HPA test. The peak pressure circled in the figure is the maximum sealing pressure, denoted as the sealing pressure.

## 4. TESTING RESULTS

A total of 80 tests were performed. Table 3 and Table 4 list the results of the 25 ml/min (HPA) tests and the instantaneous flow tests, respectively.

Figure 3 displays the plot of the sealing pressure vs. the wall angles. The graph shows a negative trend between them with a correlation coefficient ($r^2$) of 0.84.

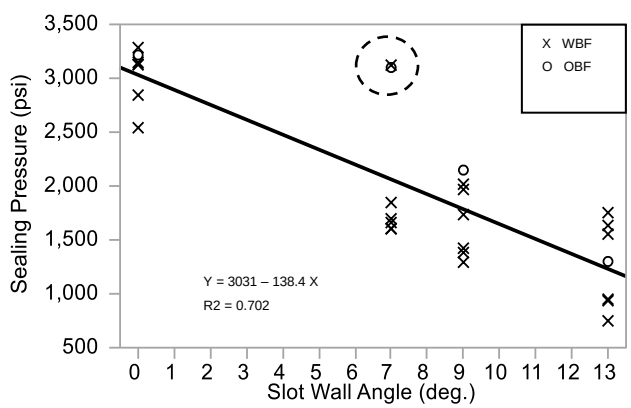


Figure 3. The plot between maximum sealing pressure vs. time obtained from the 0°, 7°, 9° and 13° wall angle tests.

Table 3. Testing results from the sealing under wall angle and thickness variation tests.

| Based Fluids | LCM blend and concentration | Discs code | Disc thickness | Wall angle (deg.) | Sealing pressure (psi) | Avg. fluid loss (ml/cycle) |
|---|---|---|---|---|---|---|
| WBF | NS 50 ppb | SS2-R | 6.35 | 0 | 3,285 | 6.9 |
| | | | | | 3,126 | 15 |
| | | | | | 2,844 | 8.1 |
| | | TS2-R7 | | 7 | 1,847 | 7.6 |
| | | | | | 1,696 | 7.5 |
| | | | | | 1,661 | 8.2 |
| | | TS2-R9 | | 9 | 1,735 | 8.6 |
| | | | | | 1,383 | 9.2 |
| | | | | | 2,017 | 8.8 |
| | | TS2-R13 | | 13 | 1,753 | 6.1 |
| | | | | | 950 | 14 |
| | | | | | 749 | 11 |
| | | SS2-T | 25.4 | 0 | 3,278 | 6.3 |
| | | | | | 3,233 | 7.3 |
| | | | | | 3,097 | 4.1 |
| | | TS2-T9 | | 9 | 1,945 | 7.1 |
| | | | | | 2,747 | 6.9 |
| | | | | | 2,334 | 6.5 |
| | | | | | 1,707 | 6.2 |
| | G & SCC 105 ppb | SS2-R | 6.35 | 0 | 3,128 | 6.2 |
| | | | | | 3,147 | 5 |
| | | | | | 2,541 | 7.1 |
| | | TS2-R7 | | 7 | 1,606 | 7 |
| | | | | | 1,603 | 5.3 |
| | | | | | 3,122 | 4.2 |
| | | TS2-R9 | | 9 | 1,293 | 6.8 |
| | | | | | 1,423 | 8.9 |
| | | | | | 1,968 | 5 |
| | | TS2-R13 | | 13 | 936 | 14.3 |
| | | | | | 1,634 | 6.5 |
| | | | | | 1,554 | 6.3 |
| | | SS2-T | 25.4 | 0 | 1,923 | 4.8 |
| | | | | | 2,107 | 6 |
| | | | | | 1,560 | 4.7 |
| | | TS2-T9 | | 9 | 2,487 | 6.8 |
| | | | | | 2,496 | 8 |
| | | | | | 3,123 | 15 |
| OBF | G & SCC 105 ppb | SS2 | 6.35 | 0 | 3,216 | 4.2 |
| | | TS2-R7 | | 7 | 3,100 | 12 |
| | | TS2-R9 | | 9 | 2,148 | 8.3 |
| | | TS2-R13 | | 13 | 1,300 | 13.8 |
| | | SS2-T | 25.4 | 0 | 3,156 | 8.6 |
| | | TS2-T9 | | 9 | 3,263 | 19 |

Table 4. Testing results from the instantaneous flow tests.

| LCM Blend and concentration | Discs code | Differential pressure: Pre-charge pressure (psi) | Sealing time (s) | Stabilized pressure (psi) | Fluid Loss (ml) |
|---|---|---|---|---|---|
| NS 50 ppb | TS2 R7 | 100 : 150 | 5.0 | 141 | 137 |
| | | | 1.0 | 147 | 35 |
| | | | 2.5 | 143 | 100 |
| | | | 2.5 | 144 | 85 |
| | | 100 : 300 | 2.5 | 261 | 175 |
| | | | 4.5 | 245 | 275 |
| | | | 3.5 | 248 | 250 |
| | | 200 : 300 | 2.0 | 287 | 120 |
| | | | 1.0 | 292 | 75 |
| | | | 1.3 | 290 | 90 |
| | | 200 : 600 | 1.5 | 547 | 110 |
| | | | 1.0 | 562 | 75 |
| | | | 1.3 | 554 | 105 |
| G&NS 40 ppb | TS15 R7 | 100 : 150 | 4.5 | 141 | 170 |
| | | | 2.5 | 145 | 85 |
| | | | 3.5 | 141 | 115 |
| | | 100 : 300 | 2.5 | 264 | 175 |
| | | | 1.5 | 277 | 110 |
| | | | 1.0 | 282 | 70 |
| | | 200 : 300 | 3.3 | 272 | 260 |
| | | | 2.8 | 272 | 225 |
| | | | 2.0 | 281 | 150 |
| | | 200 : 600 | 1.0 | 566 | 70 |
| | | | 2.5 | 502 | 225 |
| | | | 1.5 | 548 | 130 |
| G & SCC 105 ppb | TS2 R7 | 100 : 150 | 2.0 | 141 | 135 |
| | | | 2.0 | 141 | 130 |
| | | | 1.5 | 146 | 40 |
| | | 100 : 300 | 1.5 | 274 | 125 |
| | | | 5.5 | 248 | 260 |
| | | | 2.5 | 265 | 150 |
| | | 200 : 300 | 2.0 | 280 | 165 |
| | | | 1.0 | 291 | 75 |
| | | | 2.3 | 279 | 180 |
| | | 200 : 600 | 2.5 | 545 | 102 |
| | | | 1.0 | 555 | 95 |
| | | | 1.0 | 575 | 50 |

The scatter points in Figure 3 have a considerably high distribution within each group and overlap between adjacent groups. To evaluate the statistically significant difference of sealing pressure resulting from the wall angle variation, the authors applied the analysis of variance (ANOVA) using the Tukey-Kramer honest significant difference (Tukey HSD) method (Sall et al., 2001). The results revealed that the sealing pressures were significantly different between the pairs of 0°–7° and 7°–13° ($p = 0.004$ and 0.01, respectively), but not significantly different between 7°–9° and 9°–13° ($p = 0.41$ and 0.29, respectively). The overlapping difference of means between the 7°–9° and 9°–13° was suspected to not be significant because of the small difference of the wall angles between them (i.e., 2° and 4°).

Assuming that the correlation in Figure 3 is true, the straight line equation was used to calculate the sealing pressures in the case that the wall angles were varied with 1° increment. A Tukey HSD statistical analysis performed with the calculated results suggested that the sealing pressure would be significantly different between any pair of the discs with a wall angle difference of at least 5° between them. The results were also separately analyzed within the group of based fluids and LCM formulations obtaining slightly different straightt lines of the sealing pressure-wall angle relationship.

Two points of 7° angle results (broken circle) were found to have higher values deviated from the rest of the results in the same group. These results will be discussed in the Discussion section. Table 3 contains the detailed results of the 28 tests of wall angle variation. With a focus on the effect of disc thickness on the sealing pressure, a Tukey HSD statistic test showed that the sealing pressures had a positive correlation with the disc thickness among the 9° tapered slot discs ($p = 0.02$). The sealing pressures were not statistically significant between the different thicknesses of 0° slot discs.

Figure 4 shows the effect of disc thickness on sealing pressure testing in 9°, tapered slot discs (the results in detail can be found in Table 3). The 25.4 mm-thick disc had higher sealing pressure than the 6.35 mm-thick disc for all the LCM formulation and base fluids.

The instantaneous flow tests resulted in effective sealing in all 37 tests. The LCM provided effective seals with stabilized pressures dropped down from the preset differential pressures varying from 3% to 16% with the flow time ranging from 1 to 5.5

seconds. Fluid losses collected from the tests varied from 35 to 275 ml. The results validate the results obtained previously from the HPA tests in terms of LCM sealing ability (Mortadha et al., 2014b, 2014c). Table 9 contains the results of the instantaneous flow condition tests.

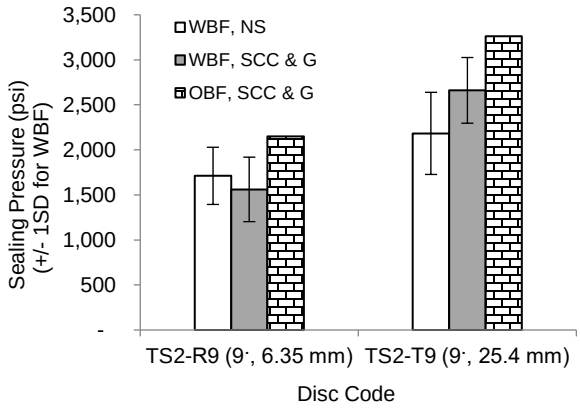


Figure 4. Sealing pressure in tapered discs with 6.35 and 25.4 mm thickness.

Figure 5 shows a scatterplot of the fluid losses volume corresponding to the four flow conditions. The Tukey HSD method showed that the fluid loss significantly increased with the differential pressure in the case of 100 psi precharged pressure ($p = 0.046$), but not significantly decreased in the case of 200 psi precharged pressure ($p = 0.43$).

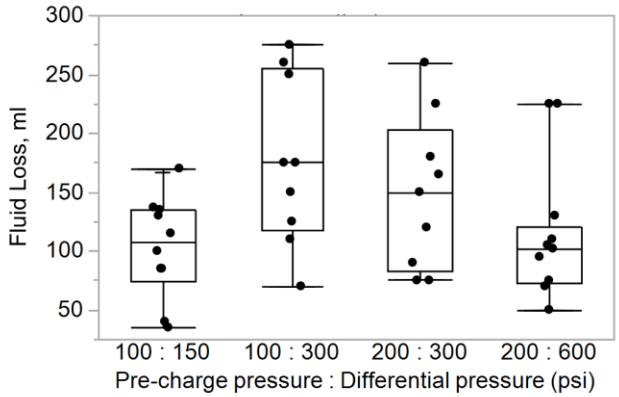


Figure 5. The plot displays fluid losses obtained from the instantaneous flow tests.

# 5. DISCUSSIONS

Figure 3–5 in the Results section confirm that significantly different results could be obtained from the different testing conditions designed and used among researchers, but before discussing further on the results of the experiment, the sealing mechanism must first be presented. Diagrams, graphs, and pictures taken from the experiments will be presented in the following discussions.

## 5.1 IMPLICATIONS FROM THE EXPERIMENT

Figure 6 a) through d) shows the seals on a straight slot disc (with 0° wall angle) compared to a 7° tapered slot disc. The seal on the straight slot could withstand injecting pressure higher than 2,500 up to 3,000 psi, while the seal on the tapered slot mostly failed to reform a seal at a pressure below 2,000 psi (Figure 3). Looking from the upstream of the flow direction, the seal on the straight slot in Figure 6 a) formed a better mound shape compared to the seal on a tapered slot in Figure 6 b); the seal on the tapered slot disc had indications of breaking and failed to rebuild. Both discs had LCM particles accumulated and formed mound shape seals covering the slot aperture and the adjacent area.

Observing the slots from the tip side, one can find that the straight slot as shown in Figure 6 c) is empty, while the tapered slot in Figure 6 d) is filled with particles down to the tip. In the straight slot disc, the coarse LCM particles larger than the slot width (2000 microns) will not pass through the slot entrance, but instead have to bridge at the entrance of the slot. In the tapered slot disc with 2000 microns width at the tip with a wider width at the entrance, the coarse particles can pass the entrance and set inside the slot where their sizes fit with the space available between the walls [Figure 6 d), f), and g)]. For both types of disc, smaller particles transported through the fracture will fail to establish a bridging structure due to the insufficient sizes. However, those small particles that pass in after the bridging process will occupy the intergranular spaces to complete the seal structure. The difference in the bridging mechanism of coarse particles provides different sealing integrity between the straight slot discs and the tapered slot discs.

Figure 6 f) and g) show a close view of the coarse particles set inside two tapered slot discs from two tests of NS and SCC formulations. The coarse particles arranged

themselves successfully as the first barrier inside the slot, being forced to move down to the tip. In Figure 6 f) and 6 g), some particles are about to leave the slot tip.

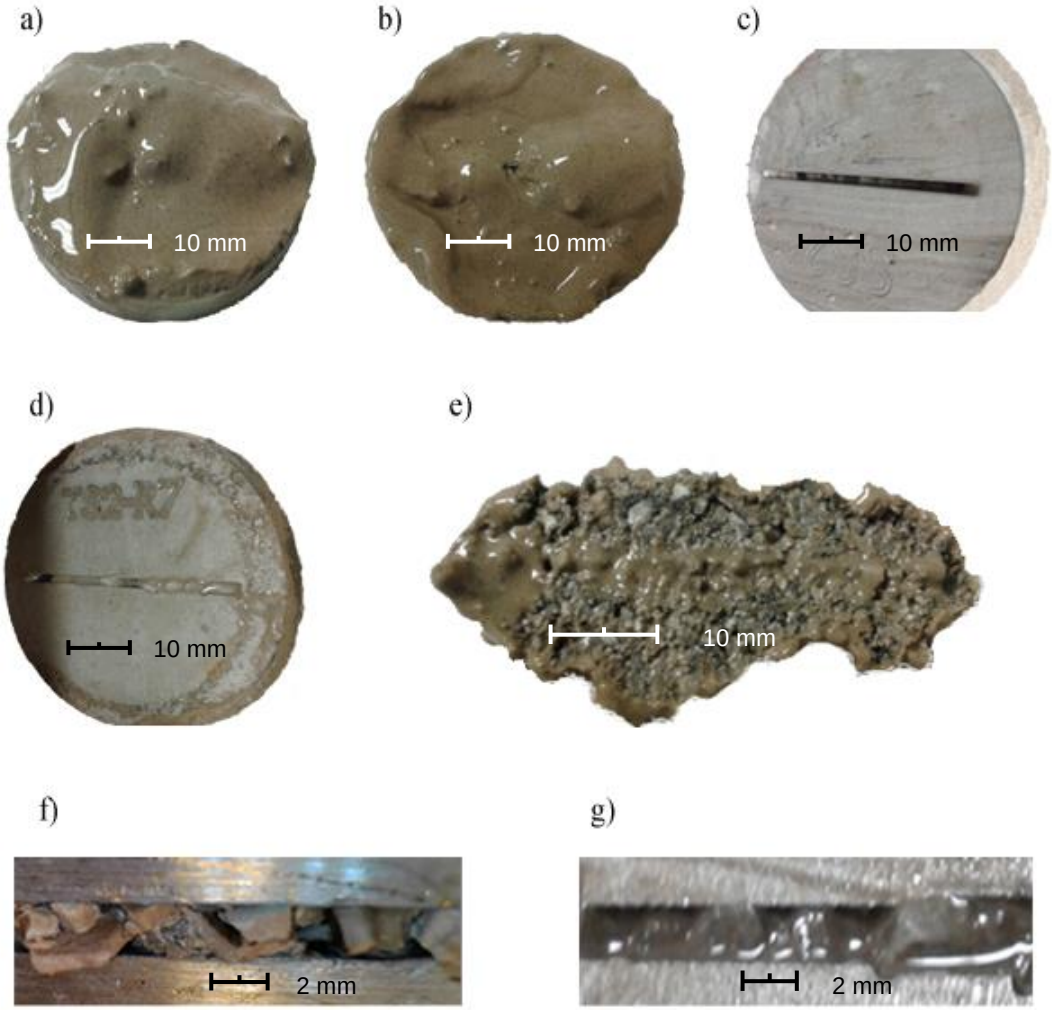


Figure 6. Seals from the straight slot and tapered slot. a) A seal formed across straight slot (SS2-R) in a mound shape. b) A seal form on a tapered slot (TS2-R7) also formed in a mound shape with a damaged point in the middle of the seal. c) LCM particles seal on the straight slot stay only on the slot mouth; they cannot be observed from the tip side. d) Coarse LCM particles settle in the tapered slot (TS2-R7) down to the tip. e) The seal removed from the straight slot reveals no coarse LCM particle passed through the slot entrance (it lost some particles sticking right at the slot mouth). f) and g) Coarse particles settle in the slot from using NS 50 ppb in WBF, and G & SCC 105 ppb in OBF, correspondingly (photos were taken from the fracture tips).

The coarse particles bridged the slot mostly in single particle row and aligned their long edge parallel to the long edge of the slot [Figure 6 f) and g)]. This behavior might be explained by their behavior during transportation. When packed into the tapered slot, the coarse particles were forced to rearrange their orientation to be more in line with the confining wall. This alignment condition caused them to require less deformation to be able to pass through the tip, correspondingly weaker in terms of load bearing capacity compared to the particles aligned in other directions, especially when the long side set perpendicular to the slot's long edge.

The bridging mechanism of the straight slot promotes consistently higher sealing integrity compared to tapered slot discs (Figure 3 in the Results section). The particles set at the entrance of the straight slot have arbitrary orientations and created stronger bridging because they need more stress to create enough deformation to fail. Some tests of the 0° slot discs might be able to withstand higher than 3,000 psi, but the tests were stopped at this point to prevent slotted disc damage.

A pair of the recorded pressures higher than 3,000 psi in two of the 7° disc tests shown in Figure 3 (inside broken circle, one from WBF and one from OBF) resulted from different sealing structures. Observation during disc removal indicated a thicker mound shape of the seal body on the disc. Instead of the bridging structure set between the tapered walls failing at a lower pressure, the bridging structures occupied more space in the slot and up on the slot entrance. This rare seal formation might be the reason why those two tests resulted in abnormally high sealing pressures compared to the results in the same wall angle.

Behind the bridging structure, more particles are needed for a complete seal development. Figure 7 shows two dried seals removed from the slot entrance area of 6.35 mm thick discs. Figure 7 a), c), and e) were taken from the seal on a 2000-microns straight slot (0°) disc, while Figure 7 b), d), and f) were taken from the seal on 2000-microns (7°) tapered slot discs. Note that some part of the seal from the tapered slot disc is missing because the particles set inside the slot were stuck tightly to the slot walls and broken off during the seal removal process.

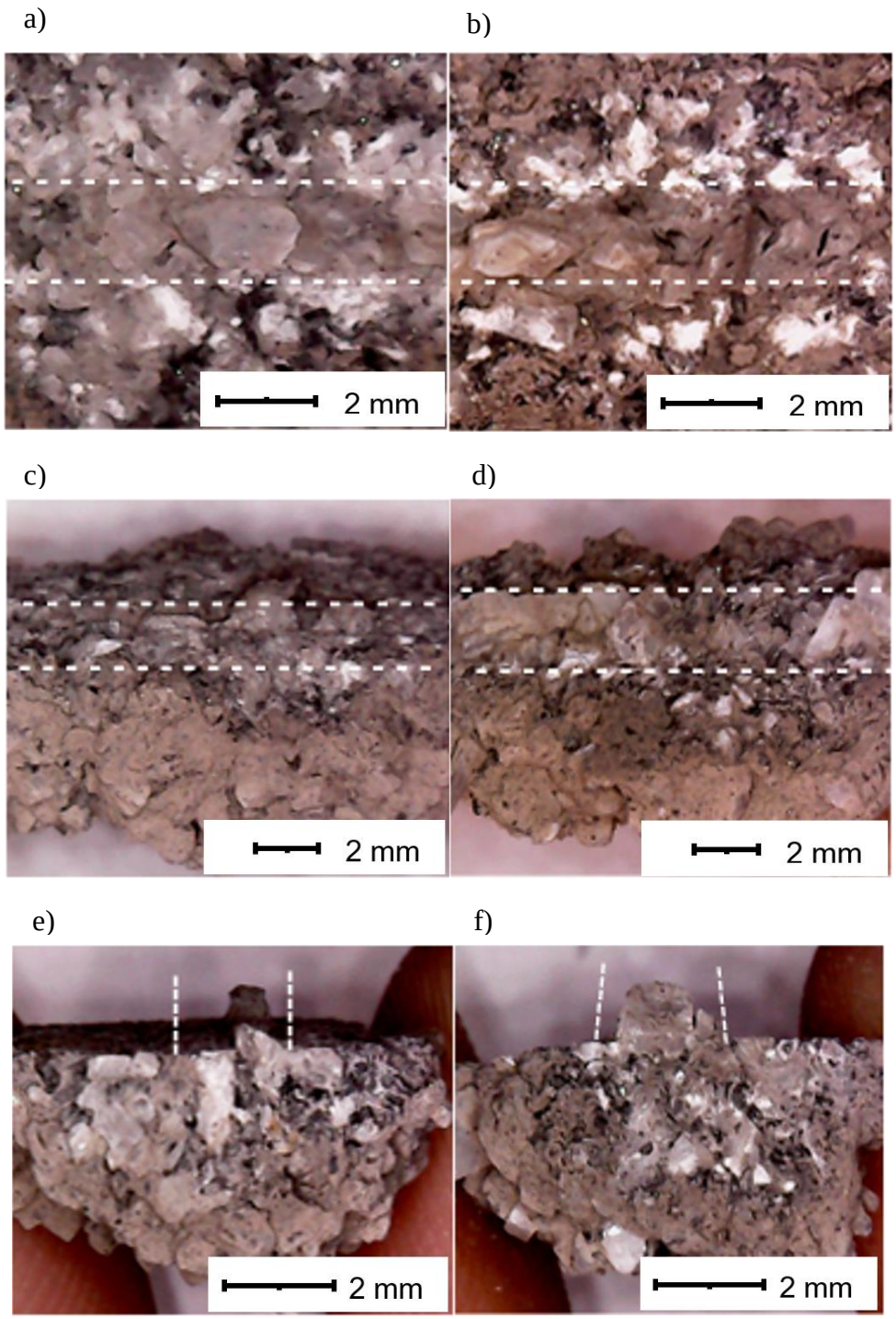


Figure 7. Seals formed on a straight slot (G&SCC 105 ppb formulation). a) top view, c) side view and e) cross-sectional view; compare to tapered slot b) top view, d) side view and f) cross-sectional view. Broken lines indicate slot opening area. Note that in Figure 7 d) and f), the sealing structure inside the tapered slot was broken off during seal removal.

These figures present how the LCM particles distribute themselves in the seals behind the bridging. The lighter color shows the compact area of a porous material forming up, which is mainly composed of larger size particles of SCC and small black spots of G particles in this case. The brown color areas consisted of the finer particles and bentonite, which packed in and filtered the fluid trying to pass through. Mostly fine particles played an important role in this layer. As shown in Figure 7 a) through 7 f), the mound shape seals developed in the straight slot and tapered slot are very similar in terms of the structure. The difference in sealing pressure between the straight slot and the tapered slot discs should be the result of the different bridging structure.

Figure 8 shows the concept of a bridge forming mechanism by a single particle and double particles on a straight slot entrance (Loeppke et al., 1990). The study presented the bridging mechanisms of coarse LCM particles settled at the fracture entrance. It also presented that if the fracture width increases from the pressure variation, the particles may move in and bridge in-between the fracture walls. Bridging can also form by single or multiple particles. All the observations carefully performed in these straight slot experiments [as shown in Figure 6 c)] agree with the concept of the bridging mechanism in Figure 8.

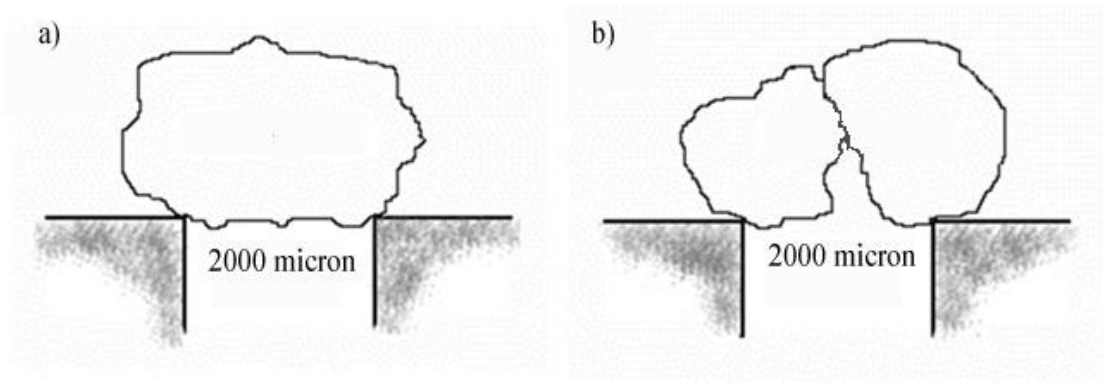


Figure 8. Bridging mechanism of LCM in straight slots at the slot entrance. a) Single particle bridging or b) double particles bridging (modified from Loeppke et al., 1990).

The bridging structure is found to be very important in the sealing mechanism. Under equilibrium conditions where the bridging structure is set inside the slot as shown

in Figure 6 f) and 6 g), the overlying finer particles cannot move through the slot if the bridging structure provided an effectively strong foundation.

At any time where the sealing structure remains at rest, the system of forces and moments must satisfy the equilibrium condition or else the system will not remain static. The summation of external forces in a three-dimensional coordinate system must be zero (Bedford & Fowler, 1998). This concept should be true for the entire sealing structure, a seal element, or a particle of interest, especially while the seal is under a stable sealing pressure.

While considering the seal as a granular system, the load acting across the slot opening area will be transferred nonuniformly via the chain-like structure connected by the contact points between the neighbor particles and the confining wall (Mehta, 2007). If the pressure downstream of the slot is negligibly small, the bodies that will equilibrate the system of the forces and moments are the slot walls where the entire load is supported. The lateral component of the forces will be distributed to the slot walls, while the axial component (parallel to the flow direction) will be transferred to the bridging structure. This component is the only one system of forces acts on the bridging particles and causes the seal failure. The bridging structure starts to carry a load immediately at the start of the bridging process, holding the structure against the flow.

The force transmitted at the points of contact are composed of normal forces and frictional (tangential) forces (Johnson, 1985). These forces support the particles to remain at rest. Regardless of a single or multiple particle types of the bridging mechanism, the balance of forces and moments will not let the bridging particles move until the load acting on the particles goes beyond the force holding the particles in place. The particle must withstand the distributed and localized stresses or they fail and move. Local deformation must not be so significant that it will affect the balance of forces and moments. Otherwise, the bridging particles will move (translate, rotate, or both) along the slot through the tip, and the sealing structure at that point will fail until the bridging structure can reform.

As shown in Figure 6, 7, and 8, a better bridging mechanism in straight slot disc is the main reason for receiving higher sealing pressure compared to tapered slot discs. Under flexural loading conditions, single or multiple particles set on the slot entrance

interlocking with the adjacent contacting particles use the slot entrance corners as the anchors for the bridge. Deformation of the bridging particles will increase the contact area, increasing stability and friction at the anchoring points and improve the overall seal integrity. The seal will fail if the bridging structure at the entrance is broken.

For particles set inside the tapered slots, no anchorage is available inside the slot. The flat walls essentially provide a weaker frictional support holding the particle in place compared to the anchor points. Under compression, the small contact areas will result in high local stress concentration at the contact points. The particles could be locally deformed or fail at the contact areas depending on the strength of the materials. The deformation or failure decreases the particle size needed to match the slot width. The bridging particles may lose the frictional support forces when they are locally damaged and shear through the tip [Figure 6 f) and 6 g)], or be broken apart due to the compressive or flexural stress within the structure.

Figure 9 illustrates how changing the wall angle affects the sealing integrity. First, increasing the wall angle increases the load acting area inside the slot, which transfers higher forces to the bridging particles. The sealing structure carries a higher load at the same differential pressure. Second, the distance between the slot walls increases with the wall angles. Increasing the space allows the coarse particles to bridge closer to the tip of the slot and increases the possibility to be pushed through the tip. These are the two main reasons for the negative relationship between the sealing pressure and wall angles shown

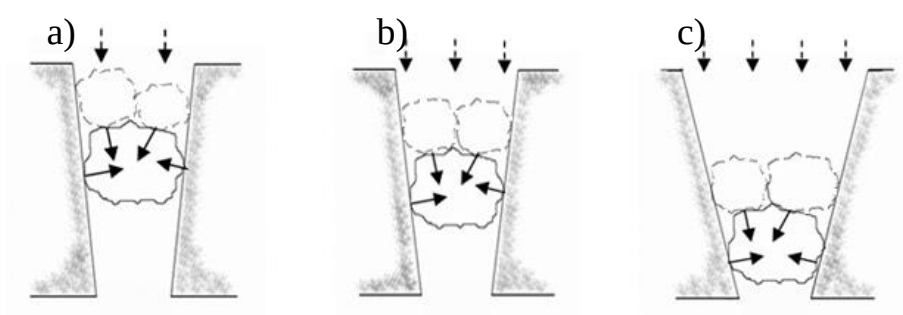


Figure 9. Possible changing in load magnitudes and orientations acts on the same front line of the bridging particles in different wall angle. a) 7°, b) 9°, c) 13°. In more inclined wall angle, the slot allows the coarse particles to set near the slot tip, causing the bridging particle more likely to be more easily sheared out through the tip.

in Figure 3. According to the experiment, the particles supporting the seal in the slot with higher wall angle would fail at a lower pressure.

Based on the observation on the seals removed from the straight slot tests, the sealing profile indicated that if LOC problems occur in parallel plane fractures cured by using LCM with coarse particles larger than the fracture entrance, the bridging process is essentially formed at the fracture entrance on the borehole wall. Even though this kind of seal performs a strong barrier capable of holding back a high pressure, the bridging set at the fracture entrance might not be preferable compared to the bridging inside the fracture. The seal on the fracture entrance could be removed out by the drill string or downhole tools. It would be hard to reinitiate the bridging without the coarse particles available in the system. In the case of tapered fractures, some of the bridging structure occupied inside the fracture will remain in place even though the outer part of the (mound shape) seal may be removed. The seal should be able to reform itself because fine particles are usually available in the drilling fluids. Reforming of the seal from a bridging structure is easier than starting over in the open fractures.

Figure 10 a) and c) show how NS forms a seal on a 6.35 mm-thick disc while Figure 10 b) and d) show a seal on a 25.4 mm-thick disc. Both discs have a wall angle of 9° and tips of 2000 microns. The LCM filled up from the slot tip and formed a mound on the 6.35 mm-thick disc while it stayed only inside the slot of the 25.4 mm-thick disc.

The reason for the different sealing profiles is that the space available inside the two types of discs are different. The thinner discs have insufficient space to allow the LCM to develop a strong seal by staying inside the slots compared to the thicker one. After the coarse particles bridge the open area and some finer particles are transported in to fill in the void spaces during the seal development, the thin discs are filled with LCM before a strong seal is completely developed. In other words, the seals are still permeable while the spaces inside the slots are running out. As injection continues, smaller and finer particles will accumulate until a complete seal is developed. This process creates the mound shape seals on the surface of the 6.35 mm-thick discs.

Figure 10 e) and f) show the LCM placement profile obtained from a test in the 25.4 mm-thick disc. These figures might be used to explain why 25.4 mm-thick discs perform better than 6.35 mm thick discs (Figure 4). The seal of the 25.4 mm-thick disc

formed completely inside the fracture with a thicker wedge or trapezoidal cross-sectional shape. Because there is more depth for the force chain development, the seal can transfer the load to the slot wall more effectively along the deep seal profile, resulting in less load acting on the bridging structure compared to the seal in 6.35 mm-thick discs. The difference in sealing mechanism provides the difference in sealing pressure between the thin discs and the thick discs. The layers of the coarse, medium and fine particles appear in Figure 10 e) and 10 f). The particle arrangement in this study is similar to the fracture plugging idea of Kageson-Loe et al. (2009), even though the article presented the sealing of fractures in permeable formations.

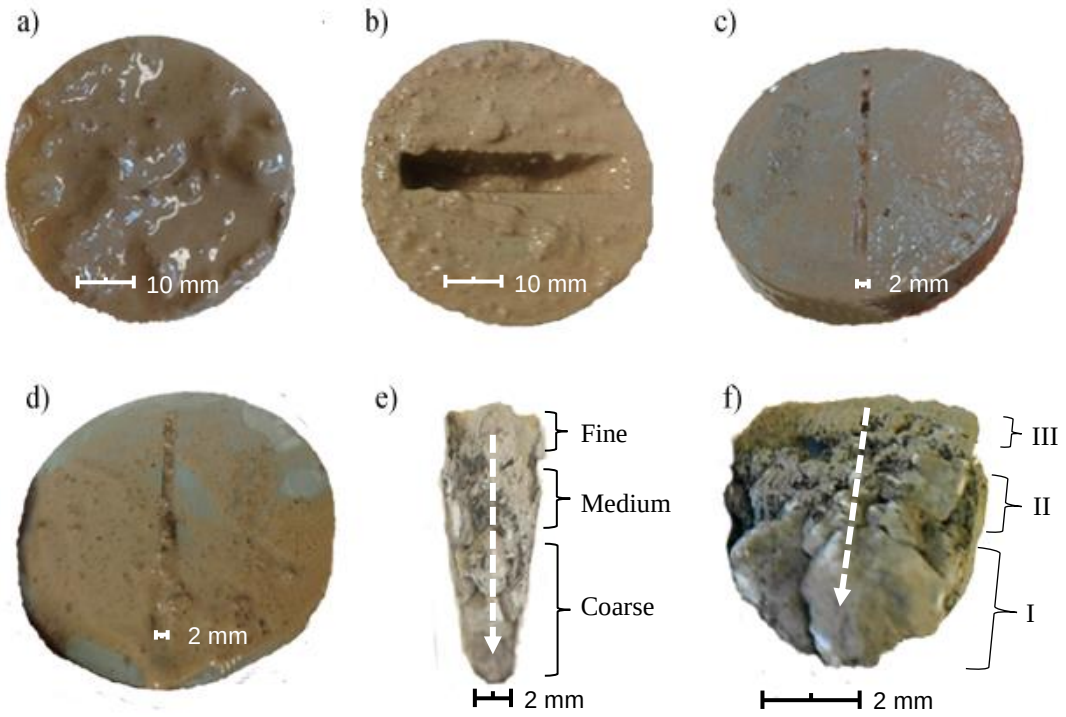


Figure 10. Comparison of seals on 6.35 mm and 25.4 mm thick discs. a) Seal on a 6.35 mm thick disc, b) Seal developed in a 25.4 mm thick disc formed a wedge shape inside the slot. c) Coarse particles remained at the end of the tip in 6.35 mm thick disc, and d) 25.4 mm thick disc. e) Close cross-sectional view of the wedge shape seal shows the grains sequence along the flow direction (broken line). f) Side (inclined) view of the same piece as e) shows the three regions of LCM settlement with respect to the flow direction (broken line), I-the bridging structure, II-filling medium particles and III sealing-off with fine particles and the filter cake.

From the results of the instantaneous flow tests, LCM sealing behavior can be linked to the sealing mechanism in the tests with the 25 ml/min injection rate. Figure 11 a) shows plots of pressure behavior attained from three successfully sealed tests under instantaneous flow conditions. A fail test plot also is presented at the bottom of the graph in Figure 11 a). It was additionally run using a formulation with an insufficient PSD in respect to the fracture width to verify the sealing inability under the rapid flow condition. The flow did not stop from seal development in the fracture, but instead from the insufficient supply of the injecting fluid. The failed test resulted in a lower pressure curve compare to the successful ones.

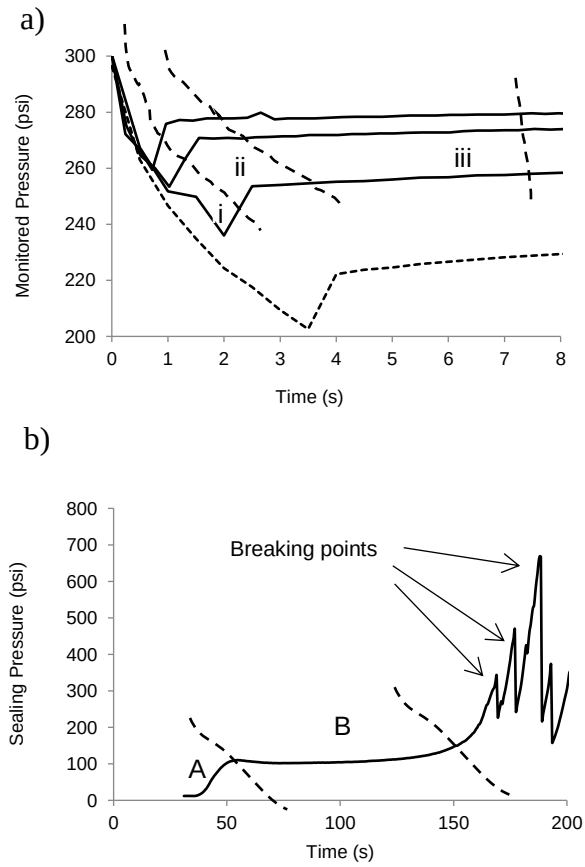


Figure 11. Comparison of the plot from the instantaneous flow tests and a slow injection test. a) The plot shows three regions of monitored pressures from three instantaneous flow tests. The bottom broken line is an intentionally failed test where the flow stops due to an insufficient amount of drilling fluid. b) The pressure plot obtained from one of the slow injection tests can also be divided into the first two regions of seal forming.

Conceptually, the three (successful tests) pressure curves in Figure 11 a) can be divided into three different regions demonstrating the sealing mechanism. The first region (i) displays rapid decreasing of the upstream pressure, indicating the sample (drilling fluid and LCM mixture) suddenly flows through the slot at a high flow rate. At this point, some coarse particles are moving into the bridging positions, but not affect the flow rate. The second region (ii) is where the pressure curves suddenly buildup, representing a rapid flow restriction, the reduction of the flow area, due to the bridging structure formation. The smaller particles following the coarse particles also promptly accumulate on the seal. The third region (iii) is where the pressure slowly increases until it reaches a stabilized (equilibrated) pressure. It is a complete-compaction region where fine particles seal off the tiny pore spaces. These graph regions provide the link to the procedure of sealing mechanism.

The same process also can be observed from the HPA tests shown in Figure 11 b) where Region (i) and (ii) are denoted as A and B area, respectively. The difference is that HPA tests are conducted at a much slower pace and no stabilized pressure can be established because the continuous injection will bring the pressure up until the seal is broken. As a result of injecting pressure fluctuation, Region (iii) cannot be seen in Figure 11 b). These chronological processes represent the nature of the sealing mechanism.

Figure 12 shows a seal removed from a wall angle test terminated at approximately 3,000 psi sealing pressure. Close observation reveals that it consists of three layers. These layers formed correspondingly to the same sealing procedure as obtained from the pressure response analysis in Figure 11 a).

The coarse particles (some are missing due to being stuck in the slot while removing process) developed a bridging structure, as shown in Region I. As these particles bridged on the seal, they decreased the permeability of the slot significantly, from flow through the open channel to flow through porous media. Following the bridging process, smaller particles as shown in Region II would be transported in by the flow stream filling the void spaces, which were the flow paths. Note that bentonite was washed away by clean drilling fluid filtrate, resulting in a lighter color in Region I and II, and revealing clear black spots of graphite particles. This observation shows that the

structure behaves like a porous media where filter cake could develop on its surface. The three regions can be seen clearly in Figure 7 e), 7 f) and Figure 10 e), 10 f).

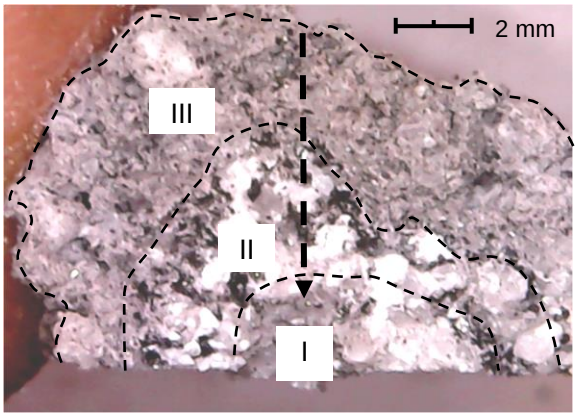


Figure 12. A cross-section view of a seal. Region-I (coarse particles), Region-II (smaller particles), and Region-III (much finer particles) arranged themselves as a strong seal. The broken arrow displays the flow direction.

In Region III, finer particles arbitrarily mixed with coarser particles accumulated on the seal. This region reduces the rate of fluid flow until the thin filter cake formed at the outer of the area boundary. This step is connected to the third region of the pressure response curve [Figure 11 a)]. In this HPA test, the pump was shut down at about 3,000 psi; the slot was sealed off, and the pressure was stabilized similar to the stabilized pressure in the instantaneous flow tests.

The discussion above supports the chronological forming idea of sealing mechanism on the fracture mouth or inside the slot. The presence of the LCM particles' settling sequence combined with pressure behavior reveals the sealing process, which can be divided into three phases: bridging, filling, and sealing. This idea agrees with a previous study stating that "large grains of LCM plug the throat and smaller grains fill the gaps" (Mostafavi et al., 2011). In this study, the particles arrangement with time was additionally presented with the fact that the fine particles not only fill the gaps between larger particles but also shut off the communication between fluids of both sides of the seal by making it impermeable.

## 5.2 SEALING MECHANISM APPLIED TO LCM TREATMENT

Sealing in severe lost circulation must start with a bridging process, as this step will change the situation from high flow rate out through opening channel of fracture, reducing to a slower seepage flow through a strip of human-made porous media. In this phase, the sufficiently strong flow with high energy transports coarse particles into the slot. Particles slightly larger than the fracture width will stop at the set points where the sizes of particles agree or match with fracture width (Alsaba et al., 2016).

After the bridging structure develops, filling the void space can occur under a slower flow condition. Governed and directed by the stream of flow, smaller particles follow the flow path towards the pore spaces. The small particles settle into the pore space instead of being transported freely through the slot. The small particles will decrease the seal permeability to a small value. The pressure drop across the seal will be higher as the flow area decreases significantly. Only tiny pore throats are left after this process.

The last step in the sealing mechanism is to seal off the tiny pores. Fine to very fine solid particles will develop a very low permeability filter cake. The fracture will be completely sealed and the structure will stay in equilibrium if the pressure stays stable below the sealing integrity.

This experiment started with knowing the slot width beforehand. The LCM formulation was effectively selected to ensure that the coarse particles will seal the slot opening because the sizes of the coarse particles are bigger than the slot entrance or the tip width. These tests confirm that knowing the fracture width is very important in terms of LCM selection and design that can lead to success in the laboratory and field applications.

In instantaneous flow experiments, the LCM forms a seal as a response to the driving differential pressure. Once the seal forms, a stabilized pressure develops similarly to the sealing under a constant bottomhole condition. The difference is that the stabilized pressure is slightly lower than the preset differential pressure due to energy lost during seal forming. During the tests, one test for each flow condition was randomly run to confirm the seal integrity. By closing the gas accumulator valve and using a syringe pump to inject drilling fluid into the system, the pressure response could be recorded with time.

All results from the tests proved that the seals were strong enough to withstand injecting pressure higher than the preset differential pressures.

Figure 13 shows the pressure response of a seal integrity test performed after sustaining a stabilized pressure from an instantaneous flow test. The bladder accumulator valve was closed, and the syringe pump injected the mud at 25 ml/min flow rate. The pressure built up and dropped with time similarly to the results from HPA tests in Figure 2, i.e., build up and break down in a cyclical behavior with higher peak pressures. This behavior shows that LCM can form a strong seal with the seal integrity higher than the driving differential pressure. The seals should be able to reform and adjust themselves under the pressure fluctuation with a relatively constant fracture width fracture, as long as the LCM with proper concentration and size distribution is still available in the system. However, further study is required for the case that the fracture width is changing with the bottomhole pressure.

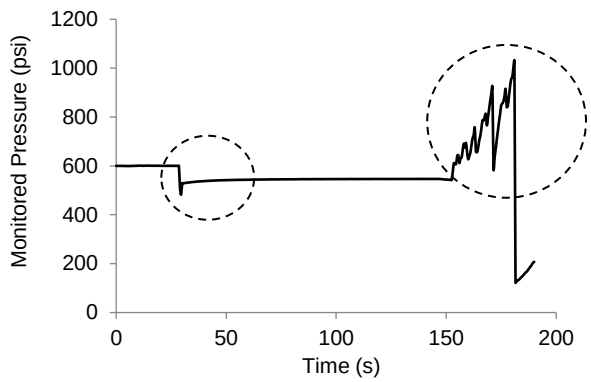


Figure 13. The plot shows the instantaneous flow test (small broken circle) and the response pressure from a seal integrity test (big broken circle) after the pressure stabilized. Injection resulted in pressure built up similar to the graph in Figure 2.

The results of instantaneous flow tests presented in Figure 5 show that trends of the fluid loss volume varied with the differential pressure under different precharge pressure. The different initial flow velocity, the change in driving pressure, and the flow velocity with time from the gas expansion strongly affect the amount of fluid spent during

the seal formation. Further study is required to understand the behavior of LCM under these flow conditions compares to the actual subsurface flow.

## 6. CONCLUSIONS

- Different wall angle testing discs result in different measured sealing integrity. Increasing the wall angle tends to decrease the maximum sealing pressure. From this study, the sealing pressure can be significantly different if the wall angle was varied by 5° or more.

- No correlation was found between the averaged fluid loss per cycle of seal initiation and the wall angle or thickness variation.

- Increasing disc thickness in 9° tapered slot discs from 6.35 mm to 25.4 mm resulted in higher sealing pressure due to the improvement of the bridging structure formed inside the slot.

- Shape and dimensions of the tapered slot discs strongly affect the seal integrity. This observation implies that the same effects could also happen with the fractures under the actual subsurface conditions, likely much-complicated environment.

- LCM formulations used to perform a strong seal in HPA tests also sealed the fracture effectively under the instantaneous flow condition. The results confirm the HPA approach measuring the maximum sealing pressure for LCM evaluation.

- The pressure behavior with time and the arrangement of LCM particles in the seal help understand how LCM works during seal development. Observation shows that the seals consist of three layers performing different tasks in the sealing mechanism.

- The experimental setup can change the results of the experiment, so caution should be taken when quantitatively comparing LCM tests on slot disks from different experiment setups.

## ACKNOWLEDGEMENT

The authors would like to acknowledge Det Norske Oljeselskap ASA (now Aker BP ASA) for the financial support for the research group; and Mortadha T. Alsaba (PhD) and Mohammed F. Al Dushaishi (PhD) for their help in experiment design and the statistical analysis.

**REFERENCE**

Almagro B, Frates C, Garand J & Meyer A (2014). Sealing fractures: Advances in Lost Circulation Control Treatments. Oilfield Review Journal, 26(3), pp. 4–13.

Alsaba M T, Nygaard R, Hareland G & Contreras (2014a). Review of Lost Circulation Materials and Treatments with an Updated Classification. In: the AADE Fluids Technical Conference and Exhibition, Houston, Texas, 15–16 April. http://www.aade.org/technical-papers/2014-fluids-conference-paper/.

Alsaba M T, Nygaard R, Saasen A & Nes O-M (2014b). Lost Circulation Materials Capability of Sealing Wide Fractures. In: the SPE Deepwater Drilling and Completions Conference, Galveston, Texas, 10–11 September. doi: 10.2118/170285-MS.

Alsaba M T, Nygaard R, Saasen A & Nes O-M (2014c). Laboratory Evaluation of Sealing Wide Fractures Using Conventional Lost Circulation Materials. In: the SPE Annual Technical Conference and Exhibition, Amsterdam, The Netherlands, 27–29 October. doi: 10.2118/170576-MS.

Alsaba M T, Nygaard R, Saasen A & Nes O-M (2016). Experimental Investigation of Fracture Width Limitations of Granular Lost Circulation Treatments. Journal of Petroleum Exploration and Production Technology, 1-11. doi: 10.1007/s13202-015-0225-3

Bedford A, Fowler W (1998). Engineering Mechanics: Statics, Addison-Wesley, second edition, pp.109, 499.

Canson B E (1985). Lost Circulation Treatments for Naturally Fractured, Vugular, or Cavernous Formations. In: SPE/IADC Drilling Conference, New Orleans, Louisiana, 6–8 March. doi: 10.2118/13440-MS.

Hettama M, Horsrud P, Taugbol K, Friedheim J, Huynh H, Sanders M W & Young S (2007). Development of an Innovative High-Pressure Testing Device for the Evaluation of Drilling Fluid Systems and Drilling Fluid Additives within Fractured Permeable Zones. In: the Offshore Mediterranean Conference and Exhibition, Ravenna, Italy, 28–30 March.

Howard G C & Scott P P (1951). An Analysis and the Control of Lost Circulation. In: the Annual Meeting of the ATME, Missouri, 19–21 February. doi: 10.2118/951171-G.

Johnson K L (1985). Contact Mechanics, Cambridge University Press, pp. 1-5.

Kageson-Loe N, Sanders M W, Growcock F, Taugbøl K, Horsrud P, Singelstad A V & Omland T H (2009). Particulate-Based Loss-Prevention Material--The Secrets of Fracture Sealing Revealed! In: the IADC/SPE Drilling Conference, Orlando, Florida, 4–6 March. doi: 10.2118/112595-PA.

Kefi S, Lee J C, Shindgikar N D, Brunet-Cambus C, Vidick B & Diaz N I (2010). Optimizing in Four Steps Composite Lost-Circulation Pills Without Knowing Loss Zone Width. In: the Asia Pacific Drilling Technology Conference and Exhibition, Ho Chi Minh City, Vietnam, 1–3 November. doi: 10.2118/133735-MS.

Kumar A, Savari S, Jamison D E & Whitfill D L (2011). Lost Circulation Control and Wellbore Strengthening: Looking Beyond Particle Size Distribution. In: AADE National Technical Conference and Exhibition, Houston, Texas, 12–14 April.

Loeppke G E, Glowka D A & Wright E K (1990). Design and Evaluation of Lost-Circulation Materials for Severe Environments. SPE Journal of Petroleum Technology, March. 328-337. doi: 10.2118/18022-PA.

Mehta A. (2007). Granular Physics, Cambridge, pp. 233-237.

Mostafavi V, Hareland G, Belayneh M & Aadnoy B S (2011). Experimental and Mechanistic Modeling of Fracture Sealing Resistance with Respect to Fluid and Fracture Properties. In: the US Rock Mechanics / Geomechanics Symposium, San Francisco, California, 26–29 June.

Nayberg T M (1986). Laboratory Study of Lost Circulation Materials for Use in Both Oil-Based and Water-Based Drilling Muds. SPE Drilling Engineering, September. doi: 10.2118/14723-PA.

Salehi S & Nygaard R (2012). Numerical Modeling of Induced Fracture Propagation: A Novel Approach for Lost Circulation Materials (LCM) Design in Borehole Strengthening Applications of Deep Offshore Drilling. In: the SPE Annual Technical Conference and Exhibition, San Antonio, Texas, USA, 8–10 October.

Sall J, Lehman A & Creighton L (2001). JMP® Start Statistics, Duxbury, pp. 171-193.

Scott P P & Lummus J L (1955). New Developments in the Control of Lost Circulation. In: the Annual Fall Meeting of the Petroleum Branch of the American Institute of Mining and Metallurgical Engineers, New Orleans, 2–5 October. doi: 10.2118/516-G.

White R J (1956). Lost-circulation Materials and their Evaluation. In: the Spring Meeting of the Pacific Coast District, Division of Production, Los Angeles, May.

Whitfill D (2008). Lost Circulation Material Selection, Particle Size Distribution and Fracture Modeling with Fracture Simulation Software. In: IADC/SPE Asia Pacific Drilling Technology Conference and Exhibition, Jakarta, Indonesia, 25–27 August.

Xu C Y, Kang Y-l, You L-j, Li S & Chen F (2014). High-Strength, High-Stability Pill System To Prevent Lost Circulation. In: the International Petroleum Technology Conference, Bejing, China, 26–28 March. doi: 10.2118/172496-PA.

# II. EFFECT OF TESTING CONDITIONS ON THE PERFORMANCE OF LOST CIRCULATION MATERIAL: UNDERSTANDABLE SEALING MECHANISM


## ABSTRACT

Lost circulation materials (LCM) are added to drilling fluids to mitigate or prevent lost circulation (LOC) problems. Designing the fluid requires a good understanding of sealing mechanisms and all the parameters affecting the sealing performance. Laboratory testing apparatuses are the key concept for LCM evaluation ensuring that the field applications will succeed.

The high-pressure cylindrical test cell containing simulated fracture discs is an effective tool among the broadly-designed apparatuses. A variety of LCM physical properties has been studied to develop effective LCM formulations for overcoming the problems. Recently, the testing conditions such as the slot wall angles, the fracture disc thickness have significant effects on the evaluation results. However, the effect of the base fluids, fluid density, types of weighting materials and aging conditions on the sealing ability have not been truly addressed.

In this study, two different base fluids, water-based fluids and oil-based fluid were used to compare the base-fluid effect. Drilling fluid density was raised up using barite and/or hematite to investigate the effect of weight agents. Barite was sieved and tested to study the effect of fine particles on the sealing. Finally, the dynamic aging tests were conducted in LCM-treated WBF using two temperature levels (200 °F and 400 °F) and two aging periods (24 and 72 hours).

The results showed that the effect of base fluids on sealing performance depended on LCM properties providing the complex interaction between the solid particles and the fluids. Adding weighting agents tended to improve the seal integrity. Adding proper size of fine particles improved the sealing performance of the used formulations. Aging conditions affected LCM properties depending on the thermal stability of the materials.

## 1. BACKGROUND

Lost circulation (LOC) is a challenge for many drilling operators. It significantly increases drilling expenses due to the loss of massive amounts drilling fluids and potentially loses expensive downhole equipment or even the entire well section (Howard and Scott 1951; Clapper et al. 2011; Almagro et al. 2014; Alsaba et al. 2014a; Ghalambor et al. 2014). The problem also consumes some valuable time spent for regaining the circulating system and solving subsequence problems known as the nonproductive time (NPT) (Salehi et al. 2012; Almagro et al. 2014; Feng et al. 2016). The serious concern is that LOC can lead to a well control issue, which can potentially lead to a life-threatening blowout accident (Horn 1950; Kaageson-Loe et al. 2009).

The industry usually performs operations classified as either preventive or corrective approach to eliminate LOC problem (Whitfill and Miller 2008; Kumar and Savari 2011; Ghalambor et al. 2014; Feng et al. 2016). The differences between the approaches are the treatments taken before the main problem occurs as prevention, or after the serious LOC detection as the loss mitigation. Regardless the method of solving, lost circulation materials (LCM) blended with drilling fluids is a common solution for the problems (Robinson 1940; White 1956; Canson 1985; Bourgoyne et al. 1986; Fuh et al. 1992; Alsaba et al. 2014a). The materials might be dispersed in the active system or placed as a concentrated mixture against the loss zones (Clapper et al. 2011; Almagro et al. 2014). Proper selection and design process of the LCM treatment is vital to the success of the problem-solving processes.

Laboratory studies were continuously and comprehensively run to understand how LCM works, how to evaluate the performance, and how to improve the sealing ability in the field application (Scott and Lummus 1955; Abrams 1977; Nayberg 1986; Dick et al. 2000; Hettema et al. 2007; Kaageson-Loe et al. 2009; Kefi et al. 2010; Clapper et al. 2011; Alsaba et al. 2014b; 2014c; 2016). The knowledge of the sealing behavior, capability and limitation help select and design for the proper LCM raw materials, blending, and treatment processes to be applied in the field operations. The testing results also gain confidence that the sealing would successfully seal at the loss spots as in the test cells.

As the laboratory studies were conducted to overcome LOC problems, testing apparatuses with similar sealing surroundings as in the loss formations were developed to simulate the environment so that the tests represented the actual sealing process as close as possible. To search for the desirable materials and formulations, various LCM types with different physical properties and blending were tested in the developed apparatuses depending on the objective of the investigations (Alsaba et al. 2014b, 2014c; Hettama et al. 2007; Loeppke et al. 1990; Scott and Lummus 1955).

Focusing on fracture sealing in the impermeable rock matrix, Alsaba et al. (2014c, 2016) presented the effects of LCM type, shape, concentration, particle size distribution (PSD), and temperature on the seal integrity with respect to differential pressure at different fracture widths. It was found that LCM can effectively seal the fractures if the D90 value is equal to or slightly larger than the anticipated fracture width; however, the size of conventional LCM particles is limited by the risk of plugging the downhole tools. The irregular shapes of LCM particles with the ability to deform of LCM particles under pressure promoted the sealing integrity. Increasing of the treatment concentration was found to improve the sealing ability within an optimum range, while the broad-range sorting of PSD was needed for a good sealing performance. The effect of fracture width was found to agree with the D90 requirement, and LCM swelling property under higher temperature improved the sealing ability in an LCM formulation.

Jeennakorn et al. (2017) conducted further laboratory investigation on the effect of changing the slot wall angle, the disc thickness, and the instantaneous flow condition on the sealing efficiency. The experiment showed that increasing the slot wall angle tended to decrease the sealing pressure. Increasing simulated disc thickness in taper slot discs improved the sealing pressure. The study provided some ideas about the effect of testing conditions that change the testing results and should be considered in LCM sealing evaluation. Observation during the experiment provided more understanding about the bridging and sealing mechanism.

The objective of this study, as a continuous work, is to investigate the effect of the missing testing conditions: the effect of the base fluids, drilling fluid density, weight material types, PSD of weighting materials, and the dynamic aging condition. The

experiment was continuously run using the high-pressure LCM tester as an evaluation method (Alsaba et al. 2014 b, 2016).

## 2. EXPERIMENTAL METHODOLOGY

### 2.1 TESTING APPARATUS

The experiment was conducted using the high-pressure LCM tester (Figure, **1**) in conjunction with tapered slots that simulate different fracture width ranging from 1000 to 2000 microns (Table 1). The apparatus consisted of four main components: a plastic accumulator used to transfer the drilling fluids to the metal accumulator, a metal accumulator used to inject the drilling fluids into the cell, the testing cell that can be pressurized up to 10,000 psi, and a high-pressure syringe pump.

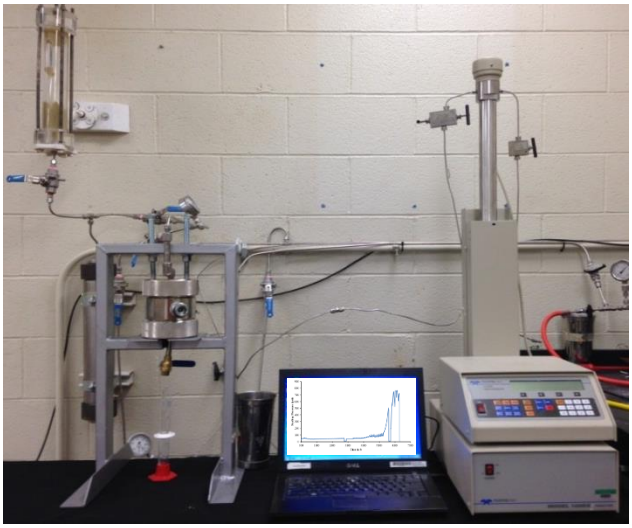

Figure 1. High-pressure LCM testing apparatus (Alsaba et al. 2014b).

Table 1. Tapered slots specifications.

| Disc Code | Diameter (inches) | Thickness (inches) | Slot Aperture (microns) | Slot Tip (microns) |
|---|---|---|---|---|
| TS1-R7 | 2.5 | 0.25 | 2500 | 1000 |
| TS15 R-7 | 2.5 | 0.25 | 3000 | 1500 |
| TS2-R7 | 2.5 | 0.25 | 3500 | 2000 |

Fluids containing LCM treatment are forced to pass through the known fracture width by injecting fluids at a flow rate of 25 ml/min using the attached Isco$^{TM}$ pump. Injection continues through the initiation of the seal until a rapid increase in the pressure is observed, which indicates fracture sealing. Once the fracture is sealed, fluids are further pressurized until a significant drop in the pressure is observed due to breaking or leakage of the formed seal. Figure, **2** shows an example of the plot of pressure with time; the maximum sealing pressure is the parameter of interest.

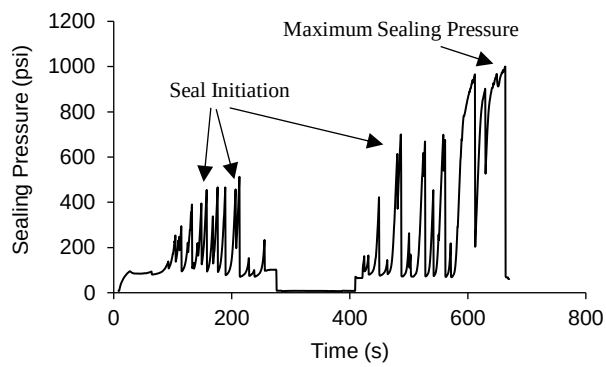


Figure 2. Pressure vs. time plot obtained from a test using 30 ppb G & SCC mixed with 14.5 ppg OBF using 1000 microns fracture width. The maximum pressure would be recorded as the sealing pressure.

## 2.2 DRILLING FLUID AND ADDITIVES

Two types of drilling fluids were used in this experiment: water base fluid (WBF) and oil base fluid (OBF). The WBF consists of 7% (by weight) bentonite in 93% fresh water, 8.6 ppg. The WBF might be weighted up with barite or hematite to get a required density of the testing program before mixing with a specific LCM formulation and concentration.

The OBF was a ready-mixed environmental-friendly drilling fluid supplied by an oil company with a density of 11 ppg. It is known that the original OBF was mixed and contained some amount of barite. To get a lower desired density, the 11 ppg OBF was diluted by adding the based oil (6.3 ppg). To get a higher density, as in the case of WBF, the 11 ppg OBF would also be weighted using barite or hematite.

In this experiment, the effect of base fluid was investigated using two sets of testing where the drilling fluid density for each pair of base fluid was kept constant. The first set of tests using the 7% bentonite WBF and the diluted OBF at a density of 8.6 ppg was tested to compare the results. Some of the available testing results from the previous study using WBF (Alsaba et al. 2014a, 2014b) were brought in for the comparison. In the second set, OBF at the original density of 11 ppg and the WBF raised up to 11 ppg using barite were used. Both sets of 8.6 ppg and 11 ppg drilling fluids were treated with three different formulations of LCM before being tested in the HPA. The sealing pressures were then used as an indicative variable to study the effect of base fluid on LCM slot sealing performance.

For the effect of drilling fluid density on the sealing pressure, the drilling fluid densities for both WBF and OBF were adjusted to be six different densities varying from 8.6 ppg to 16.5 ppg. The WBF was simply weighted up from 8.6 ppg using barite, while the OBF was either diluted with the base oil or barite was added to get the desired densities. The blending of graphite and sized calcium carbonated (G & SCC) with a concentration of 30 ppb was used for each sample treatment before being tested in the HPA. The difference in the sealing pressure would indicate the effect of increasing the drilling fluid density on LCM treatment effectiveness.

To study the effect of using different weighting materials, hematite was introduced into the experiment. Along with barite, hematite was added to the density of OBF (11 ppg) or WBF (8.6 ppg) samples to get a density of 12.5, 14.5, and 16.5 ppg. Then, the drilling fluid samples were treated with 30 ppg G & SCC blend and tested in the HPA. Comparing the same base fluid and density, the effect on sealing ability of different weighting material can be observed.

When sieving the barite and hematite, the results were slightly different from what was stated in API specification due to the very fine particles tended to stick with the coarse particles; however, the results presented that hematite contained much finer particle compared to barite. The used weighting materials both came from a reliable manufacturer and met API specification, so it was used for the analysis instead of the sieving results.

By API Specification 13A – 8.1.2 to 8.1.2, drilling grade hematite produced from ground hematite ores will have residue particle sizes greater than 45 microns at a maximum mass fraction of 15% (and greater than 75 microns no more than 1.5% mass fraction), while the particles smaller than 6 microns will have a maximum mass fraction of 15%. This information implies that at least 70 % mass fraction of the hematite particles are between 6 to 45 microns. One of the previous studies showed that decreasing the particle sizes improves the weighting materials' suspending properties (Xiao et al. 2013). Hematite particles need to be ground finer to get higher surface area per volume (or mass) for easier suspension in the drilling fluids and prevention of sagging problems during circulation.

The effect of fine particles of weighting materials on the sealing ability was validated through an investigation. The 11 ppg OBF used some sieved barite with different ranges of particle size were tested after mixing with LCM. In this paper, both the LCM and the weighting agent underwent PSD analysis. API Specification 13A – 7.1.1 states that the standard drilling grade barite products should have residue particles greater than 75 microns at a maximum mass fraction of 3% and particle sizes less than 6 microns at a maximum mass fraction of 30%. Barite particles ranged from 6 to 75 microns can be approximately 67% mass fraction (or more).

To get the different grade of barite to be mixed with the drilling fluids, the barite was sieved to get three ranges of particle size: course (C), medium (M), and fine (F). The C particles were larger than 90 microns (remaining on sieve #170). The M particles were equal to or smaller than 90 microns but larger than 50 microns (passing through sieve #170 but remaining on sieve #270). The F particles were 50 microns or finer (passing through sieve #270). Compared to the specification of hematite above, F barite particles (50 microns or finer) are very close in size compared to many of the hematite particles (45 microns or finer). Even though using this separating method could not ensure that smaller particles will not remain with the larger one, the fineness grade of the particles in this experiment was efficiently controlled for the smaller sizes, especially in the F sample.

The result of using the ordinary (no sieve) barite would be available from the effect of density tests; three samples of 12.5 ppg OBF were additionally prepared. They

were weighted up to be 12.5 ppg by adding each range of sieved barite, C, M, or F, respectively. The 12.5 ppg fluid samples were treated with G & SCC at 30 ppb concentration before being tested in the HPA. The effect of weight agent particle sizes was then achieved by comparing the four sealing pressure results.

Aging tests using aging cells heated in a roller oven were performed to inspect the effect of aging conditions on LCM sealing performance. WBF treated with three different LCM formulations was load into the aging cells and placed in the hot rolling oven at a predetermined temperature. After reaching the aging time, the sample was left to cool down to room temperature before testing in the HPA to get the sealing pressure as a performance indicator. The tests were run following the procedure provided in the manufacturer's aging cell instruction manual (OFITE 2013).

### 2.3 LCM FORMULATIONS

Table 2 shows the formulations in ppb used in this paper. Seven formulations of LCM were used in this experiment. The blending concentration is shown in pound per barrel (ppb). The specification of each ingredient is indicated by the D50 values as obtained from the materials data sheet provided by the manufacturers.

Table 3 presents the PSD regarding D10, D25, D50, D75, and D90 of the LCM formulation after blending the entire ingredient as indicated in Table 2 and conducting the sieve PSD analysis. A previous study (Alsaba et al. 2016) proposed that the PSD of the LCM blend affects the formulation sealing ability significantly and is one of the reasons why one LCM formulation gives a different sealing pressure compared to the others. However, the comparison between each formulation is not the objective of this paper.

Table 2. LCM Treatment formulations.

| Type and D50 (microns) | LCM Blend | | | | | | |
|---|---|---|---|---|---|---|---|
| | G & SCC#1 | G & SCC#2 | G & SCC#3 | G & SCC#4 | G & NS | G, SCC & CF | NS |
| Graphite (G) | | | | | | | |
| 50 | 3 | - | - | - | 2 | 2 | - |
| 100 | 3 | - | - | - | 2 | 2 | - |
| 400 | 4.5 | 35 | - | - | 3 | 3 | - |
| 1000 | 4.5 | - | - | - | 3 | 3 | - |

Table 2. LCM Treatment formulations. (continued)

| Type and D50 (microns) | LCM Blend | | | | | | |
|---|---|---|---|---|---|---|---|
| | G & SCC#1 | G & SCC#2 | G & SCC#3 | G & SCC#4 | G & NS | G, SCC & CF | NS |
| Sized calcium carbonate (SCC) | | | | | | | |
| 5 | 1 | - | - | - | - | 2.4 | - |
| 25 | 1 | - | - | - | - | 2.4 | - |
| 40 | - | 35 | - | - | - | - | - |
| 50 | 2 | - | - | - | - | 5.2 | - |
| 400 | 3 | - | - | - | - | 8.4 | - |
| 600 | 4 | - | - | - | - | 10.8 | - |
| 1200 | 4 | - | - | - | - | 10.8 | - |
| 1400 | - | 35 | 70 | 35 | - | - | - |
| 2400 | - | - | - | 35 | - | - | - |
| Nut Shells (NS) | | | | | | | |
| 620 | - | - | - | - | 3.3 | - | 16.6 |
| 1450 | - | - | - | - | 3.3 | - | 16.6 |
| 2300 | - | - | - | - | 3.4 | - | 16.8 |
| Fine G & SCC Blend | | | | | | | |
| 500 | - | - | 35 | 35 | - | - | - |
| Cellulosic Fiber (CF) | | | | | | | |
| 312 | - | - | - | - | - | 2.5 | - |
| 1060 | - | - | - | - | - | 2.5 | - |

Table 3. LCM particle size distribution obtained from blending the formulations in Table 2.

| LCM Blend | Concentration (ppb) | PSD (microns) | | | | |
|---|---|---|---|---|---|---|
| | | D10 | D25 | D50 | D75 | D90 |
| G & SCC # 1 | 30 | 78 | 100 | 460 | 900 | 1300 |
| G & SCC # 2 | 105 | 65 | 90 | 420 | 1100 | 1400 |
| G & SCC # 3 | 105 | 90 | 400 | 700 | 1200 | 1400 |
| G & SCC # 4 | 105 | 170 | 650 | 1300 | 1900 | 2600 |
| G & NS | 20 | 65 | 180 | 500 | 1300 | 1900 |
| G, SCC & CF | 55 | 55 | 100 | 450 | 850 | 1200 |
| NS | 50 | 180 | 400 | 1000 | 1600 | 2400 |

## 3. RESULTS AND DISCUSSIONS

Table 4 shows a summary of the testing results both from the previous studies (Alsaba et al. 2014a, 2014b) and this study. The information will be used to compare between different testing conditions discussed below.

Table 4. Summary of the results from previous studies (Alsaba et al. 2014a, 2014b) and this study.

| LCM Blend | Total LCM (ppb) | Base Fluid | Disc Code | Weighting Material | Base Fluid Density (ppg) | Sealing Pressure (psi) |
|---|---|---|---|---|---|---|
| *G & NS* | *20* | *WBM* | *TS1-R7* | *N/A* | *8.6* | *2,372* |
| *G, SCC & CF* | *55* | *WBM* | *TS1-R7* | *N/A* | *8.6* | *1,011* |
| *G & SCC # 1* | *30* | *WBM* | *TS1-R7* | *N/A* | *8.6* | *487* |
| G & SCC # 2 | 105 | WBM | TS1-R7 | Barite | 11 | 2,050 |
| G & SCC # 3 | 105 | WBM | TS1-R7 | Barite | 11 | 2,859 |
| G & SCC # 4 | 105 | WBM | TS15-R7 | Barite | 11 | 2,571 |
| G & NS | 20 | OBM | TS1-R7 | N/A | 8.6 | 2,398 |
| G, SCC & CF | 55 | OBM | TS1-R7 | Barite | 8.6 | 1,505 |
| G & SCC # 1 | 30 | OBM | TS1-R7 | Barite | 8.6 | 737 |
| G & SCC # 2 | 105 | OBM | TS1-R7 | Barite | 11 | 1,569 |
| G & SCC # 3 | 105 | OBM | TS1-R7 | Barite | 11 | 1,489 |
| G & SCC # 4 | 105 | OBM | TS15-R7 | Barite | 11 | 1,708 |
| G & SCC # 1 | 30 | WBM | TS1-R7 | Barite | 9.5 | 1,205 |
| | | | TS1-R7 | Barite | 11 | 901 |
| | | | TS1-R7 | Barite | 12.5 | 912 |
| | | | TS1-R7 | Barite | 14.5 | 1,037 |
| | | | TS1-R7 | Barite | 16.5 | 1,344 |
| | | OBM | TS1-R7 | Barite | 9.5 | 1,049 |
| | | | TS1-R7 | Barite | 11 | 1,050 |
| | | | TS1-R7 | Barite | 12.5 | 1,191 |
| | | | TS1-R7 | Barite | 14.5 | 1,214 |
| | | | TS1-R7 | Barite | 16.5 | 1,238 |
| G & SCC # 1 | 30 | WBM | TS1-R7 | Barite + Hematite | 12.5 | 1,507 |
| | | | | | 14.5 | 1,334 |
| | | | | | 16.5 | 1,842 |
| | | OBM | TS1-R7 | Barite + Hematite | 12.5 | 1,269 |
| | | | | | 14.5 | 1,305 |
| | | | | | 16.5 | 1,283 |
| G & SCC # 1 | 30 | OBM | TS1-R7 | Barite (C) | 12.5 | 1,073 |
| | | OBM | TS1-R7 | Barite (M) | 12.5 | 1,134 |
| | | OBM | TS1-R7 | Barite (F) | 12.5 | 1,249 |

* The results from the previous study (Alsaba et al. 2014a, 2014b) were italicized.

Table 5 shows the results both in WBF from the aging condition tests. Data sets from Table 4 and Table 5 will be used for the analysis and discussion of this paper.

Table 5. Aging condition testing results.

| Aging Condition | LCM formulation and Concentration | Disc Code | Density (ppg) | Sealing Pressure (psi) |
|---|---|---|---|---|
| No aging | NS, 50 ppb | TS2 R7 | | 755 |
| | G & NS, 40 ppb | TS15 R7 | 8.6 | 1,713 |
| | G, SCC & CF, 55 ppb | TS1 R7 | | 1,011 |
| | G & SCC#4, 105 ppb | TS2 R7 | 11 | 1,606 |
| 24 hrs @ 200 · F | NS, 50 ppb | TS2 R7 | 8.6 | 1,713 |
| | | | | 750 |
| | | | | 638 |
| | G & NS, 40 ppb | TS15 R7 | 8.6 | 676 |
| | | | | 988 |
| | | | | 1,474 |
| | | | | 682 |
| | G, SCC & CF, 55 ppb | TS1 R7 | 8.6 | 1,427 |
| | | | | 1,979 |
| | | | | 614 |
| | G & SCC#4, 105 ppb | TS2 R7 | 11 | 1,879 |
| | | | | 1,242 |
| 72 hrs @ 200 · F | NS, 50 ppb | TS2 R7 | 8.6 | 3,021 |
| | | | | 1,167 |
| | G & NS, 40 ppb | TS15 R7 | 8.6 | 421 |
| | | | | 1,425 |
| | | | | 470 |
| | G, SCC & CF, 55 ppb | TS1 R7 | 8.6 | 1,544 |
| | | | | 1,593 |
| 24 hrs @ 400 · F | NS, 50 ppb | TS2 R7 | 8.6 | 196 |
| | | | | 136 |
| | G & NS, 40 ppb | TS15 R7 | 8.6 | 99 |
| | | | | 106 |
| | G, SCC & CF, 55 ppb | TS1 R7 | 8.6 | 1,124 |
| | | | | 820 |
| | G & SCC#4, 105 ppb | TS2 R7 | 11 | 994 |
| | | | | 1,105 |
| 72 hrs @ 400 · F | NS, 50 ppb | TS2 R7 | 8.6 | 161 |
| | G & NS, 40 ppb | TS15 R7 | | 104 |
| | G, SCC & CF, 55 ppb | TS1 R7 | 8.6 | 111 |
| | | | | 42 |
| | G & SCC#4, 105 ppb | TS2 R7 | 11 | 3,067 |
| | | | | 1,790 |

### 3.1 THE EFFECT OF THE BASE FLUIDS

Figure 3 shows a comparison between each pair of base fluids with the same density treated with the same LCM formulations. Three pairs of the 8.6 ppg samples are shown on the left-hand side, while three pairs of the 11 ppg samples are shown on the right. All blends were tested using a slot width of 1000-microns (TS1-R7) except the last pairs on the right which were tested with a slot width of 1500 microns (TS15-R7). Results show that different types of base fluids (WBF and OBF) provided different sealing pressures even though they have the same density. Different LCM formulations and concentrations also have different sensitivity to the base fluids.

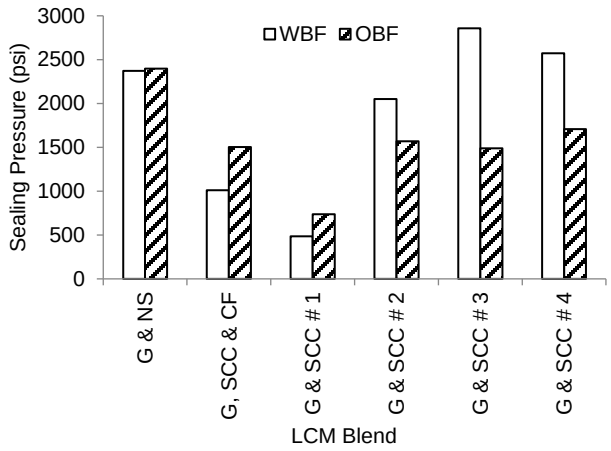


Figure 3. Base fluid effects on sealing pressure for each LCM formulation. The three pairs of WBF and OBF on the left were the results from 20, 55, and 30 ppb varied concentration, while the three pairs on the right were 105 ppb.

The first group on the left-hand side shows the results of the three formulations: G & NS; G, SCC & CF; and G & SCC#1 with a concentration of 20, 55, and 30 ppb, respectively. With the density of 8.6 ppg and considerably lower LCM treatment concentrations, OBF performed better than WBF. The sealing pressure in the G, SCC & CF and (G & SCC#1) formulations increased by approximately 50% when used in OBF compared to WBF.

Normally, OBF has a better lubricating property compared to WBF (Bourgoyne et al. 1986). This property can reduce friction between solid contact points and decrease the seal integrity. On the other hand, with the same drilling fluid density, OBF tends to

have more solid weight fraction (and volume fraction) than WBF because it contains less density base fluid. Potentially, the presence of barite particles remaining in the diluted OBF promoted the LCM sealing performance, forming a stronger solid seal and overcoming the lubricating effect. The simple 7% bentonite WBF containing only bentonite particles and water, with the same LCM treatment with OBF, could not perform as well as the OBF. At this point, the difference in lubricating property and solid volume fraction between WBF and OBF were believed to be the main factors affecting the sealing efficiency of both base fluids. The effect of the weighting material particles on the used LCM sealing ability will be evaluated in the following sections when the comparisons were done between the same base fluid.

The G & NS formulation also sealed better in OBF but had a less increasing sealing pressure between the pair. This formulation was less affected by the base fluids under the testing condition. Considering the PSD of LCM formulations shown in Table 3, the D90 value of the G & NS formulation is 1900 microns, which is much larger than the tested slot width (1000 microns). While the (G, SCC, & CF) and (G & SCC#1) formulations have D90 of 1200 and 1300 microns, respectively (Table 3), the D90 sizes are just slightly larger than the tested slot width (1000 microns). The significantly larger size of the bridging particles of NS compared to the slot width might reduce the effect of the base fluids in the G & NS case.

The second group on the right-hand side of Figure 3 shows the effect of base fluids in a different way (i.e., WBF performed better than OBF). The performance of the other three different LCM formulations; G & SCC#2, G & SCC#3, and G & SCC# 4; increased by 30%, 92%, and 50% when they were used in WBF compared to the OBF. One different between the two groups of results is that in the second group, higher density (11 ppg) drilling fluid samples were treated with a much higher LCM concentration (105 ppb) compared to the first group (8.6 ppg drilling fluid with 20 to 55 ppb of LCM). It is believed that the higher concentration of the LCM, the higher concentration of barite, and the lubricating property of OBF supported the LCM performance better in WBF environment than in OBF environment. The results presented here provide strong evidence that base fluids do affect the LCM sealing performance. However, its overall effect seems to depend on the type of LCM and should be an area of future investigation.

### 3.2 THE EFFECT OF DENSITY

Figure 4 shows the sealing pressure from 12 HPA tests over the 1000-micron slot disc after the drilling fluid samples were treated with G & SCC#1 at a concentration of 30 ppb. The densities of WBF and OBF were adjusted using barite to be six different densities varying from 8.6 ppg to 16.5 ppg.

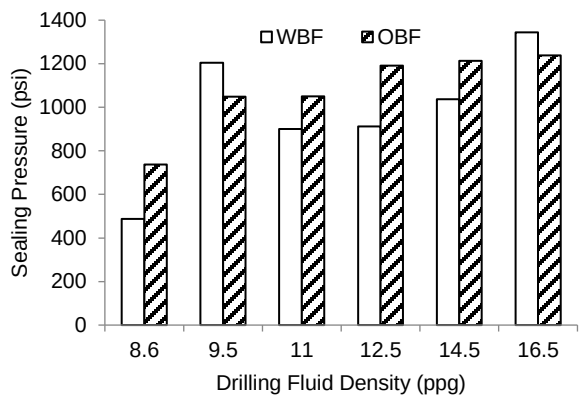


Figure 4. Effect of increasing the drilling fluid density on the sealing pressure.

The sealing pressure in OBF was increased by approximately 68% from 737 psi to 1,238 psi when the fluid density was increased from 8.6 ppg to 16.5 ppg. A higher increase of the sealing pressure, 175% increase from 487 to 1,344 psi, was observed for the same formulation in WBF when the fluid was weighted from 8.6 ppg to 16.5 ppg.

Since the only variable that was changed with the fluid density is the increasing of the barite particles within the mixture, it is believed that barite particles affect the sealing integrity. If the sealing mechanism arranged the particles inside the simulated fractures from coarse particles (as the bridging structure), fine particles (as filling material), and the very fine particles (both as filling and seal-off the permeability of the seal), the difference in seal integrity could be explained.

Applying basic engineering mechanics to the seal element, at the instant when the seal was completely developed and remained in equilibrium, the sum of external forces acting on the seal element in any direction must be zero (Bedford and Fowler 1998). The pressure forces acted within the slot opening area performed by the fluid differential

pressure (injecting pressure) was supported back by the slot wall in the form of reaction forces. The load was transferred down the seal from finer grains to the larger particles until it reached the coarsest bridging particles in the slot where no particles set beyond that barrier (Jeennakorn et al. 2017). When the particles remained in equilibrium, the balance of forces would not allow any particle to move but to stay at rest. Under loading condition, the particles deformed locally at the contact points due to the stress indentation (an elastic or elastic-plastic type of deformation–depending on the material properties) (Fischer-Cripps 2000). If the load acting on the bridging particles did not exceed the strength of the particles and the sizes of the particles under the local deformation were still greater than the slot space, no part of the seal would fail. On the other hand, if a bridging particle failed or if the local deformation reduced the size of the particle to be less than the gap between the slot walls, the particle would slip deeper into the slot and finally pushed through the slot. The seal would then suddenly fail because smaller particles accompanying the base fluid can move or flow through the suddenly available flow path. The failure condition would go on until the bridging structure was reformed by other coarse particles and the seal was in equilibrium again. The bridging structure (coarse particles) acted as the foundation or backbone of the seal, played an important role in the seal integrity.

The forces in the granular system normally distribute in the form of the “force chains” (Mehta 2007), which is heterogeneous due to different grain sizes and arbitrarily set structure and void spaces. The nonuniform stress distribution weakens the seal structure because it creates the weak point (i.e., the point with a higher local stress that would cause failure while the other points can or try to stay in equilibrium). In this situation, the forces are more difficult to balance. Particles tend to move, and the seal would fail easier. The fine barite particles help occupy the remaining pore space of the seal, either between the solid particles or against the solid particles and the wall. They turn the granule-packed seal into a more homogeneous wedge-shaped object, increase the overall strength of the seal by increasing the contact points within the granular system and improve the forces-distribution to be more uniform. Increasing the number of contact points and the contact areas also reduces the local stress concentration within the bridging particles, which decreases the chance of the particles to be locally deformed.

Since forces transmitted at the points of contact are composed of normal forces and frictional (tangential) forces (Johnson 1985), the slot walls support the seal element by both the normal component and the friction component. While the coarse particles set in place as the first barrier, the normal and frictional forces control the equilibrium of the seal. As discussed above, better force distribution improves both the normal and friction force distribution to be more uniformed within the seal element. Improving the normal force distribution to the walls also improves the friction, and the better the friction, the higher the seal element can withstand the overall load. Overall, the load can be transferred more uniformly toward the slot walls and better shared among the particles, resulting in higher seal integrity. The barite particles may also improve the friction coefficient between the contact particles, which can improve the magnitude of the frictional force holding the seal in place as in the case of hematite, which will be discussed later.

From the flattened increasing of sealing pressure in 12.5 – 16.5 ppg (Figure 4), appears that there might be an optimum point where the proper size distributed particles in the system are just right to fill the pore spaces. The LCM performance will not improve beyond that point.

### 3.3 THE EFFECT OF WEIGHTING MATERIALS: BARITE VS. HEMATITE

From the result of the effect of density tests, some experiments were continued to investigate the effect of changing the weighting material types on the sealing ability. The same G & SCC#1 blended at 30 ppb was used to treat the drilling fluid samples. The 11 ppg OBF (with some amount of barite) and the 8.6 ppg WBF was weighted with hematite to get the desired densities of 12.5, 14.5, and 16.5 ppg.

Figure 5 compares the results from using hematite as a weighting agent with the previous results of using barite. The results confirm that in the range of density from 12.5 to 16.5 ppg, increasing the density slightly improved the sealing pressure for both WBF and OBF. In OBF, adding hematite into barite-weighted samples resulted in a slight increase of the sealing pressures (broken arrows), but in WBF, using only hematite improved the sealing ability of the LCM treatment significantly (solid arrows).

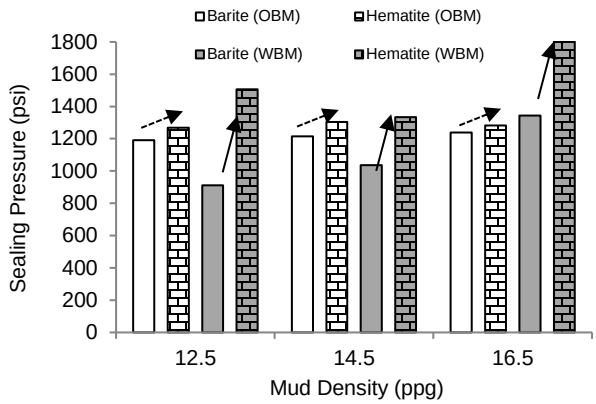


Figure 5. The effect of weighting materials between barite and hematite. In WBF, the weighting agent was used only barite or hematite, but in OBF, the 11 ppg barite-treated drilling fluid's density was increased to the target density using barite or hematite.

Like the case of adding barite, the finer hematite particles of hematite could better fill in the pore spaces of the particulate system, providing a stronger seal barrier against the slot walls. Another reason that can explain the sealing pressure improvement using hematite comes from the previous study that states the hematite particles are more abrasive than the barite particles (Tehrani et al. 2014). It is then believed that the hematite particles not only increase the contact points and contact areas, but also improve the frictional force component (friction coefficient) to be higher than using barite, and helps further increase the sealing ability of the LCM. Note that OBF contained some amount of barite from the originally supplied drilling fluid. A Smaller amount of hematite was added to increase the OBF 11-ppg density to the desired densities compared to WBF, where only hematite was added to the 8.6-ppg (7% by weight) bentonite drilling fluid. This might be the reason why the sealing ability improved less in OBF compared to WBF.

Figure 6 shows the sealing pressure obtained from the test using different sizes of sieved barite to increase the WBF density from 8.6 ppg to 12.5 ppg before applying G & SCC#1 treatment at 30 ppb. Compared to the regular barite (no sieve), the fluid sample with fine barite (F) gave a better sealing pressure, while the medium (M) and coarse particles (C) decreased the sealing performance.

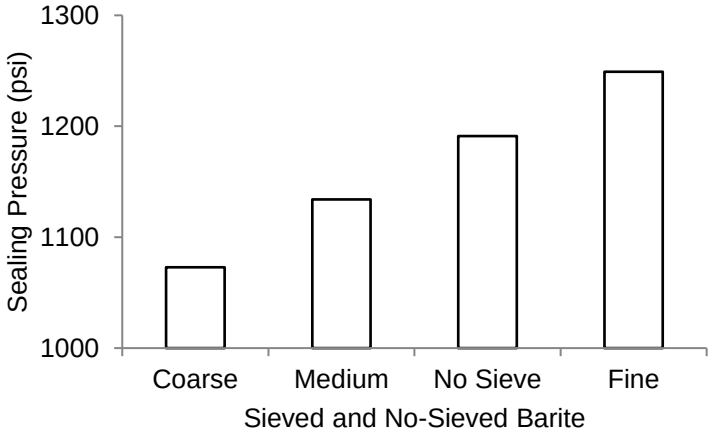


Figure 6. Effect of adding three ranges of sieved barite particles on the sealing pressures of 12.5 ppg OBF treated with G & SCC#1 at 30 ppb. Variation of barite particle sizes causes the sealing pressures to be varied from 1,073 psi to 1,249 psi.

Using F barite brought the sealing pressure up from the case of non-sieve barite (1,191 psi) to a higher pressure (1,249 psi); it is closer and comparable to the result of the 11-ppg OBM adding hematite (1,269 psi) under the same condition. The size of F barite particles is 50 microns or less, while the size of hematite particles is 45 microns or less for 70% or more by weight. Considering the PSD of the used LCM formulation (G & SCC#1), it is noticeable that this formulation had a D10 value of 78 microns. It was likely that both barite and hematite particles fulfilled the gap-filling requirement of the sealing system, where the improvement was found to be smaller in OBF. However, the results confirmed the idea that weight agent particle size affects the seal integrity.

### 3.4 THE EFFECT OF DYNAMIC AGING CONDITIONS

This experiment was set up to investigate the effect of aging conditions on LCM performance. Using OFITE aging cells and a rolling oven, two temperature levels were selected to be used. First, a high temperature of 400 °F was used in the tests to evaluate temperature degradation of LCMs. Secondly, 200 °F was used to achieve a normal temperature condition in drilling. Two aging times, 24 and 72 hours, were selected to be run as a primary laboratory investigation.

After aging, the drilling fluid samples were moved from the oven and let cool to room temperature before being tested in HPA. Figure 7 shows the measured sealing pressure of the drilling fluid sample after a specific aging condition compared to non-aged results from previous tests.

In high temperature with aging conditions at 400 °F (Figure 7), the NS blend and G & NS blends failed to develop strong seal after applying 400 °F aging condition for 24 hours, but the G, SCC, & CF formulation still had the ability to seal after 24 hours, then failed in a 72-hour test. The 400 °F aging condition does not affect the sealing ability of the G & SCC#4 formulation for at least 72 hours of the aging test. The thermal stability of the LCM particles controls how LCM performs in the aging tests.

Figure 7 also shows the results of the lower temperature aging condition at 200 °F for 24 hours and 72 hours of aging time. The NS formulation tends to increase sealing efficiency with aging time. This result confirms the previous study on the effect of temperature on LCM sealing efficiency (Alsaba et al. 2014c).

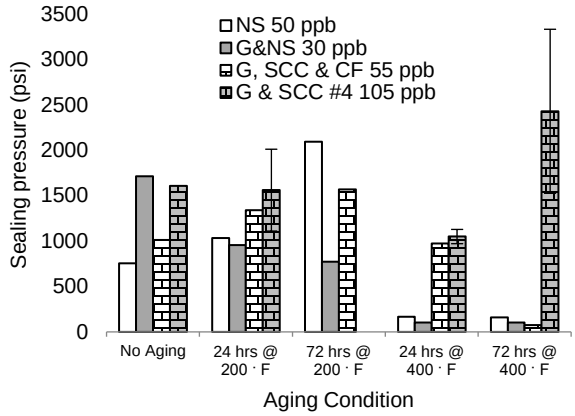


Figure 7. Sealing pressure of the drilling fluids treated with different LCM after subjected to different aging conditions.

Inversely, the G & NS blend (which has 50% weight of G) tends to decrease sealing ability with the aging time. While the NS improved the sealing pressure, the G strongly decreased the sealing ability of the mixture. The previous study about LCM shear degradation presented the idea about the decreasing in size of LCM particles under

the dynamic flow of drilling fluids (Valsecchi 2014). The degree of degradation of LCM depends on the density of the particles, the density of drilling fluids, the size of particles, and the fluid viscosity. It was possible that some of the G particles decreased their sizes under the rolling conditions, resulting in lower sealing efficiency. Further study is needed to understand the behavior of G under this aging conditions.

The G, SCC & CF blend contained only 18% weight of G, so it was not affected much by the aging conditions, but still gave the same trend as NS, where sealing pressure increased with time of aging. Obviously, CF (9% weight) should have the same swelling property as NS that improves sealing pressure under higher temperature. From this experiment, the G & SCC #4 formulation was not affected by the aging condition in terms of sealing efficiency. The formulation contains less than 30% G, which still showed a good sealing integrity under a 72-hours of aging time.

## 4. CONCLUSIONS

- Different LCM formulations respond differently to the different testing conditions depending on the physical properties of the individual ingredient and the effect of the testing conditions on them.

- LCM behaves and performs differently in different base fluids.

- The interactions between fluid and solid grains under dynamic conditions and the static of formed seal with complex interactions between the solid grains need further study.

- Increasing the drilling fluid density before applying any LCM treatment tends to increase the seal integrity, interrelating with the added solid particles.

- Increasing the weighting material particles helps improve the sealing ability of the seal. It is believed that the proper range of particle sizes occupy the seal pore space, increase the number of contact points and contact areas, and result in more effective load distribution within the seal structure and against the slot walls.

- For each type of weighting material, adding a proper range of particle sizes can fulfill the insufficient particle sizes in the LCM formulation, promoting the sealing ability of the mixture.

- Increasing drilling fluids' density using hematite improves LCM performance

better than using barite alone. It is believed that the proper size of fine particles, combined with the grain abrasiveness, improve the seal strength and the frictional forces supporting the seal structure.

- The PSD of the mixture is the final PSD that affects the sealing ability, not only the PSD of the LCM alone.

- The aging condition affects the performance of LCM differently. It might promote or reduce the sealing pressure at a practical temperature (200 °F) depending on the LCM thermal properties.

- Some formulations failed to perform a strong seal at a higher temperature (400 °F) especially the ingredients made from natural plant products.

- The sealing ability of the formulation containing G & SCC was not affected by aging conditions for up to at least 72 hours due to the temperature stability of the materials.

## ACKNOWLEDGEMENT

The authors would like to acknowledge Det Norske Oljeselskap ASA for the financial support under research agreement # 0037709 to the research group, Dr. Galecki from Missouri University of Science and Technology for his help with the PSD analysis work, and John Tyler and Jeff Heniff from Missouri University of Science and Technology for their assistance in manufacturing the testing apparatuses.

## REFERENCE

Abrams A (1977). Mud Design to Minimize Rock Impairment due to Particle Invasion. Petroleum Technology May:586–592.

Almagro B S P, Frates C, Garand J & Meyer A (2014). Sealing Fractures: Advances in Lost Circulation Control Treatments. Oilfield Review 26(3):4–13.

Alsaba M, Nygaard R, Hareland G & Contreras O (2014a). Review of Lost Circulation Materials and Treatments with an Updated Classification. In: AADE Fluids Technical Conference and Exhibition, Houston, Texas, 15–16 April.

Alsaba M, Nygaard R, Saasen A & Nes O (2014b). Lost Circulation Materials Capability of Sealing Wide Fractures. In: SPE Deepwater Drilling and Completions Conference, Galveston, Texas, 10–11 September.

Alsaba M, Nygaard R, Saasen A & Nes O (2014c). Laboratory Evaluation of Sealing Wide Fractures Using Conventional Lost Circulation Materials. In: SPE Annual Technical Conference and Exhibition, Amsterdam, The Netherlands, 27–29 October.

Alsaba M, Nygaard R, Saasen A & Nes O (2016). Experimental Investigation of Fracture Width Limitations of Granular Lost Circulation Treatments. Petroleum Exploration and Production Technology:1–11.

Bedford A & Fowler W (1998). Engineering Mechanics: Statics. Addison-Wesley.

Bourgoyne A, Millheim K, Chenevert M & Young F S (1986). Applied Drilling Engineering. SPE.

Canson B E (1895). Lost Circulation Treatments for Naturally Fractured, Vugular, or Cavernous Formations. In: SPE/IADC Drilling Conference, New Orleans, Louisiana 6–8 March. doi: 10.2118/13440-MS.

Clapper Dennis K, Szabo Joseph J, Spence Steven P, Otto Mike, Creelman Brian, Lewis Tom G & McGuffey Gary (2011). One Sack Rapid Mix and Pump Solution to Severe Lost Circulation. In: SPE/IADC Drilling Conference and Exhibition, Amsterdam, The Netherlands, 1–3 March.

Dick M A, Heinz T J, Svoboda C F, Aston M (2000). Optimizing the Selection of Bridging Particles for Reservoir Drilling Fluids. In: SPE International Symposium on Formation Damage, Lafayette, Louisiana, 23–24 February.

Feng Yongcun, Jones John F & Gray K E (2016). A Review on Fracture-Initiation and Propagation Pressures for Lost Circulation and Wellbore Strengthening. SPE Drilling and Completion, June:134–144.

Fisher-Cripps A C (2000). Introduction to Contact Mechanics. Springer.

Ghalambor Ali, Salehi S, Mojtaba P & Shahri (2014). Integrated Workflow for Lost Circulation Prediction. In: SPE International Symposium and Exhibition on Formation Damage Control, Lafayette, Louisiana, 26–28 February.

Fuh G-F, Morita N, Boyd P A & McGoffin S J (1992). A New Approach to Preventing Lost Circulation While Drilling. In: Annual Technical Conference and Exhibition of the Society of Petroleum Engineers, Washington DC, 4–7 October.

Hettema M, Horsrud P, Taugbol K, Friedheim J, Huynh H, Sanders M W & Young S (2007). Development of an Innovative High-Pressure Testing Device for the Evaluation of Drilling Fluid Systems and Drilling Fluid Additives within Fractured Permeable Zones. In: Offshore Mediterranean Conference and Exhibition, Ravenna, Italy, 28–30 March. OMC-2007-082.

Horn A J (1950). Well Blowouts in California Drilling Operations Causes and Suggestions for Prevention. API 50:112–128.

Howard George C & Scott Jr P P (1951). An Analysis and the Control of Lost Circulation. Petroleum Transactions, AIME192:171–182.

Jeennakorn M, Nygaard R, Nes O-M & Saasen A (2017). Testing Condition Make a Difference When Testing LCM's. Manuscript submitted to Journal of Natural Gas Science and Engineering.

Johnson K L (1985). Contact Mechanics. Cambridge University Press.

Kageson-Loe N, Sanders M W, Growcock F, Taugbøl K, Horsrud P, Singelstad A V & Omland T H (2009). Particulate-Based Loss-Prevention Material-the Secrets of Fracture Sealing Revealed! SPE Drilling & Completion, December:581–589.

Kefi Slaheddine, Jesse C Lee, Nikhil Dilip Shindgikar (2010). Optimizing in Four Steps Composite Lost-Circulation Pills without Knowing Loss Zone Width. In: Asia Pacific Drilling Technology Conference and Exhibition, Ho Chi Minh City, Vietnam, 1–3 November. doi: 10.2118/133735-MS.

Kumar A & Savari S (2011). Lost Circulation Control and Wellbore Strengthening: Looking Beyond Particle Size Distribution. In: AADE National Technical Conference and Exhibition, Houston, Texas, 12–14 April. AADE-11-NTCE-21.

Loeppke G E, Glowka D A & Wright E K (1990). Design and Evaluation of Lost-Circulation Materials for Severe Environments. SPE Petroleum Technology, March:328–337. doi: 10.2118/18022-PA.

Mehta A (2007). Granular Physics. Cambridge.

Morita N, Black A D & Fuh G-F (1990). Theory of Lost Circulation Pressure. In: Annual Technical Conferences and Exhibition of the SPE, New Orleans, Louisiana, 23–26 September.

Nayberg T M (1986). Laboratory Study of Lost Circulation Materials for Use in Both Oil-Based and Water-Based Drilling Muds. SPE Drilling Engineering, September:229–236 doi: 10.2118/14723-PA.

OFI Testing Equipment Inc (2014). Aging Cell Instruction Manual Ver. 2.13. http://www.ofite.com/doc/175-25_instructions.pdf).

OFI Testing Equipment Inc (2013). High-Temperature Roller Oven with Circulating Fan Instruction Manual. Ver.1.3. http://www.ofite.com/doc/176-00-C_instructions.pdf.

Robinson W. W. (1940). The Application of Chemicals to Drilling and Producing Operations. API 40:236–245.

Salehi S & Nygaard R (2012). Numerical Modeling of Induced Fracture Propagation: a Novel Approach for Lost Circulation Materials (LCM) Design in Borehole Strengthening Applications of Deep Offshore Drilling. In: SPE Annual Technical Conference and Exhibition, San Antonio, Texas, 8–10 October.

Scott Jr P P& J L Lummus (1955). New Developments in the Control of Lost Circulation. In: Annual Fall Meeting of the Petroleum Branch of the American Institute of Mining and Metallurgical Engineers, New Orleans, Louisiana, 2–5 October. doi: 10.2118/516-G.

Tehrani A, Cliffe Angleika, Hodder M H, Young S, Lee J, Stark J & Seale S (2014). Alternative Drilling Fluid Weighting Agents: a Comprehensive Study on Ilmenite and Hematite. In: IADC/SPE Drilling Conference and Exhibition, Fort Worth, Texas, 4–6 March.

Valsecchi P (2014). On the Shear Degradation of Lost-Circulation Materials. SPE Drilling and Completion, September:323–328.

Whitfill D L & Miller M (2008). Developing and Testing Lost Circulation Materials. In: AADE Fluids Conference and Exhibition, Houston, Texas, 8–9 April. AADE-08-DF-HO-24.

White R J (1956). Lost-Circulation Materials and Their Evaluation. In: Spring meeting of the Pacific Coast District, Division of Production, Los Angeles, May.

Xiao J, Nasr-El-Din H A & Al-Bagoury M (2013). Evaluation of Ilmenite as a Weighting Material in Oil-Based Drilling Fluids for HPHT Applications. In: SPE European Formation Damage Conference & Exhibition, Noordwijk, The Netherlands, 5–7 June. doi:10.2118/165184-MS.

# III. SEALING PRESSURE PREDICTION MODEL FOR LOST CIRCULATION TREATMENTS BASED ON EXPERIMENTAL INVESTIGATIONS


## ABSTRACT

Lost circulation events are one of the major contributors towards drilling-related non-productive time (NPT). Lost circulation materials (LCMs) are often applied as a remedial action to alleviate drilling fluid losses into fractured formations. In normal overbalanced drilling operations and when designing lost circulation treatments, it is important that the formed seal within the fractures maintain at least the minimum overbalance pressure without breaking. Predicting the sealing pressure of LCMs treatments, which is defined as the maximum pressure at which the formed seal breaks and fluid losses resumes, is crucial for an effective fracture sealing. This paper presents a linear model for sealing pressure prediction.

A statistical analysis was conducted on a data set, which was developed from a previous experimental investigation, to understand the relationship between different parameters and the sealing pressure of LCM treatments. The investigated parameters include fracture width, fluid density, LCM type/blend, base fluid, and particle size distribution (PSD).

The statistical analysis showed that the sealing pressure is highly dependent on the fracture width, fluid density, and PSD. A predictive linear fit model, which could be used as a useful tool to design LCM treatment prior to field application, was developed. The developed model correlated well with the collected data and resulted in an overall model accuracy of 80%.

Knowing the dominant parameters affecting the sealing pressure will help in designing LCM treatments that are capable of sealing expected fracture widths as well as maintaining high differential pressures and thus, effectively mitigating fluid losses as soon as they occur.

## 1. INTRODUCTION

Lost circulation events are considered to be one of the challenging problems to be prevented or mitigated where approximately 1.8 million bbls of drilling fluids are lost per year (Marinescu, 2014). This number explains the operational challenges caused by lost circulation. In addition, lost circulation events could delay further drilling and thus contributing towards increased cost of drilling operations as a result of non-productive time (NPT).

Proper remedial actions, as per a pre-designed contingency plan or decision trees (Savari and Whitfill, 2016), are often taken to mitigate or stop the losses once they occur depending on the loss severity. However, these contingencies plans neglect the need for the experimental evaluation of the most effective LCM blend on the rig site (Savari and Whitfill, 2016).

To verify the effectiveness of designed treatments, laboratory evaluation is a crucial step prior to field application. Different testing methods are used to evaluate the performance of LCM treatments, based on the fluid loss volume at a constant pressure, such as the particle plugging apparatus (PPA) or the high-pressure-high-temperature (HPHT) fluid loss in conjunction with slotted/tapered discs or ceramic discs (Whitfill 2008; Kumar et al. 2011; Kumar and Savari 2011).

Other testing equipment has been developed to evaluate the sealing efficiency of LCM treatments in sealing permeable/impermeable fractured formations (Hettema et al. 2007; Sanders et al. 2008; Van Oort et al. 2009; Kaageson-Loe et al. 2009). Both particle size distribution (PSD) and total LCM concentration were found to have a significant effect on the sealing efficiency. It was also concluded that the fluid loss volume is not a good parameter to measure the sealing efficiency of LCM treatments.

PSD is often used as the designing parameter for LCM treatments where different models such as Abrams median particle-size rule (Abrams, 1977), ideal packing theory (IPT) (Andreasen and Anderson, 1930), and Vickers method (Vickers et al. 2006) are used to optimize PSD.

The effect of other LCM properties such as crushing resistance, resiliency, and aspect ratio on the overall performance of LCM blends were evaluated by Kumar et al.

(2010). It was concluded that higher crushing resistance and resiliency are desirable for both controlling fluid losses and wellbore strengthening applications.

In normal overbalanced drilling operations (i.e. drilling fluid pressure higher than formation pressure), a minimum static overbalance pressure of 150-300 psi is required to prevent formation fluid influx (Jahn et al. 2008; Rehm et al. 2012; The Drilling Manual, 2015). Therefore, when designing LCM treatments, it is important to ensure that the selected LCM blend is able to seal fractures effectively and stop losses. In addition, the formed seal within the fracture should withstand at least the minimum overbalance pressure without failing.

The main objective of this paper is to introduce the sealing pressure prediction model, which was developed based on a large data collected from experimental evaluation of different LCM blends used to seal different fracture widths at different fluid types and densities. The model can be used as a tool to evaluate the performance of the selected LCM treatment from the contingency plan without the need for extra experimental evaluation.

## 2. PREVIOUS EXPERIMENTAL INVESTIGATION

The sealing pressure of LCM treatments was previously (Alsaba, 2015) measured using a high-pressure LCM testing apparatus. The sealing pressure is defined here as the maximum pressure at which the formed seal breaks and fluid loss resumes. Figure 1 shows a schematic of the experimental setup, where a plastic accumulator (1) used to transfer the drilling fluids to the metal accumulator (2) prior to pressurizing the fluids containing LCM treatments inside the testing cell (3) through the tapered discs (4) using an Isco$^{TM}$ pump (DX100) (5) to provide injection pressure, which was connected to a computer to record pressure vs. time.

The effects of varying LCM type, formulation, concentration, fracture width, particle size distribution, base fluid, and density were studied with respect to differential pressure. The main objectives were to establish a better understanding of how these parameters could affect the sealing efficiency (in terms of pressure) of LCMs and identify their limitations in sealing fractures.

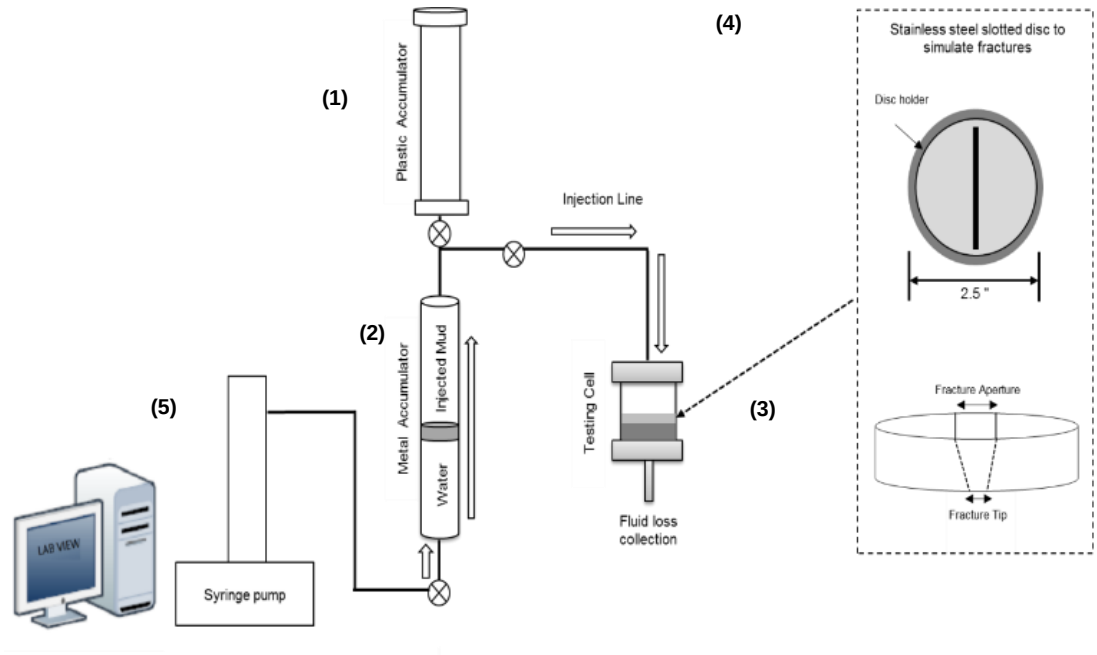


Figure 1. Schematic of the High-Pressure Testing Apparatus.

High-pressure tests were conducted on different LCM treatment formulations containing conventional LCMs such as graphite (G), sized calcium carbonate (SCC), nut shells (NS), and cellulosic fiber (CF) (Detailed formulation can be found in Alsaba, 2015) to evaluate their sealing efficiency at different fracture width varying between 1000 – 3000 microns. The LCM treatments were tested in both water-based mud (WBM) and oil-based mud (OBM) at different fluid densities ranging between 8.6 lb/gal and up to 16.5 lb/gal. The concentrations and the PSD of the LCM blends, which was measured using dry sieve analysis, used in this study are shown in Table 1.

## 3. STATISTICAL METHODS

Statistical analysis of the LCM sealing pressure results for 75 high-pressure tests was performed to define the parameters with the highest effect on the sealing pressure.

A statistical analysis was conducted using JMP$^{TM}$ statistical analysis software to understand the relationship between the different investigated parameters such as fracture width, LCM type/blend, base fluid, and PSD on the performance of LCM in terms of the sealing pressure.

First, a regression analysis was conducted by performing a multiple linear regression analysis to model a relationship between 9 explanatory variables and the sealing pressure response. The 9 variables used are fracture width, LCM type/blend, base fluid, fluid density, and the five D-values obtained from PSD analysis; D10, D25, D50, D75, and D90.

Table 1. Summary of the Particle Size Distribution Analysis for the Different LCM Blends.

| LCM Blend | Total Conc. (ppb) | Particle Size Distribution (microns) | | | | |
|---|---|---|---|---|---|---|
| | | D10 | D25 | D50 | D75 | D90 |
| G # 1 | 15 | 60 | 85 | 320 | 800 | 1300 |
| G # 1 | 50 | 60 | 95 | 340 | 800 | 1300 |
| NS # 1 | 15 | 180 | 400 | 1000 | 1600 | 2000 |
| NS # 1 | 50 | 180 | 400 | 1000 | 1600 | 2400 |
| SCC # 3 | 50 | 250 | 360 | 680 | 950 | 1200 |
| CF # 1 | 15 | 90 | 140 | 220 | 700 | 1400 |
| CF # 1 | 50 | 90 | 150 | 220 | 800 | 1400 |
| G & SCC # 1 | 30 | 80 | 100 | 460 | 900 | 1300 |
| G & SCC # 1 | 80 | 80 | 120 | 480 | 900 | 1300 |
| G & SCC # 3 | 105 | 65 | 90 | 420 | 1100 | 1400 |
| G & SCC # 4 | 105 | 60 | 150 | 500 | 700 | 900 |
| G & SCC # 5 | 105 | 90 | 400 | 700 | 1200 | 1400 |
| G & SCC # 6 | 105 | 100 | 500 | 900 | 1250 | 1400 |
| G & SCC # 7 | 105 | 170 | 650 | 1300 | 1900 | 2600 |
| G & SCC # 8 | 105 | 100 | 250 | 1000 | 1800 | 2400 |
| G & SCC # 9 | 105 | 300 | 800 | 1400 | 1800 | 2200 |
| G & NS # 1 | 20 | 65 | 180 | 500 | 1300 | 1900 |
| G & NS # 1 | 40 | 80 | 180 | 580 | 1400 | 2000 |

The probability test (F-test) was performed to test the influence of each parameter on sealing pressure. The F-test provides a P-value, where the P-value is basically a statistical probability that the predicted value (in this case the F-value) is similar or very

different from the measured value, assuming a true null hypothesis ($H_0$) that proposes no influence of a specific variable on the sealing pressure (Montgomery, 2001). With a confidence interval of 95% and type I error (α) of 0.05, P-values less than 0.05 suggests rejecting the null hypothesis ($H_0$) and accepting an alternative hypothesis ($H_1$).

The alternative hypothesis suggests that the sealing pressure is influenced by a specific variable. The F-test is calculated based on the variance of the data as:

$$F = \frac{S_1^2}{S_2^2} \tag{1}$$

where $S_1^2$ is the variance of the first sample and $S_2^2$ is the variance of the second sample. The variance can be defined as the average squared difference from the mean.

Leverage plots for the general linear hypothesis, introduced by Sall (1990), were plotted for each of the 9 variables (predictors) to show their contribution to the predicted sealing pressure. The Effect Leverage plot is used to characterize the hypothesis by plotting points where the distance between each point to the fit line shows the unconstrained residual while the distance to the x-axis shows the constrained residual by the hypothesis. The constrained sealing pressure for each parameter under the hypothesis can be written as:

$$b_0 = b - (X'X)^{-1}L'\lambda \tag{2}$$

where b is the least square, $(X'X)$ is the inverse matrix (the transpose of the matrix data being D-values and other parameter, used to enforce orthogonality), and λ is the Lagrangian multiplier for the hypothesis constraint (L). The residual constrained by the hypothesis ($r_0$) is:

$$r_0 = r + X(X'X)^{-1}L'\lambda \tag{3}$$

where the Lagrangian multiplier is defined as:

$$\lambda = (L(X'X)^{-1}L')^{-1}Lb. \tag{4}$$

The residuals unconstrained by the hypothesis (r) are the least squares residuals defined as:

$$r = \acute{y} - Xb. \tag{5}$$

The Leverage plot is constructed by plotting $v_x$ on the x-axis (Eq. 6) versus $v_y$ on the y-axis (Eq. 7). $v_x$ values represent the difference in the residuals caused by the hypothesis, which is the distance from the model fit line to the x-axis while $v_y$ values are $v_x$ plus the unconstrained residuals.

$$v_x = X(X'X)^{-1}L'\lambda. \tag{6}$$

$$v_y = r + v_x. \tag{7}$$

The sealing pressure residuals are regressed on all predictors except for the variable of interest while the x-residuals (variable of interest) are regressed on all other predictors in the model. The mean of the sealing pressure, without the effect of the variable of interest, is plotted as well as a least square fit line and confidence interval for easier interpretation of the results. The upper and lower confidence interval could be plotted using Eq. 8 and Eq. 9, respectively. The least squares fit line slope is a measure of how the tested variable affects the sealing pressure i.e. a non-zero slope implies that the tested variable will affect the sealing pressure (Sall, 1990). When x = [1 *x*] is the 2-vector of regressors,

$$Upper\ (x) = xb + t_{\alpha/2}s\sqrt{x(X'X)^{-1}x'} \tag{8}$$

$$Lower\ (x) = xb - t_{\alpha/2}s\sqrt{x(X'X)^{-1}x'}\ . \tag{9}$$

## 4. STATISTICAL ANALYSIS RESULTS

Figures 2 to 10 show the Effect Leverage plots for each parameter with the resulting P value. The blue dashed line represents the mean sealing pressure, the solid red line represents the fitted model, and the dashed red line represents the confidence interval (5% confidence level). If the mean sealing pressure is inside the confidence interval envelope the parameter does not have any significant effect on sealing pressure. If the confidence interval crosses the mean pressure at a high angle, it has a significant contribution to sealing pressure.

Figure 2 shows the effect of fracture width in the sealing pressure. The effect of fracture width is very significant since the confidence interval curves crossed the mean pressure with a high slope. The P-value of 0.0003 also indicates that the fracture width influenced the predicted sealing pressure. The effect of fluid density (Figure 3) was also pronounced since confidence curve crossed the horizontal line with a P-value that is less than 0.05 suggesting a good correlation.

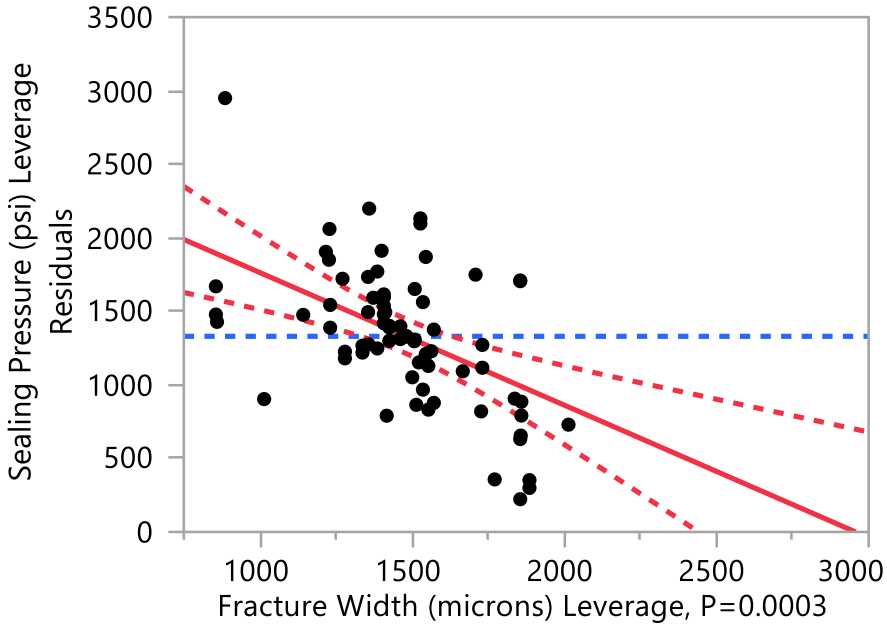


Figure 2. Leverage Plot Showing the Effect of Fracture Width on Sealing Pressure.

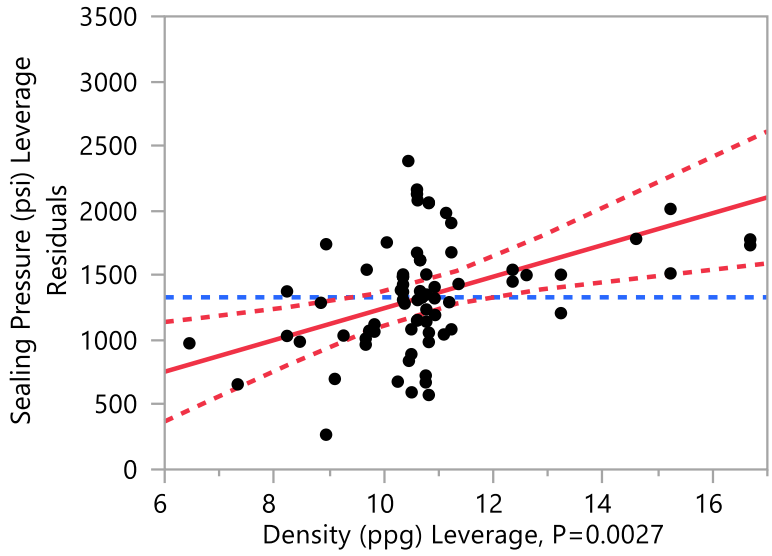


Figure 3. Leverage Plot Showing the Effect of Density on Sealing Pressure.

The effect of D90 was the third significant parameter to affect the prediction of sealing pressure. The Effect of D90 can be clearly seen (Figure 4) with a P-value that is slightly larger than 0.05. The variation in LCM blends showed also a clear effect with P-value 0.1147 (Figure 5).

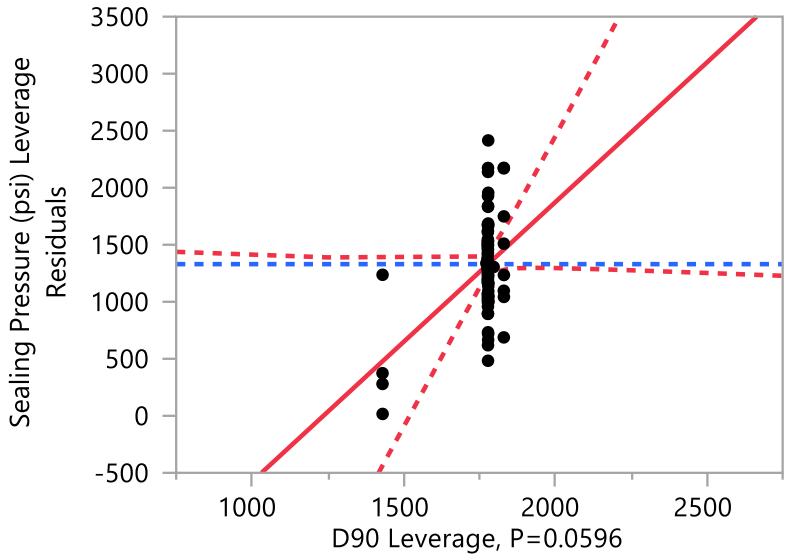


Figure 4. Leverage Plot Showing the Effect of D90 on Sealing Pressure.

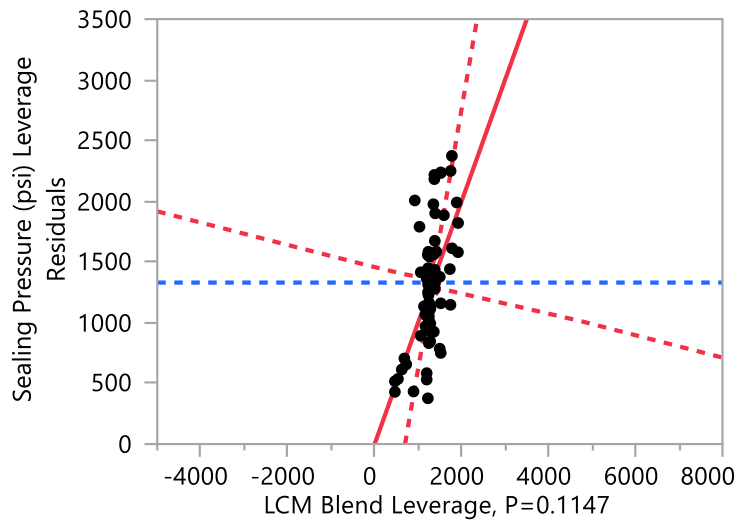


Figure 5. Leverage Plot Showing the Effect of LCM Blend on Sealing Pressure.

The Effect Leverage plots (Figures 6 – 10) for D75, base fluid, D25, D50, and D10, respectively shows less effect on the sealing pressure with P-values ranging between 0.2863 and 0.9817. However, the less significance of these parameters might be due to the outliers in the analyzed data set.

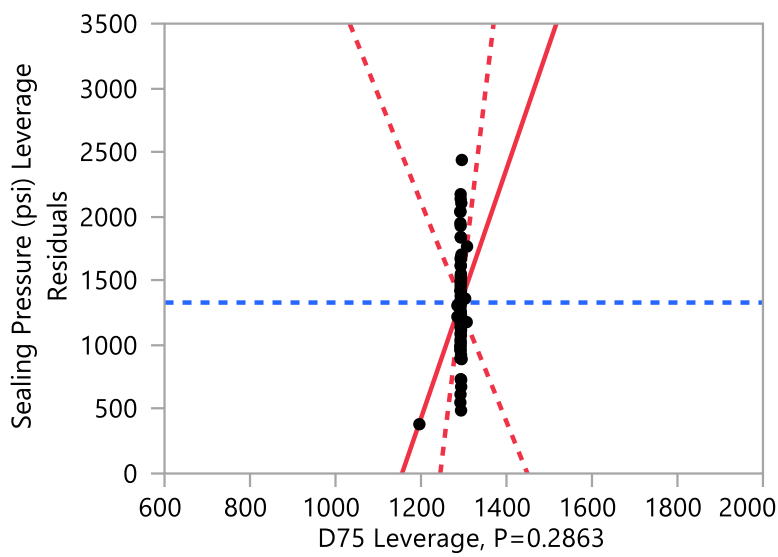


Figure 6. Leverage Plot Showing the Effect of D75 on Sealing Pressure.

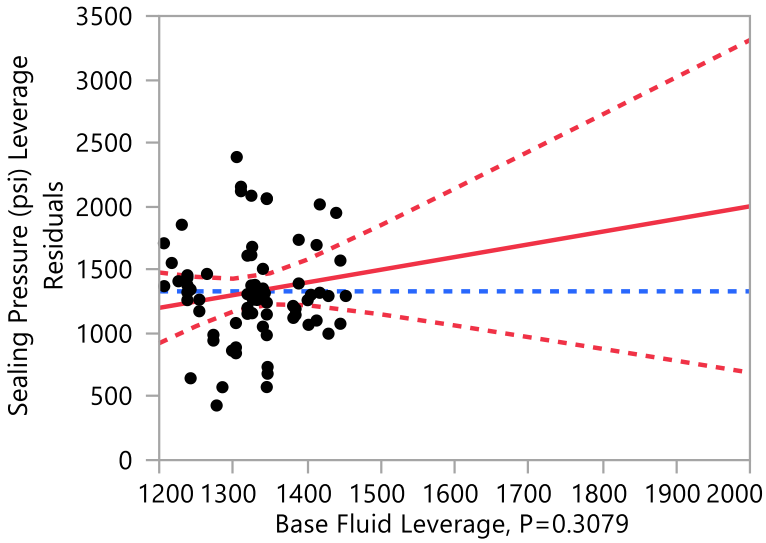


Figure 7. Leverage Plot Showing the Effect of Base Fluid on Sealing Pressure.

The predictive linear fit model shown in Figure 11 shows a good correlation with an $R^2$ of 80% and a P-value less than 0.05. The residual plot (Figure 12) showed the data being randomly distributed around the x-axis, verifying that a linear model was appropriate for the collected data. Table 2 summarizes the P-values for the different variables as well as the model fit $R^2$.

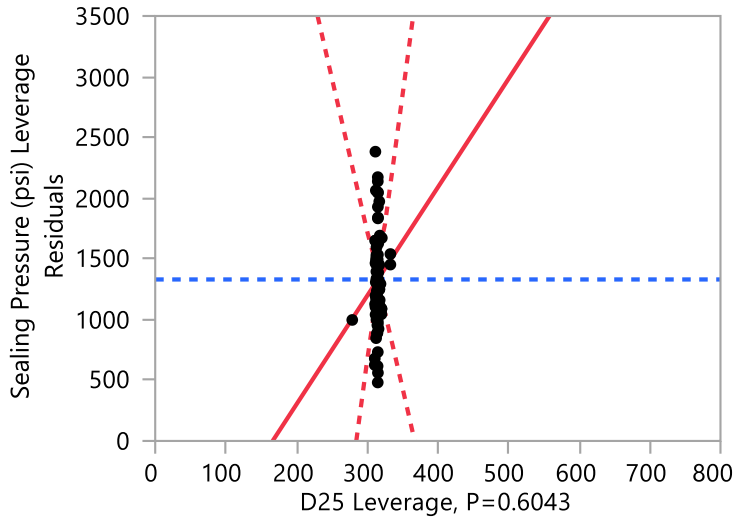


Figure 8. Leverage Plot Showing the Effect of D25 on Sealing Pressure.

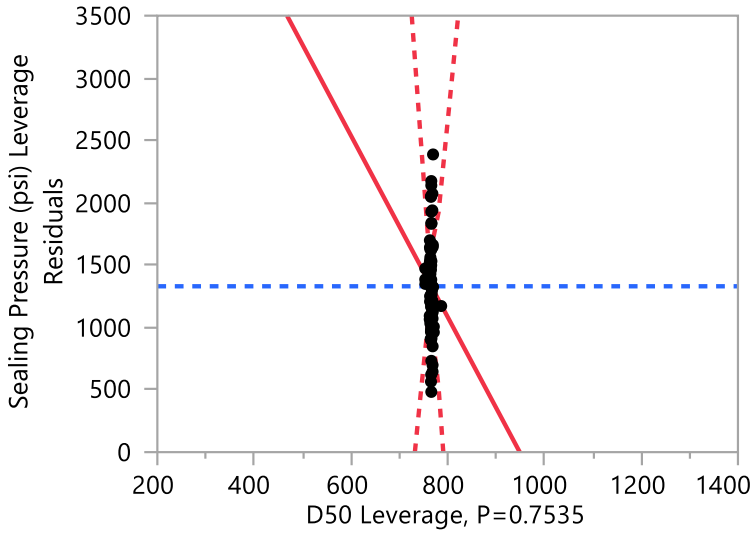


Figure 9. Leverage Plot Showing the Effect of D50 on Sealing Pressure.

From the statistical analysis, it can be seen that the sealing pressure was highly dependent on the different parameters in the following order: fracture width, fluid density, D90, LCM blend/type, D75, base fluid, D25, D50, and D10. Out of these parameters, the fracture width cannot be controlled and the fluid density should be designed based the mud weight window.

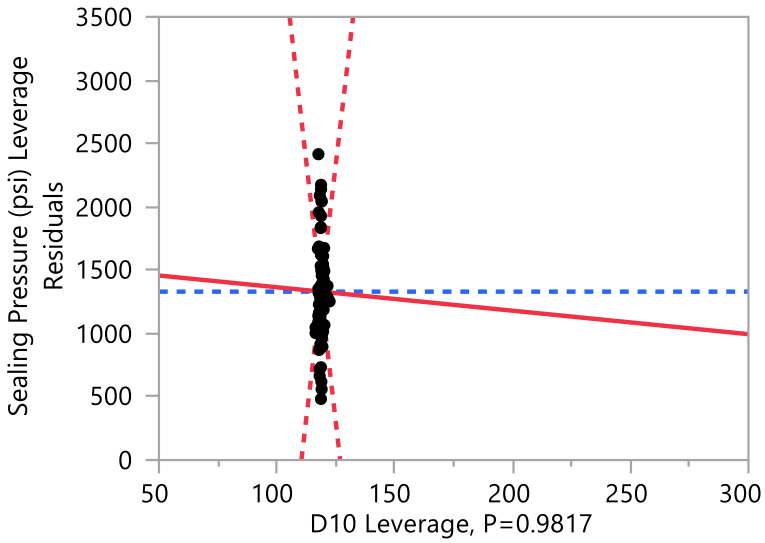


Figure 10. Leverage Plot Showing the Effect of D10 on Sealing Pressure.

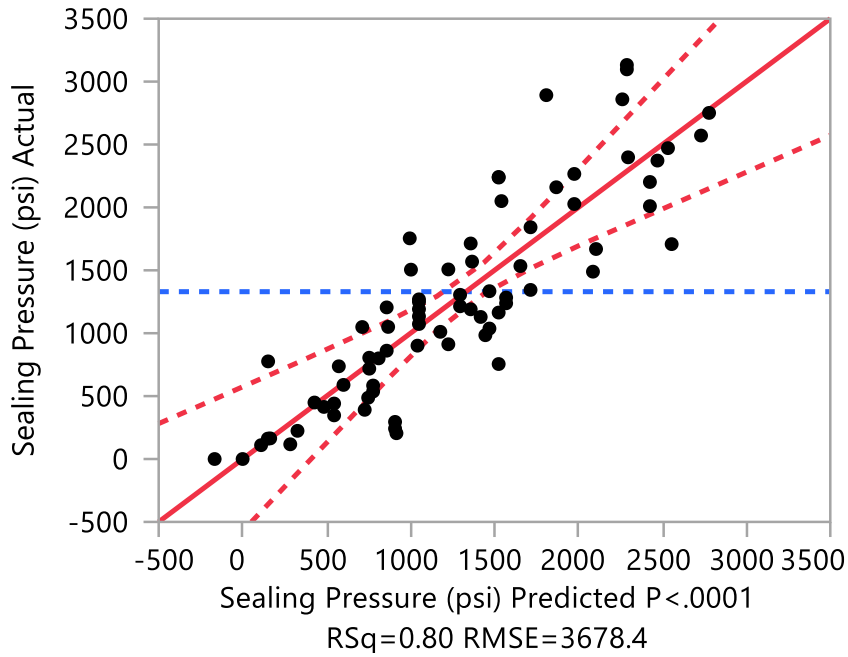


Figure 11. Leverage Plot Showing the Actual Sealing Pressure versus the Predicted Sealing Pressure using the fit model.

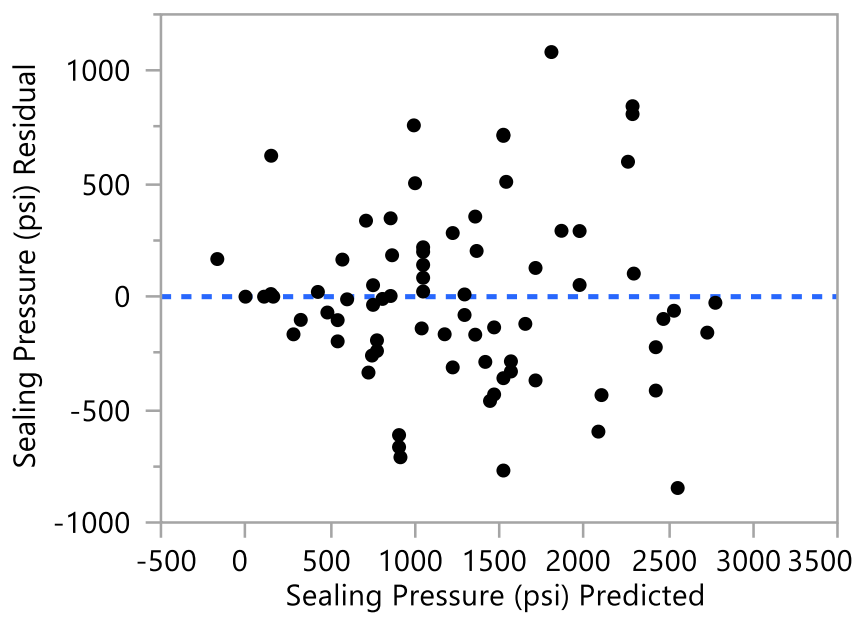


Figure 12. Residual Plot of Sealing Pressure versus the Predicted Sealing Pressure.

Table 2. Effect of Different Parameters on the Sealing Pressure and Model Fit.

| Parameter | Unit | P-Values |
|---|---|---|
| Fracture Width | (microns) | 0.00028 |
| Density | (lb/gal) | 0.00267 |
| D90 | (microns) | 0.05957 |
| LCM Blend | N/A | 0.11473 |
| D75 | (microns) | 0.28628 |
| Base Fluid | (WBM/OBM) | 0.30786 |
| D25 | (microns) | 0.60427 |
| D50 | (microns) | 0.75352 |
| D10 | (microns) | 0.98169 |
| Model Fit | | |
| $R^2$ | | 0.8 |

## 5. SEALING PRESSURE PREDICTION MODEL

Based on the multiple linear regression analysis, which was used to model the relationship between the different parameters and the sealing pressure, a predictive linear fit model to predict the sealing pressure was developed (Eq. 10).

$$Sealing\ Pressure\ (psi) = A_1 + Fluid_{Coeff.} + (A_2\ \rho_{Fluid}) + LCM_{Coeff.} + (A_3 \times F_w) + (A_4\ D10) + (A_5\ D25) + (A_6\ D50) + (A_7\ D75) + (A_8\ D90) \quad (10)$$

where the constants $A_1$ through $A_8$ are as follows:

| | | | |
|---|---|---|---|
| $A_1$ = - 12006.89 | $A_2$ = 122.4 | $A_3$ = - 0.9 | $A_4$ = - 1.85 |
| $A_5$ = 8.93 | $A_6$ = -7.28 | $A_7$ = 9.69 | $A_8$ = 2.45 |

and $\rho_{Fluid}$ = fluid density in (lb/gal), $F_w$ = fracture width in (microns), D10, D25, D50, D75, and D90 are the particle size distribution in (microns).

The other coefficient for the type of fluid and the LCM blend are tabulated in Table 3 below.

Table 3. Empirical Coefficients for the Fluid Type and the Different LCM Blends.

| Fluid Coefficient | |
|---|---|
| OBM | -87.5 |
| WBM | 87.5 |
| **LCM Blends Coefficient** | |
| CF # 1 | 2881.496 |
| G # 1 | 2995.117 |
| G, SCC, & CF # 1 | 4251.583 |
| NS # 1 | -3153.86 |
| SCC # 3 | 2418.024 |
| G & SCC # 1 | 3207.762 |
| G & SCC # 3 | 1298.886 |
| G & SCC # 4 | 5353.874 |
| G & SCC # 5 | 364.3878 |
| G & SCC # 6 | -1011.73 |
| G & SCC # 7 | -6158.57 |
| G & SCC # 8 | -4532.94 |
| G & SCC # 9 | -5785.11 |

## 6. CONCLUSIONS

- A better understanding of the reasons behind the variation in LCM performance by means of experimental results and statistical methods was achieved.

- The statistical analysis showed that the sealing pressure is highly dependent on the fracture width, fluid density, and PSD.

- Parameters with the most significant influence on sealing pressure are fracture width, fluid density, D90, LCM blend/type, D75, base fluid, D25, D50, and D10 respectively.

- A predictive linear fit model, which could be used as a useful tool to design LCM treatment prior to field application, was developed using the parameters with significant influence on sealing pressure.

- The developed model correlated well with the collected data and resulted in an overall model accuracy of 80%.

- The knowledge of the dominant parameters affecting the sealing pressure will ensure designing LCM blends that are capable of sealing expected fracture widths that can maintain high differential pressures.

- Predicting the sealing pressure of LCM blends in advance will help in mitigating fluid losses as soon as they occur without further extensive laboratory evaluations.

## ACKNOWLEDGEMENT

The authors would like to acknowledge Det Norske Oljeselskap ASA (Now Aker BP) for the financial support under research agreement # 0037709.

## NOMENCLATURE

| | |
|---|---|
| NPT | None-productive time |
| LCM | Lost circulation material |
| PSD | Particle size distribution |
| PPA | Particle plugging apparatus |
| HPHT | High pressure high temperature |
| IPT | Ideal packing theory |
| WBM | Water-based mud |
| OBM | Oil-based mud |
| G | Graphite |
| SCC | Sized calcium carbonate |
| NS | Nutshells |
| CF | Cellulosic fiber |
| Conc. | Concentration in lb/bbl |

**REFERENCE**

Abrams A (1977). Mud Design to Minimize Rock Impairment Due to Particle Invasion. Journal of Petroleum Technology. Vol. 29, pp. 586–592. http://dx.doi.org/10.2118/5713-PA

Alsaba M (2015). Investigation of Lost Circulation Materials Impact on Fracture Gradient. PhD dissertation, Department of Geological Sciences and Engineering, Missouri University of Science and Technology.

Andreasen A H M & Andersen J (1930). Kolloid Z.50: 217–228.

Hettema M, Horsrud P & Taugbol, K (2007). Development of an Innovative High-Pressure Testing Device for The Evaluation of Drilling Fluid Systems and Drilling Fluid Additives Within Fractured Permeable Zones. In: Offshore Mediterranean Conference and Exhibition, Ravenna, Italy, 28–30 March. OMC-2007-082.

Jahn F, Cook M & Graham M (2008). Hydrocarbon Exploration & Production, 2nd Edition. Elsevier Science, Oxford, UK.

Kaageson-Loe N M, Sanders M W, Growcock F, Taugbol K, Horsrud P, Singelstad A V & Omland T H (2009). Particulate-Based Loss-Prevention Material - The Secrets of Fracture Sealing Revealed! In: SPE Drilling & Completion, Vol. 24(4), pp. 581-589.

Kumar A & Savari S (2011). Lost Circulation Control and Wellbore Strengthening: Looking Beyond Particle Size Distribution. In: AADE National Technical Conference and Exhibition, Houston, Texas, USA, 12–14 April. AADE-11 NTCE-21.

Kumar A, Savari S & Jamison D (2011). Application of Fiber Laden Pill for Controlling Lost Circulation in Natural Fractures. In: AADE National Technical Conference and Exhibition, Houston, Texas, USA, 12–14 April. AADE-11 NTCE-19.

Marinescu P (2014). Loss Circulation Challenges – Current Approach and What are the Next Solutions? In: SPE Lost Circulation Workshop, Dubai, 20–22 May.

Montgomery D (2001). Design and Analysis of Experiments, 5th Edition. John Wiley & Sons, Inc., New York, NY.

Rehm B, Haghshenas A, Paknejad A S, Al-Yami A & Hughes J (2012). Underbalanced Drilling: Limits and Extremes. Gulf Publishing Company, Houston, TX.

Sall J (1990). Leverage Plots for General Linear Hypotheses. The American Statistician, Vol. 44 (4), pp. 308–315.

Sanders M, Young S & Friedheim J (2008). Development and Testing of Novel Additives for Improved Wellbore Stability and Reduced Losses. In: AADE Fluids Conference and Exhibition, Houston, USA, 8–9 April. AADE-08-DF-HO-19.

Savari S & Whitfill D L (2016). Lost Circulation Management in Naturally Fractured Formations: Efficient Operational Strategies and Novel Solutions. In: IADC/SPE Drilling Conference and Exhibition, Fort Worth, Texas, USA, 1–3 March. SPE-178803-MS.

Australian Drilling Industry Training Committee limited (2015). The Drilling Manual. Fifth Edition. CRC Press, Boca Raton, FL.

Van Oort E, Friedheim J, Pierce T & Lee J (2009). Avoiding Losses in Depleted and Weak Zones by Constantly Strengthening Wellbores. SPE Drilling and Completion 26: 519-530. doi: 10.2118/125093-PA.

Vickers S, Cowie M, Jones T & Tywnam A J (2006). A New Methodology that Surpasses Current Bridging Theories to Efficiently Seal a Varied Pore Throat Distribution as Found in Natural Reservoir Formations. In: AADE Fluids Conference and Exhibition, Houston, Texas, USA, 11–12 April. AADE-006-DF-HO-16.

Whitfill D & Miller M (2008). Developing and Testing Lost Circulation Materials. In: AADE Fluids Conference and Exhibition, Houston, Texas, USA, 8–9 April. AADE-08-DF-HO-24.

# IV. EFFECT OF EXPERIMENTAL SETUP ON LOST CIRCULATION MATERIALS EVALUATION RESULTS


## ABSTRACT

Laboratory experiments with slotted disks simulating fractures have been used extensively to evaluate loss circulation materials. The amount of fluid loss and sealing pressure have been used as evaluation criteria. The question that remains is how valuable are these tests for use in real life conditions in the wellbore when flow conditions and particle settling will be different from the laboratory tests. To address this question, a water-based mud with added loss circulation materials (LCM) were tested with four different experimental setups. For the two first experiments, the slotted disk was placed at a bottom of a cell, filled with a drilling fluid with LCM added, and the flow rate was either a constant flow rate of 25 ml/min or instantaneous pressure build up from a bladder accumulator. For the other two experiments, the slotted disk was placed upward in a cylinder, filled with drilling fluid with LCM additives, and a flow rate of 25 ml/min were used. When necessary, a paddle stired the drilling fluid to ensure a homogenous fluid. The results showed the experiments with the same flow rate of 25 ml/min gave comparable results. However, changing the flow rate from 25 ml/min to 6,000 ml/min flow rate did change the seal forming results. The effect from running the experiments with the slotted disk placed downwards or upwards did not have a significant effect on the sealing pressure. When stirring the sample, a higher fluid loss was required before the sample sealed and the maximum seal pressure was lowered. Therefore, caution should be taken when quantitatively comparing LCM tests on slot disks from different experimental setups with different flow conditions.


## 1. INTRODUCTION

Lost circulation is defined as the loss of drilling fluid in the wellbore to the formation, during drilling or completion, occurring when encountering highly permeable unconsolidated sand or gravels, cavity or cavernous, natural fracture, and induced fractured formations (Howard & Scott, 1951). The severity of the of losses can be divided as seepage losses (1-10 bbl/hr), partial losses (10 to 500 bbl/hr), and severe losses (over

500 bbl/hr) (Nayberg, 1986). To prevent loss circulation, loss circulation materials (LCM) are added to the drilling fluid. A comprehensive review of LCM types and their usage can be found in Alsaba et al (2014a). To investigate the effectiveness of the LCM laboratory experiments are conducted (Scott & Lummus, 1955; White, 1956; Loeppke et al., 1990; Hettama et al., 2007; Kageson-Loe et al., 2009; Kumar et al., 2011a, 2011b; Alsaba et al., 2014b, 2014c, 2016; Mostafavi et al., 2011; Xu et al., 2014; Baggini Almagro et al., 2014; Canson, 1895; Kefi et al., 2010).

The objective of this paper is to address how changing the experimental setup and flow conditions affect the experimental LCM performance, using steel slots to simulate fractures for lost circulation treatment in fractured impermeable formations.

## 2. EXPERIMENTAL SETUP

To study the effect of changing of setup and flowing conditions on LCM performance, the testing apparatuses were set up to meet the objectives. The variation included a slow (25 ml/min) and instantaneously high injection flow rate with the slotted disc placing at downward of the testing cell; and a slow injection rate (25 ml/min) with the disc placing at the top of the cell, with and without stirring conditions. Four different experimental setups were used along with a 2000-microns-width stainless steel, simulated fracture discs.

The first and second set of experiments were run using the first setup. Figure 1 is the schematic of the first apparatus showing the disc placed downward of the cell. The tests can be run with or without the bladder accumulator.

In the first set of tests (Condition#1), the experiments were run using a continuous flow at 25 ml/min flow rate. A syringe pump (1) provided a continuous flow of water to displace drilling fluid from the steel accumulator (2) to flow along the injecting line (3) into the testing cell (4). A slotted disc (5) was placed inside the testing cell on a spacer cylinder. The spacer provided a room for fluid and LCM that passes through the slot during the test to prevent plugging or restriction of flow at the cell outlet. The fluid sample (drilling fluid treated with LCM) placed in the space above the slotted disc was forced to flow through the slotted disc.

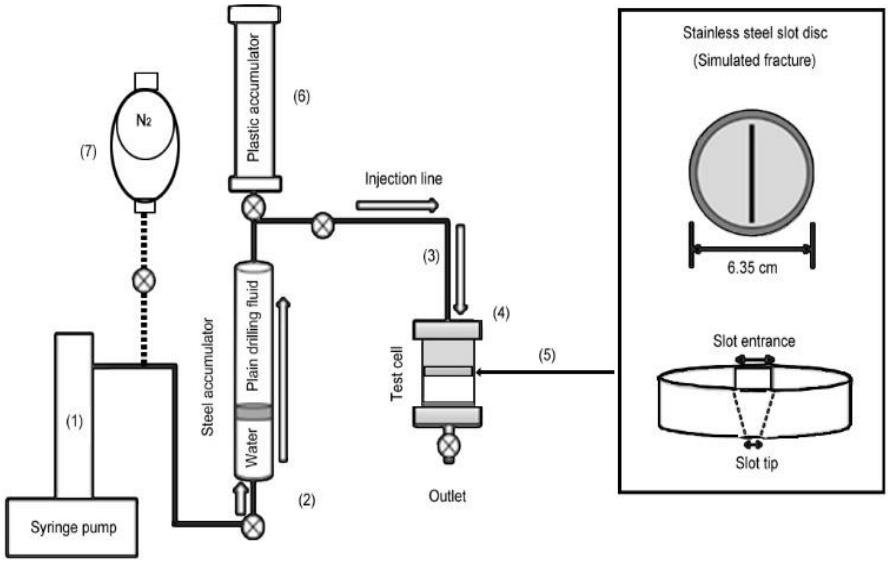


Figure 1. Schematic of the first testing apparatus (Modified from Alsaba et al. 2016).

The injecting pressure built up in the injecting line after seal development on the discs was automatically detected by the syringe pump pressure transducer. The sealing pressure and the fluid losses collected at the cell outlet were recorded and used as the performance indicator. The plastic accumulator (6) was used to supply the drilling fluid to the steel accumulator when it was empty by manipulating the valves in the system.

The second set of tests (Condition#2) were the instantaneous flow test, where the bladder-type accumulator (7) was installed. The nitrogen gas inside the bladder provided an instantaneous flow from the pneumatic spring action of the gas expansion. The flow was found to have a rate of 6,000 ml/min, comparable to a lost circulation rate of 190 gpm (270 bbl/hr) from a well with a 20-foot-long fracture (2000-micron fracture width) on the borehole wall (Jeennakorn et al. 2017).

The third (Condition#3) and the fourth set of tests (Condition#4) were run with the second set of apparatuses. The test system was a modified fluid loss tester cell where the stainless-steel cell was enclosed in a chamber which could provide an elevated temperature (elevated temperature was not used for these experiments). The schematic of the setup used for the third and fourth set of experiments is shown in Figure 2a with a picture of the system in Figure 2b.

A piston pump (1) provided a continuous flow of water (25 ml/min) to displace drilling fluid from the steel accumulator (2) to flow along the injecting line (3) into the bottom of the testing cell inside the chamber (4). The same slotted disc (Figure 1) was placed inside the top part of the testing cell with spacer cylinder (5). The fluid treated with LCM was forced to flow through the slot (from bottom to the top, upside down with the first apparatus).

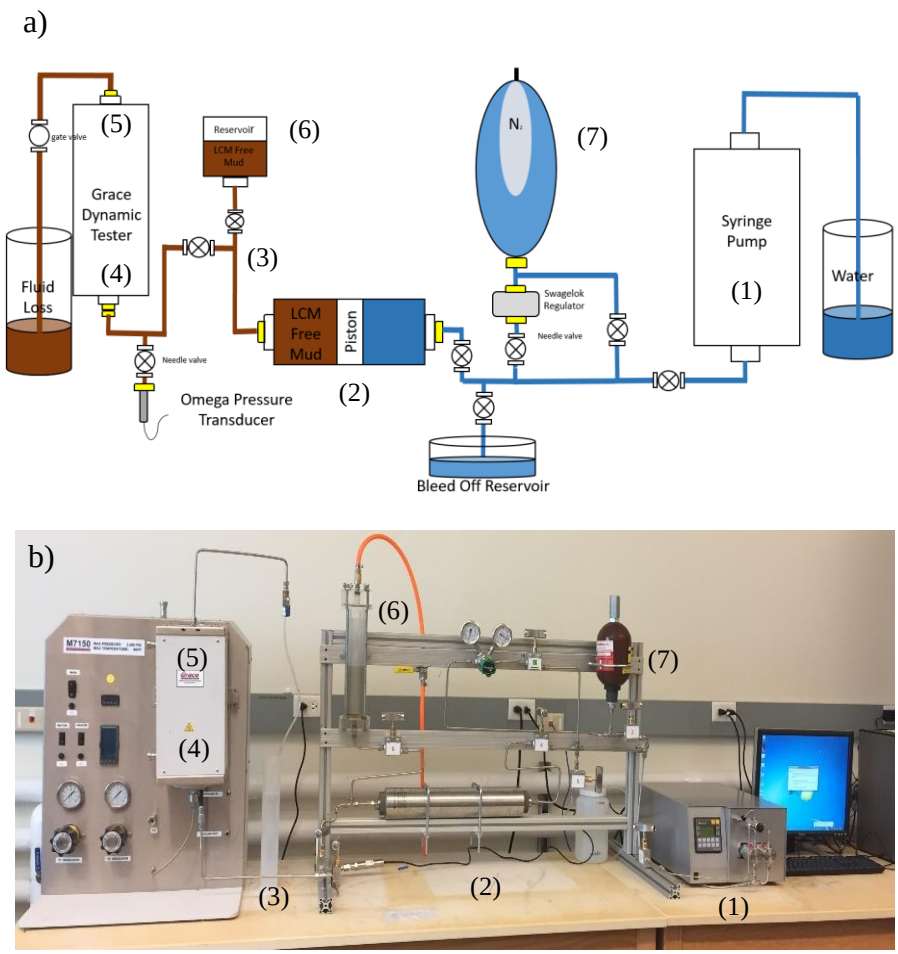


Figure 2. Schematics of the second apparatus. a) Schematics of The Dynamic Fluid Loss & Seal Efficiency Tester. b) Picture of the system.

As same as the first set up, the injecting pressure was recorded by the pressure transducer, where the fluid losses could be collected at the outlet. The plastic accumulator

(6) was used to supply the drilling fluid to the steel accumulator when it was empty. The bladder accumulator (7) was also installed in the system, but not used in this experiment.

The testing cell was equipped with a rotating paddle, installed in the test chamber (Figure 3a). The paddle was driven by a flexible shaft, providing the rotating torque from an electric motor in the panel box. The paddle was not used for the third set of tests but used to perform a circulating condition inside the cell for the fourth testing condition.

Originally, the testing cell was designed to be used in the downhole environment fluid loss tests. Modifications were made to build a room for the installation of the fracture disc with a cylinder spacer, on the top part of the cell (when the test cell was installed in the test chamber in Figure 2) as shown in figure 3b.

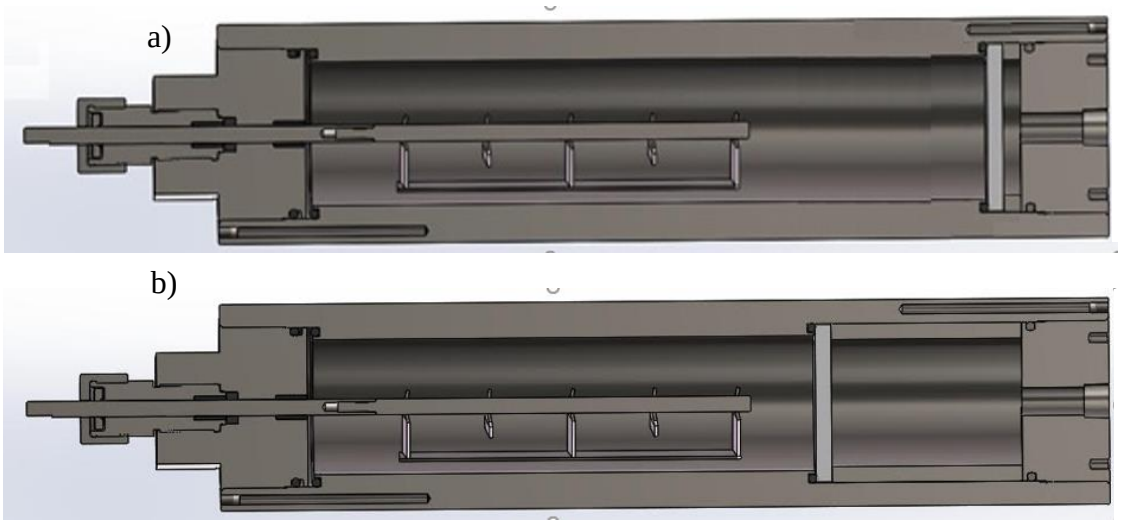


Figure 3. The testing cell of the second apparatus. a) The original from the manufacturer, and b)the modified cell for fracture disc sealing tests.

The tests in the thirds set were run under the same procedure with the first set of experiment, except the disc position was changed from the bottom part of the cell (facing up) to be installed at the top part of the cell (facing down). The fourth set of experiments were run the same as the third set, but the paddle was rotated at 150 rpm during the tests. The mixture of drilling fluid and LCM inside the cell was stirred continuously to investigate the dynamic condition on LCM performance. The sealing pressure and the fluid loss volume were also used as the evaluating parameters.

For all the four set of tests, a blending of graphite (G) and sized calcium carbonate (SCC) was used at a concentration of 105 ppb (Alsaba et al., 2014b). Table 1 shows the LCM formulations by the type of LCM with the concentration of the products with particle size distribution as indicated by the manufacturer.

Table 1. LCM formulation used in the tests.

| Type of LCM | D50 (microns) | Concentration (ppb) |
|---|---|---|
| Sized calcium carbonate (SCC) | 1400 | 35 |
| | 2400 | 35 |
| Fine G & SCC Blend | 500 | 36 |

Table 2 shows the particle size distribution of the LCM after dry blending as the formulation in Table 1.

Table 2. PSD of used LCM using sieve analysis method.

| PSD of G & SCC after blending | | | | |
|---|---|---|---|---|
| D10 | D25 | D50 | D75 | D90 |
| 170 | 650 | 1300 | 1900 | 2600 |

The drilling fluid used as the base fluid and injecting fluid was a simple 7% bentonite (by weight) water-based fluid, 8.6 ppg. It was used for the test conditions #2 to #4. The test condition #1 was previously conducted using 11 ppg which is basically the 7% bentonite drilling fluid with some barite as a weighting agent. Previous investigation (Jeennakorn et al. 2017) presented that the base fluid density has a positive effect on the sealing pressure in 1000 microns slotted disc, so the data was used carefully with the density effect in mind.

The same tapered fracture disc was used throughout the four test conditions. Table 3 shows the disc dimensions used for the four tests, installed in the first apparatus

or second apparatus to perform the simulated fracture where the LCM particles bridged and sealed the flow channel. The schematics of the used fracture simulated disc can also be found in Figure 1.

Table 3. Fracture disc dimensions.

| Dimensions | Measured |
|---|---|
| Slot entrance width (mm) | 3.5 |
| Wall angle (degree) | 7 |
| Diameter (mm) | 63.5 |
| Slot tip width (mm) | 2 |
| Slot tip length (mm) | 50 |
| Disc thickness (mm) | 6.35 |

## 3. TESTING METHODOLOGY

The first testing condition was done using the syringe pump for the energy of the flow (Figure 1). The pressure recorded with time was recorded to get an indicative parameter, the maximum sealing pressure.

Figure 4 shows a plot of the injecting pressures and time typically obtained from the first testing condition.

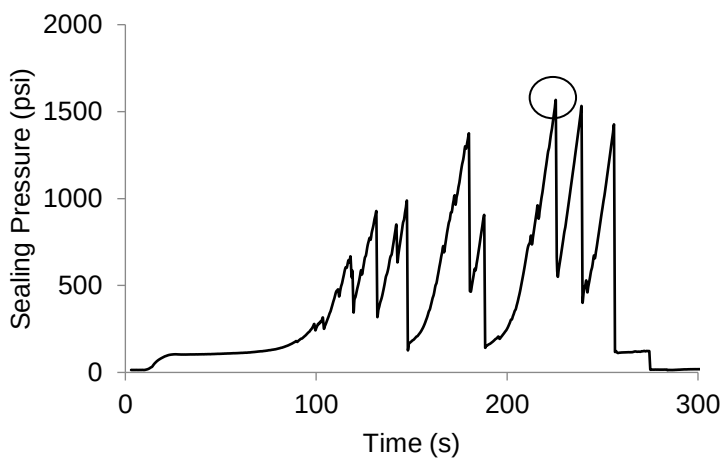


Figure 4. A plot of injecting pressure over time from a test showing the peak pressure (circled), recorded as the maximum sealing pressure.

After starting the pump, the pressure increased to 50 psi due to the static frictional effect. Fluid losses from the drilling fluid sample containing LCM particles started to flow out of the cell's outlet, first at the injecting rate, and decrease as the seal was formed. Pressure increased when the LCM started to form a seal bridge across the slot. After the seal formed, the pressure built up until the seal was broken. The bridge redeveloped quickly, where pressure rebounded up sharply. The seal was broken and reestablished many times. When the seal failed to develop or developed with very low sealing pressures, the test was stopped. If the pressure went above 3,000 psi, the test was also stopped to prevent the disc damage. From the test results, as shown in Figure 4, the sealing and breaking cycles were counted from every pressure differences of 100 psi between the peak and the bottom of the curve. The total fluid loss was divided by the number of cycles to obtain the fluid loss per cycle for the results analysis.

The second testing condition was performed using the same setup as the first one, except that the bladder accumulator was installed in the system. The nitrogen gas was precharged in the bladder with a pressure of 100 or 200 psi before water (as a hydraulic fluid) was injected in the accumulator to get a testing differential pressure varied from 150, 300 or 600 psi, respectively. Instead of using the syringe pump as an injecting tool, the fluid inside the bladder accumulator was allowed to suddenly flow and inject the drilling fluid in the steel accumulator to flow into the testing cell instead. The pressure of the system will drop sharply, then the rate of decreasing with respect to the time was reduced significantly, indicating the development of the seal. The pressure transducer monitored the pressure with time to be used for the analysis. Fluid loss volume was recorded after the pressure was stabilized. Figure 5 shows a plot of the monitored pressure over the testing time. The graph shows multiple forming of the seal comparable as the forming-breaking cycle as in the first testing condition but under the pressure lower than the differential pressures.

The third testing condition was run using the second setup as shown in Figure 2. The drilling fluid was injected at 25 ml/min and all the testing methodology and the data gathering were the same as the tests conducted in the first testing condition. The differences from the first testing condition were that the disc was placed at the top of the

cell, facing down, and the drilling fluid with LCM was placed below the disc and injected from downward.

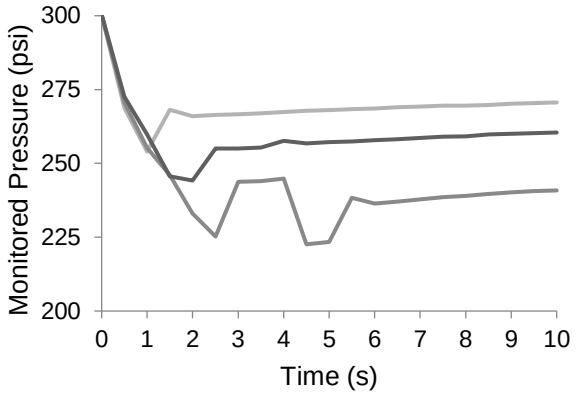


Figure 5. The plot of monitored pressure over time obtained from three tests of the second testing condition.

For the fourth condition experiment, the experiments were run as same as the third testing condition, except that the rotating paddle was turn on to provide a dynamic condition within the testing cell.

The sealing pressure (condition 1, 3, and 4) and the averaged fluid loss per cycle were used to compare the results among the four testing conditions as shown below.

## 4. TESTING RESULTS

Table 4 shows the results of the first testing condition. From the table, the obtained maximum sealing pressures indicated that strong seals were developed on the discs. The last test shows a very high sealing performance which randomly happened in the test and may be considered as an outlier; however, the other two results are consistent and show the comparable strength of the formed seals.

Table 5 provides the results from the second condition (instantaneous) flow test. The fluid loss spent during the seal development shown in Table 4 is higher compared to the fluid loss per cycle as obtained from the other tests. This is because the instantaneous flow tests had a much higher flow rate compared to the slow flow rate tests.

Table 4. Testing results from the first, third, and fourth testing conditions.

| Testing conditions | Sealing pressure (psi) | Initial fluid loss before seal forming (ml) | Avg. fluid loss (ml/cycle) |
|---|---|---|---|
| Static condition, disc placed at bottom | 1,606 | 31 | 7 |
| | 1,603 | 48 | 5.3 |
| | 3,122 | 26 | 4.2 |
| Static condition, disc placed on top | 3018 | 14 | 150 |
| | 3076 | 36 | 15 |
| | 3047 | 42 | 25 |
| Dynamic condition, top placed on top | 911 | 150 | 300 |
| | 1271 | 75 | 33 |
| | 341 | 137 | 150 |

Table 5. The results from the second testing conditions.

| Differential pressure: precharge pressure (psi) | Stabilized pressure (psi) | Spending sealing time (s) | Fluid loss (ml) |
|---|---|---|---|
| 100 : 150 | 141 | 2.0 | 135 |
| | 141 | 2.0 | 130 |
| | 146 | 1.5 | 40 |
| 100 : 300 | 274 | 1.5 | 125 |
| | 248 | 5.5 | 260 |
| | 265 | 2.5 | 150 |
| 200 : 300 | 280 | 2.0 | 165 |
| | 291 | 1.0 | 75 |
| | 279 | 2.3 | 180 |
| 200 : 600 | 545 | 3 | 102 |
| | 555 | 1 | 95 |
| | 575 | 1 | 50 |

Figure 6 shows the averaged sealing pressure obtained from the Condition#1 (static fluid condition with disc at the bottom of the cell), Condition #2 (static fluid condition with disc at the top of the cell), and Condition #4 (dynamic fluid condition with disc on the top of the cell), respectively.

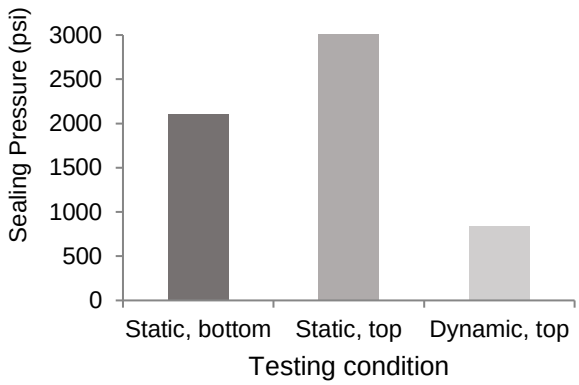


Figure 6. Graph comparing the averaged sealing pressure from condition#1, condition#3, and condition#4.

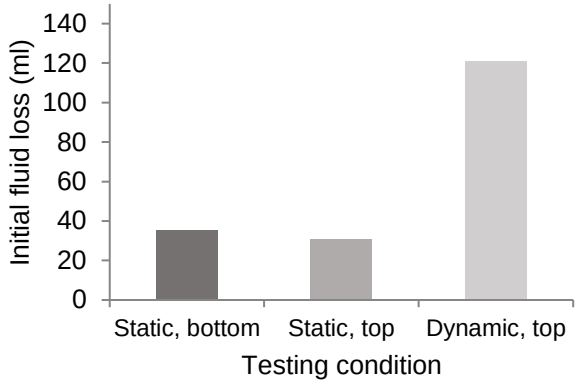


Figure 7. Graph comparing the averaged initial fluid loss from condition#1, condition#3, and condition#4.

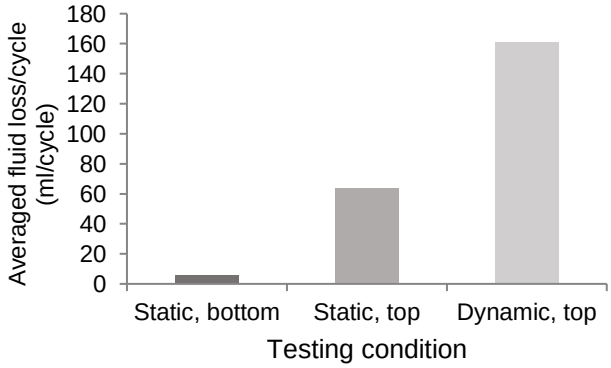


Figure 8. Graph comparing the averaged fluid loss per cycle (seal formed and breaking) from condition#1, condition#3, and condition#4.

## 5. DISCUSSION

From the results, the fluid under static and dynamic shear condition significantly affected the sealing ability, the initial fluid loss, and the fluid loss per cycle of the used LCM. The results from the static condition test with the disc at the bottom of the cell (Condition #1) seems to agree with the static condition with the disc on the top of the cell (Condition #2), even though the based fluid density was different between them.

In Figure 6, the sealing pressure was higher when the tests were done in static fluid conditions (Condition #3) but yielded a low sealing pressure when the test was done under the dynamic shear condition (Condition #4). In Figure 7, the initial fluid loss volume, the fluid loss volume that was spent before the sealing pressure buildup occurred, was lower when the tests were run under the static condition with the disc on the top of the cell (Condition #3), but it required much higher volume of fluid loss in the dynamic shearing condition and the same disc position (Condition #4). The fluid loss per cycle of the static fluid condition with the disc on the top of the cell in Figure 8 (Condition #3) was also found to be smaller compared to fluid loss per cycle in the dynamic shear condition (Condition #4) even though they had the same disc position at the top of the cell, thus confirms the fluid loss consumption of the dynamic shear condition.

These results indicated that the fluid transported LCM particle better under a static fluid condition, compared to a dynamic shearing condition. The fluid loss per cycle is very high compared to the total fluid loss used in the instantaneous flow tests as presented in Table 5.

The initial fluid loss, the fluid loss per cycle, and the total fluid loss obtained from these tests confirmed that the drilling fluids required for LCM transportation to form the seal or fix the broken seal varied with the fluid flow condition and shearing condition in the laboratory. It tends to require more fluid loss per cycle when the mixture flow in the opposite direction the gravity, under the higher fluid flow rate, and dynamic shear conditions.

All of these conditions tested in the laboratory can also occur in the field treatment. The difference of the conditions can cause the indicative parameters to be significantly different from the laboratory evaluation run before the field application. The treatment results can also be significantly different from field to field.

## 6. CONCLUSIONS

- Testing disc position and the flow direction, testing flow characteristics, and the fluid shearing condition affected the testing results significantly.

- Shearing condition of the fluid in the tested cell strongly decreased the sealing integrity, increased the initial fluid loss during the seal forming and the seal redevelopment.

- Overall, fluid losses obtained from static fluid tests (disc on bottom) were significantly small compared to the static fluid tests (disc placed on top) and the dynamic fluid condition.

- Experimental setup strongly affects results. Care must be taken when compare the results from different testing setup and the application from laboratory evaluation to the field treatment.

- Similarly, the actual treatment in the field with different operating environment compared to the pilot testing in the laboratory can be significantly different from the laboratory results.

## NOMENCLATURE

| | |
|---|---|
| LCM | Lost circulation material |
| WBF | Water-based fluid |
| G | Graphite |
| SCC | Sized calcium carbonate |
| ppb | Concentration in lb/bbl |

## REFERENCE

Baggini Almagro S P, Frates C, Garand J, Meyer A (2014). Sealing Fractures: Advances in Lost Circulation Control Treatments. Oilfield Review 26(3):4–13.

Alsaba M, Nygaard R, Hareland G, Contreras O (2014a). Review of Lost Circulation Materials and Treatments with an Updated Classification. In: AADE Fluids Technical Conference and Exhibition, Houston, Texas, 15–16 April.

Alsaba M, Nygaard R, Saasen A, and Nes O (2014b). Lost Circulation Materials Capability of Sealing Wide Fractures. In: SPE Deepwater Drilling and Completions Conference, Galveston, Texas, 10–11 September.

Alsaba M, Nygaard R, Saasen A, and Nes O (2014c). Laboratory Evaluation of Sealing Wide Fractures Using Conventional Lost Circulation Materials. In: SPE Annual Technical Conference and Exhibition, Amsterdam, The Netherlands, 27–29 October.

Alsaba M, Nygaard R, Saasen A, and Nes O (2016). Experimental Investigation of Fracture Width Limitations of Granular Lost Circulation Treatments. Petroleum Exploration and Production Technology:1–11.

Canson B E (1895). Lost Circulation Treatments for Naturally Fractured, Vugular, or Cavernous Formations. In: SPE/IADC Drilling Conference, New Orleans, Louisiana 6–8 March. doi: 10.2118/13440-MS.

Hettema M, Horsrud P, Taugbol K, Friedheim J, Huynh H, Sanders M W, Young S (2007). Development of an Innovative High-Pressure Testing Device for the Evaluation of Drilling Fluid Systems and Drilling Fluid Additives within Fractured Permeable Zones. In: Offshore Mediterranean Conference and Exhibition, Ravenna, Italy, 28–30 March. OMC-2007-082.

Howard George C, and Scott Jr P P (1951). An Analysis and the Control of Lost Circulation. Petroleum Transactions, AIME192:171–182.

Kageson-Loe N, Sanders M W, Growcock F, Taugbøl K, Horsrud P, Singelstad A V, Omland T H (2009). Particulate-Based Loss-Prevention Material-the Secrets of Fracture Sealing Revealed! SPE Drilling & Completion, December:581–589.

Kefi Slaheddine, Jesse C Lee, Nikhil Dilip Shindgikar (2010). Optimizing in Four Steps Composite Lost-Circulation Pills Without Knowing Loss Zone Width. In: Asia Pacific Drilling Technology Conference and Exhibition, Ho Chi Minh City, Vietnam, 1–3 November. doi: 10.2118/133735-MS.

Kumar A, Savari S (2011a). Lost Circulation Control and Wellbore Strengthening: Looking Beyond Particle Size Distribution. In: AADE National Technical Conference and Exhibition, Houston, Texas, 12-14 April. AADE-11-NTCE-21.

Kumar A, Savari S, Jamison Dale E, and Whitfill Donald L (2011b). Application of Fiber Laden Pill for Controlling Lost Circulation in Natural Fractures. In: AADE National Technical Conference and Exhibition, Houston, Texas, 12-14 April. AADE-11 NTCE-19.

Loeppke G E, Glowka D A, Wright E K (1990). Design and Evaluation of Lost-Circulation Materials for Severe Environments. SPE Petroleum Technology, March:328–337. doi: 10.2118/18022-PA.

Mostafavi V, Hareland G, Belayneh M, and Aadnoy B S (2011). Experimental and Mechanistic Modeling of Fracture Sealing Resistance with Respect to Fluid and Fracture Properties. In: US Rock Mechanics / Geomechanics Symposium held in San Francisco, California, June 26-29.

Nayberg T M (1986). Laboratory Study of Lost Circulation Materials for Use in Both Oil-Based and Water-Based Drilling Muds. SPE Drilling Engineering, September:229–236 doi: 10.2118/14723-PA.

Scott P, J L Lummus (1955). New Developments in the Control of Lost Circulation. In: Annual Fall Meeting of the Petroleum Branch of the American Institute of Mining and Metallurgical Engineers, New Orleans, Louisiana, 2–5 October. doi: 10.2118/516-G.

Hinkebein T E, Behr V L & Wilde S L (1983). Static Slot Testing of Conventional Lost Circulation Materials. Report from Sandia National Laboratories to the National Technical Information Service, US Department of Commerce, Springfield, Virginia. https://www.osti.gov/scitech/servlets/purl/6471455/

White R J (1956). Lost-circulation Materials and Their Evaluation. In: Spring meeting of the Pacific Coast District, Division of Production, Los Angeles, May.

Xu C Y, Kang Y-l, You L-j, Li S, and Chen F (2014). High-Strength, High-Stability Pill System To Prevent Lost Circulation. In: The International Petroleum Technology Conference held in Bejing, China, 26–28 March. doi: 10.2118/172496-PA.

# SECTION

# 3. DISCUSSION AND CONCLUSIONS

## 3.1 DISCUSSION

1) The significantly different results among the different apparatuses, the simulated discs, the test flow rate, and the surrounding conditions show that the parameters strongly affect the LCM evaluation. Therefore, the results from laboratories must be used with care and cannot be quantitatively compared between experiment to experiment if the testing conditions and surroundings are different between apparatus.

2) The fracture discs in this study can be considered unrealistic from their simplification compared to the rock fractures. Many points of the simulated fracture did not ideally represent the actual fracture and may be improved in the future studies depending on the researchers' consideration. The parameters that the author would like to discuss are the fracture length in the flow direction, the material used in the discs manufacturing, the fracture surface roughness, the disc positioning, and the pressure controlled fracture width.

2.1) The fracture dimension in the fracture propagating direction (in this case, the disc thickness) is relatively small compared to the distance that real fractures propagate. The real fracture can extend away from the wellbore to reach the natural fracture networks. In this experiment, the space available inside the test cell limited the thickness of the discs, where the length of fracture in the fluid flow direction for the thin and thick discs were set to be only 6.35 and 24.5 mm, respectively. This distance is sufficient only for the investigation of the fracture sealing at or close to the fracture entrance because there is no space for LCM to form seal deeper into the fracture. To study the LCM sealing performance at a longer distance from the fracture entrance, an apparatus modification is required. The seal development may differ from this set of experiments.

2.2) Deformable material with mechanical properties close to the rock formation may be used to manufacture the simulated discs. The experiment using solid fracture discs seemed to have a constant fracture aperture during the tests. It may be questionable about the effect of the steel physical properties that are different compared to the rock formation. With this idea, using the materials having similar physical properties

compared to the actual rock to construct the simulated fracture should yield more realistic results in the future study.

2.3) The fracture roughness is another interesting factor that may be introduced to the future studies. The relatively smooth surface of the slotted steel discs, cut by a water jet machine, were used in this study. It is expected that surface roughness also has the significant effects on the LCM sealing behavior and performance. The rough surface increases the frictional force component supporting the seal structure, and possibly act as the particle anchorage points. The rough surface may also change the contact areas between the particles and the fracture walls, increases or decreases the local stress concentration on the particles, which may change the bridging particles mode of failure from shear mode to compression or flexural mode. It is a good idea to construct the discs with surface machining to imitate the real formation as similar as possible.

2.4) Placing the fracture simulated disc on the top or bottom of the cell, facing the fracture entrance to the flow-in direction has been tested in this study. In the future study, placing the disc horizontally, perpendicular to the flow direction and the gravitational field might be a more permissive way to fully understand the sealing processes.

2.5) In many models explaining the fluid flows in fractures, the fracture width is a function of the wellbore pressure, i.e., non-linearly proportional to the wellbore pressure. Even though it not currently possible to construct the apparatus that has an exactly true relationship between the wellbore (injecting) pressure and the fracture width, it is a good idea to investigate the LCM sealing ability in a pressure controlled fracture, where the width and fracture angle can vary with the wellbore pressure. The apparatus will simulate the situation when the developed seal element is subjected to the wellbore pressure fluctuation which in turns affect the fracture width and the angle of the fracture planes. The results will gain confidence on LCM sealing success if such condition happened downhole.

3) The slow injection rate testing method has both advantages and disadvantages. In this form of LCM tests, the maximum sealing pressure indicating the highest differential pressure that the seal can withstand and the fluid loss are obtained. They are essential measurable parameters that can be used in the LCM testing as comparing

criteria. Better LCM blend should have a high seal integrity, at least higher than the expected differential pressure the seal has to hold back. The formulation with smaller fluid loss means the sealing effectiveness both during the seal formation and the service time. The disadvantage is that the testing condition may not simulate the operational conditions accurately if the loss flow rate is not a constant parameter and the flowing pressure (differential pressure) does not start from a close-to-zero pressure.

4) The instantaneous flow testing method can provide some other useful information.

4.1) Even though during the LOC curing, the loss rate will be kept as low as possible and sometimes the hesitating injection technique (inject-stop and observe cycles) may be used, the instantaneous flow tests replicates the flow process better when the flowing pressure does not start from zero. Moreover, it can simulate a sudden flow occurred from either an induced fracture initiation and propagation to a natural flow network or an immediate opening of a natural fracture when LCM is available inside the wellbore.

4.2) With a preset differential pressure, the instantaneous flow setup was not designed to measure the possible maximum sealing pressure of any LCM formulation at such flow rate, but the purpose is to test whether the LCM can form a seal against the fast flow that withstands the driving differential pressure (in this experiment, 300 and 600 psi). If the sealing capability at a higher differential pressure is required, a higher differential pressure can be preset respect to the apparatus pressure capacity.

4.3) The pressure drop from the nitrogen gas expansion, the difference between the differential pressure and the stabilized pressure after the seal forming, can be reduced to a negligible value by using a large unit of bladder accumulators. A small fraction of the fluid loss volume compared to the energized fluid in the accumulator can create a flow with a very small pressure drop that can be more realistic bottomhole pressure. This experiment was conducted with a limited volume of the bladder accumulator, but it may be better if this limitation can be eliminated in the future studies.

4.4) The changing of the fluid loss rate over time can be used for tracking and explaining the sealing steps: the bridging, filling, and sealing-off. The rate of fluid loss may be monitored by a direct measurement of the fluid loss at the outlet, or it can be

calculated using the accumulator pressure over time or an indirect calculation of the gas expansion volume from the pressure-volume relationship. Unfortunately, the tools to obtain the fluid loss rate over time was not available, and the pressure transducer had an insufficient frequency response (not enough data points per second) to clearly detect the pressure changing in the quick sealing processes occurring within only a few seconds. This may be improved in the future work to confirm the chronological sealing processes in the instantaneous flow.

5) PSD of the solid particles against the fracture zones.

5.1) Before knowing the effect of the weighting materials, the previous study considered PSD of the LCM alone as the parameter affecting the sealing ability of a specific LCM formulation without taking other solid particles in the drilling fluid into account. From the effect of weighting materials tests, it suggested that the weighting materials particles strongly affect the sealing ability of the LCM while they collaboratively contribute together in the sealing process. This implies that any solid particles available in the drilling fluid, both WBF and OBF, can also affect the sealing process of LCM.

5.2) In the actual LOC situation, it may not practical to mix a new drilling fluid to be used for the LOC treatment (as being used in this experiment). The drilling fluid generally available in an active circulating system is usually contaminated by the drilled solid particles which cannot be absolutely eliminated by the solid control system. Some of the drilled solids are always left in the active tanks and recirculated back downhole blending with the newly drilled solid particles. The future experiment may be conducted while some types of drilled solids (from different formation types) disperse in the drilling fluid to observe the effect of those drilled solid particles.

5.3) The practical solid PSD affecting sealing process should be the actual PSD of the drilling fluid and LCM mixture available before the fracture zone. It is questionable that the placement processes transporting the mixture from the mixing tank through the pumps and drill string will cause a non-uniform particles distribution (segregation) in the mixture or not. Different slip velocity of different size (and density) particles subjected to the various fluid velocity profile may cause the PSD of solid particles in the mixture

deviating from the PSD of the mixture used in the laboratories or mixed in the drilling fluids.

6) The preferred sealing profile: completely set in-between the fracture walls.

6.1) Typically, after the LOC treatment, various drilling operations have to be conducted to finish the well sections. The drill stem must be tripped in and out of the well several times to reach the target depth. These drill string movements can potentially destroy the seal element on the wellbore wall surface.

6.2) Also, during the casing running, the casing collars, casing centralizers and wall scratcher (usually applies to the wellbore wall to remove the filter cake in the purpose of a better bond of cement between the steel casing and the formation) are going to cut or wipe off some part of the seal element on the fracture entrance. These seal disturbing processes can potentially reactivate the LOC problems.

6.3) Thus, the sealing profile with all the sealing element completely set inside the fracture is more desirable than the seal setting at the fracture entrance as a cross-sectional mound shape. In parallel or nearly parallel fracture planes (according to the observation made in these experiments) conventional granular LCM may not be capable of creating the appropriate sealing profile inside the fractures.

6.4) The preferred sealing profile can be applied by using the expandable (granular) materials in the form of expandable particle materials, the like materials applied in the expandable elastomeric production packers. The materials may be used in combination with the granular LCM. The idea is the expandable particles, slightly smaller in sizes compared to the fracture width, will be allowed to pass through the fracture entrance into the available spaces in-between the fracture walls while the coarse granular LCM particles will bridge at the fracture entrance, temporally hold back the flow. The expandable particles entering the fracture space will increase in size over time. Scraper tools, if applicable, may be used to open the seal at the fracture entrance to allow more expandable material occupy the space between the fracture walls. Once the expandable particles enlarge themselves inside the fracture, they essentially become the bridging structure readily for the seal development inside the fracture. The materials are not yet available and need further study to bring them into the LOC application.

6.5) Another possible application, presented as one of the possible bridging mechanism in parallel fracture by Loeppke et al (1990), is that the coarse particles can enter the fracture entrance while the fracture width is increased by the increasing of the wellbore pressure. With this idea, the seal can form at the fracture mouth to stop the flow, then the wellbore pressure can be carefully and slowly increased by adding a surface pressure on the column of the drilling fluid inside the well. The increasing pressure will widen the fracture planes allowing the bridging structure to be slowly squeezed or into the fracture. The pressure is then relieved at a later time. This application can also be done with the expandable materials in the LCM system.

7) Laboratory vs. downhole conditions and the surroundings, the knowledge can be applied to the field treatment.

7.1) In the author's understanding after reviewing the literature and conducting many experiments, it is preferable if one can develop a perfect testing apparatus that can take every physical process into account. All the researchers previously conducted the LCM experiments tried to create the testing apparatus to most accurately simulate the operating conditions as actually present in the subsurface conditions.

7.2) Knowing the strong effect of testing conditions on the evaluation results, it is then very important to design the testing apparatuses to represent the field conditions. The limitation is that it is difficult to combine every simulated condition with only one set of apparatus and only one set of experiments. The complexity of the natural physical processes with many affecting variables, the scale of the problems, and the variation of some variables with the other variables and time create more difficulties comparable to solving the LOC problem itself.

7.3) Because the sealing ability varies with the environment, this knowledge implies that the results from a set of testing conditions which are different to the field conditions have less value to the field application. If the field conditions are so different from the testing conditions, it may not be applicable at all, and the success field treatment following such laboratory experiment just happened by chance. This probably was the reason why some field applications were not effective or successful even though the selected LCM showed good performance in the laboratory.

7.4) Field treatment sometimes fails or needs multiple attempts to mitigate the LOC incidents. Unconventional treatments with higher cost and side effects can be unnecessarily applied prior to truly understand what should be corrected. For example, switching from healing with conventional granular LCM to the polymer or cement-gunk method without an improvement in the LCM granular particle size with respect to the fracture geometry.

7.5) Even though the LCM fracture sealing is considerable a temporary (short-term) treatment before the well section is protected by the casing and cementing processes, the following drilling operations can cause the seal to fail and LOC to resume. In a long well section, drilling parameters can change significantly from the starting of the section to the casing and cementing processes. Since all involving parameters can affect the sealing ability of the LCM, laboratory evaluation should cover the range of expected parameters and the predicted downhole environment in each well section.

7.6) The ideal apparatus may or may not be innovated in the future; however, in the meantime, the error of LCM evaluation can be decreased by using a combination of testing apparatus while trying to control the involving parameter as accurate as possible.

8) The experiment needs the statistical methods applying to the data processing.

8.1) The resulting analysis indicates that using the same set of apparatus, the results of each testing condition or environment is not constant, but tend to distribute within a specific range. Even though all the parameters are completely kept constant, the non-uniformity (the variety in shape, size, PSD, local concentration, and composition) of the granular particles got from the storage containers, and thereafter randomly dispersed in the liquid mixture, are the uncontrollable factors that arbitrarily affect the scattering of the results.

8.2) The number of experiments is important if the results are found to spread in a wide range of data. The central of tendency using the statistical method is generally used as the representative result; however, the worse result is also important depending on the probability that the similar event will happen in the actual application. Worst case may be used as a performance indicator to increase the chance of success of the field application if it is not considered as an outlier.

9) The statistical model in Paper III was created with a 90% accuracy while using for sealing integrity (sealing pressure) estimation. This model can be used as a tool to predict the performance of a known data of LCM formulation. Under a range of uncertainty, the model can be used to eliminate the unnecessary trial and error in the formulation development. However, as the overall experiment showed that the testing conditions strongly affect the testing results, the detailed tests under the expected treatment conditions should be performed to get the most accurate results for field application.

10) The aging conditions with the temperature of 200 and 400 °F were investigated in this experiment. These temperatures were set as the base case to know the LCM performance in a normal temperature and an extremely high temperature for a high-pressure high-temperature drilling operation. In the case of the other temperature between the tested temperature or with a different aging period, the experiment should be conducted for that specific case with the used based fluid, fluid density, temperature, aging period, etc. Loop flowing in the pipe instead of rolling shear condition may better simulate the aging environment better than the standard testing methodology used in this experiment. However, this aging condition tests can be used as an initial idea for further study due to the lack of the information about LCM aging test in the petroleum industry.

11) The industry standard or recommendation practice for LCM fracture-sealing testing methods is not updated. The standard testing methodology for the LCM evaluation purpose is not well established in the petroleum industry. It is a good idea to set up a standard testing methodology or recommendations to be used in research and apply in the drilling operation.

## 3.2 CONCLUSIONS

Based on this study, the overall conclusion is that the experimental setup and the fluid properties creating different sealing environments can change the results of the tests, so caution should be taken when quantitatively comparing LCM tests on slot disks from different experiment setups and surrounding conditions. Additionally, the following conclusions can be drawn

1) Slot disc configurations were varied in this study and found to affect the evaluation results significantly. The specific testing condition effects seen were;

1.1) Increasing the discs' wall angle tends to decrease the maximum sealing pressure. The same behavior could happen in subsurface fractures if they are tapered in shape with an open end at the tip.

1.2) No correlation was found between the average fluid loss per cycle of seal initiation and the sealing pressure, the wall angle or disc thickness variation in slow injection tests. Fluid losses might not be a good indicative parameter for an effective fracture sealing in impermeable rock.

1.3) The depth of the fractures with parallel planes propagating into the formation had no effect on sealing efficiency since the large-size particles would bridge the fracture entrance. No test resulted in particles smaller than the fracture width forming the bridging structure inside the parallel walls to resist the flow.

1.4) In the Fractures tapered towards the tip, the bridging particles could set wherever the sizes agree with the fracture width. Setting the seal completely in-between the fracture walls was found to improve the sealing integrity, forming a more effective sealing profile compared to sealing at the fracture entrance.

1.5) For the tested LCM formulation, shape and dimensions of the tapered slot discs affected the seal integrity. This observation implies that the same behavior could also happen with different experimental setup used by laboratories, as well as in the real fractures under subsurface conditions. Imaginably, the subsurface fracture sealing occurs with higher complexity.

2) The experimental results showed that a proper range of solid particle sizes was very important and confirmed the effect of PSD on sealing efficiency. In addition, the following behavior of the drilling fluid and LCM was observed.

2.1) The base fluid effects did not show consistent results. That was because many factors were involved in creating the seal, where the interaction between the base fluids containing different solids and LCM particles resulted in different sealing performance.

2.2) Increasing the drilling fluid density before applying any LCM treatment tends to increase the seal integrity, interrelating with the increase of the solid particles

within the mixture. The flattened rate of the sealing pressure increasing implied the optimum point where the best performance occurred.

2.3) For each type of weighting material, adding a proper range of particle sizes fulfilled the missing particle sizes in the LCM formulation. Sufficient sizes and concentration of fine particles increased seal integrity.

2.4) From the effect of density and weighting materials on the sealing integrity, where the solid particles in the based drilling fluid influenced the overall performance, the PSD should be considered in the final mixed fluid, not only the added LCM solid particles.

2.5) Observation shows that the seals consisted of three layers forming chronologically during the seal development. The layers performed different essential tasks in the sealing mechanism and the sealing procedure was more understood.

2.6) An analytical flow model was developed from the statistical method and might be used to predict sealing pressure from the same testing condition when the input parameters are known.

3) Downhole conditions with higher pressure, temperature, and dynamic shearing significantly affected the application of some LCM formulation.

3.1) Aging the treated fluid strongly affected the performance of LCM. It might promote or reduce the sealing pressure at a moderate downhole temperature (200 °F) depending on the LCM thermal properties.

3.2) Some LCM formulations that contained natural plant products failed to perform a strong seal at a higher temperature (400 °F). Aging tests should be conducted if the high temperature is expected in the downhole conditions.

4) Having the disk placed on top or at the bottom of the cell did not significantly change the results of sealing integrity; however, flow pattern did significantly change the results in the following way:

4.1) Apparatus with disc installed at the upward position resulted in decreasing of the sealing pressure under a dynamic shearing condition. The setup increased the initial fluid loss and the fluid loss during seal redevelopment. This created a more accurate representation of the downhole sealing environment.

4.2) Instantaneous flow conditions did not affect the ability of LCM to form a seal. The seal integrity of a specific LCM formulation obtained from a slow injection test was useful for quantifying the LCM sealing strength and LCM selection, while the seal forming ability can be proved in the sudden flow tests. Testing using a high-pressure cell approach was validated to be used in LCM evaluation.

# BIBLIOGRAPHY


Abrams A (1977). Mud Design To Minimize Rock Impairment Due To Particle Invasion. Journal of Petroleum Technology, 5713, 586–592. https://doi.org/10.2118/5713-PA.

Alberty M W & McLean M R (2001). Fracture Gradients in Depleted Reservoirs-Drilling Wells in Late Reservoir Life. In: SPE/IADC Drilling Conference. https://doi.org/10.2118/67740-MS.

Alsaba M, Al Dushaishi M F, Nygaard R, Nes O-M & Saasen A (2017). Updated Criterion to Select Particle Size Distribution of Lost Circulation Materials for an Effective Fracture Sealing. Journal of Petroleum Science and Engineering, 149 (January 2016), 641–648. https://doi.org/10.1016/j.petrol.2016.10.027.

Alsaba M, Nygaard R, Hareland G & Contreras O (2014). Review of Lost Circulation Materials and Treatments with an Updated Classification. In: AADE Fluids Technical Conference and Exhibition, Houston, Texas. 15–16 April. http://www.aade.org/technical-papers/2014-fluids-conference-paper/.

Baggini Almagro S P, Frates C, Garand J & Meyer A (2014). Sealing Fractures : Advances in Lost Circulation Control Treatments. Oilfield Review, 26(3), 4–13. http://www.slb.com/resources/publications/industry_articles/oilfield_review/2014/or2014aut01_sealing.aspx.

Bourgoyne A, Millheim K, Chenevert M & Young F S (1986). Applied Drilling Engineering.

Canson B E (1985). Lost Circulation Treatments for Naturally Fractured, Vugular, or Cavernous Formations. In: SPE/IADC Drilling Conference, New Orleans, Louisiana. 5–8 March. https://doi.org/10.2118/13440-MS.

Cedola A E, Akhtarmanesh S, Qader R, Caldarola V T, Hareland G, Nygaard R & Alsaba M. (2016). Nanoparticles in Weighted Water Based Drilling Fluids Increase Loss Gradient. In: American Rock Mechanics/Geomechanics Symposium, Houston, Texas. 26–29 June.

Chaney P. (1949). Abnormal Pressures and Lost Circulation. Drilling and Production Practice.

Contreras O, Hareland G, Husein M, Nygaard R & Alsaba M (2014). Wellbore Strengthening in Sandstones by Means of Nanoparticle-Based NPs Applications in Drilling Industry. In: SPE Deepwater Drilling and Completions Conference Galveston, Texas. 10–11 September.

Deeg W F J (2004). Changing Borehole Geometry and Lost-Circulation Control. In: The North America Rock Mechanics Symposium (NARMS), Houston, Texas. 5–9 June.

Dick M A, Heinz T J, Svoboda C F & Aston M (2000). Optimizing the Selection of Bridging Particles for Reservoir Drilling Fluids. In: SPE International Symposium on Formation Damage, Lafayette, Louisiana. 23–24 February.https://doi.org/10.2118/58793-MS.

Fuh G-F, Beardmore D & Morita N (2007). Further Development, Field Testing, and Application of the Wellbore Strengthening Technique for Drilling Operations. In: SPE/IADC Drilling Conference, Amsterdam, The Netherlands. 20–22 February. https://doi.org/10.2118/105809-MS.

Ghalambor A, Salehi S, Shahri M & Karimi M (2014). Integrated Workflow for Lost Circulation Prediction. In: SPE International Symposium and Exhibition on Formation Damage Control, Lafayette, Louisiana, 26–28 February.

Gockel J F, Gockel C E & Brinemann M (1987). Lost Circulation: A Solution Based on the Problem. SPE/IADC Drilling Conference, New Orleans, Louisiana. 15–18 March. https://doi.org/10.2118/16082-MS.

Growcock F B, Friedheim J, Sanders M W & Bruton J (2009). Wellbore Stability, Stabilization and Strengthening. In: Offshore Mediterranean Conference and Exhibition, Ravenna, Italy. 25–27 March.

Hands N, Kowbel K, Maikranz S, Nouris R (1998). Drill-in Fluid Reduces Formation Damage, Increases Production Rates. Oil & Gas Journal, Vol.96(28), 65-69.

Hettema M, Horsrud P, Taugbol K, Asa S, Friedheim J, Huynh H, Sanders M W & Young S (2007). Development of an Innovative High-Pressure Testing Device for the Evaluation of Drilling Fluid Systems and Drilling Fluid Additives within Fractured Permeable Zones. In: Offshore Mediterranean Conference and Exhibition, Ravenna, Italy, 28–30 March. OMC-2007-082.

Howard G C & Scott P P (1951). An Analysis and the Control of Lost Circulation. Journal of Petroleum Technology, 3(6), 171–182. https://doi.org/10.2118/951171-G.

Ivan C, Bruton J & Bloys B (2003). How Can We Best Manage Lost Circulation? In: AADE National Technology Conference “Practical Solutions for Drilling Challenges”, Houston, Texas, April 1–3.

Kang Y, Xu C, Tang L, Li S & Li D (2014). Constructing a Tough Shield Around the Wellbore: Theory and Method for Lost-Circulation Control. Petroleum Exploration and Development, 41(4), 520–527. https://doi.org/10.1016/S1876-3804(14)60061-6.

Kefi S, Lee J C, Shindgikar N D, Brunet-cambus C, Vidick B & Diaz N I (2010). Optimizing in Four Steps Composite Lost-Circulation Pills Without Knowing Loss Zone Width. In: IADC/SPE Asia Pacific Drilling Technology Conference and Exhibition, Ho Chi Minh City, Vietnam. 1-3 November. https://doi.org/10.2118/133735-MS.

Kumar A & Savari S (2011). Lost Circulation Control and Wellbore Strengthening: Looking Beyond Particle Size Distribution. In: AADE National Technical Conference and Exhibition, Houston, Texas, USA, 12–14 April. AADE-11 NTCE-21. http://www.aade.org/technical-papers/2011-national-technical-papers/.

Kumar A, Savari S & Jamison D (2011). Application of Fiber Laden Pill for Controlling Lost Circulation in Natural Fractures. In: AADE National Technical Conference and Exhibition, Houston, Texas, USA, 12–14 April. AADE-11 NTCE-19.

Loeppke G E, Glowka D A & Wright E K (1990). Design and Evaluation of Lost-Circulation Materials for Severe Environments. Journal of Petroleum Technology, 42(3), 328–337. https://doi.org/10.2118/18022-PA.

Onyla E C (1994). Experimental Data Analysis of Lost · Circulation Problems During Drilling With Oil · Based Mud. SPE Drilling & Completion (13), 25–31. https://doi.org/10.2118/22581-PA.

Opedal N, Cerasi P & Ytrehus J D (2013). Dynamic Fluid Erosion on Filter Cakes. In: SPE European Formation Damage Conference and Exhibition, Noordwijk, The Netherlands. 5–7 June.

Rahimi R, Alsaba M & Nygaard R (2016). Analysis of Analytical Fracture Models for Wellbore Strengthening Applications: An experimental approach. Journal of Natural Gas Science and Engineering, 36, 865–874. https://doi.org/10.1016/j.jngse.2016.11.022.

Salehi S & Nygaard R (2011). Numerical Study of Fracture Initiation, Propagation, and Sealing to Enhance Wellbore Fracture Gradient. In: 45th US Rock Mechanics / Geomechanics Symposium. http://www.scopus.com/inward/record.url?eid=2-s2.0-82555186524&partnerID=tZOtx3y1.

Salehi S & Nygaard R (2012). Numerical Modeling of Induced Fracture Propagation: A Novel Approach for Lost Circulation Materials (LCM) Design in Borehole Strengthening Applications of Deep Offshore Drilling. In: SPE Annual Technical Conference and Exhibition, San Antonio, Texas. 8–10 October. https://doi.org/10.2118/135155-MS.

Sanders M W, Scorsone J T, Friedheim J E & Swaco M (2010). High-Fluid-Loss, High-Strength Lost Circulation Treatments. In: SPE Deepwater Drilling and Completions Conference, Galveston, Texas. 5-6 October. https://doi.org/10.2118/135472-MS.

Sanders M W, Young S, Friedheim J & Waco M S (2008). Development and Testing of Novel Additives for Improved Wellbore Stability and Reduced Losses. In: SPE Annual Technical Conference and Exhibition, Denver, Colorado. 21-24 September.

Savari S & Whitfill D L (2016). Lost Circulation Management in Naturally Fractured Formations: Efficient Operational Strategies and Novel Solutions. In: IADC/SPE Drilling Conference and Exhibition, Fort Worth, Texas, USA, 1–3 March. SPE-178803-MS.

Scott P P & Lummus J L (1955). New Developments in the Control of Lost Circulation. In: the Annual Fall Meeting of the Petroleum Branch of the American Institute of Mining and Metallurgical Engineers, New Orleans, 2–5 October. doi: 10.2118/516-G.

Vajargah K & Oort V (2016). Initiation and Propagation of Drilling Induced Fractures. In: US Rock Mechanics / Geomechanics Symposium, Houston Texas. 26–29 June.

Van Oort E, Friedheim J, Pierce T & Lee J (2011). Avoiding Losses in Depleted and Weak Zones by Constantly Strengthening Wellbores. SPE Drilling & Completion, 26(4), 519–530. https://doi.org/10.2118/125093-PA.

Vickers S, Cowie M, Jones T & Tywnam A J (2006). A New Methodology that Surpasses Current Bridging Theories to Efficiently Seal a Varied Pore Throat Distribution as Found in Natural Reservoir Formations. In: AADE Fluids Conference and Exhibition, Houston, Texas, USA, 11–12 April. AADE-006-DF-HO-16.

Wang H, Soliman M y (2009). Strengthening a Wellbore with Multiple Fractures : Further Investigation of Factors for Strengthening a Wellbore. In: the US Rock Mechanics Symposium and U.S.-Canada Rock Mechanics Symposium, Asheville, NC. 28 June– 1 July.

White R J (1956). Lost-circulation Materials and their Evaluation. In: the Spring Meeting of the Pacific Coast District, Division of Production, Los Angeles, May.

Whitfill D (2008). Lost Circulation Material Selection, Particle Size Distribution and Fracture Modeling with Fracture Simulation Software. In: IADC/SPE Asia Pacific Drilling Technology Conference and Exhibition, Jakarta, Indonesia, 25–27 August. https://doi.org/10.2118/115039-MS.

Whitfill D & Miller M (2008). Developing and Testing Lost Circulation Materials. In: AADE Fluids Conference and Exhibition, Houston, Texas, USA, 8–9 April. AADE-08-DF-HO-24.

Zoback M D (2007). Reservoir Geomechanics. Cambridge University Press.

# VITA

Montri Jeennakorn was born in 1972. In 1988, he joined the Armed Force Academy Preparatory School. He earned his B.Sc. in Military Science (Mechanical Engineering) from the Chulachomklao Royal Military Academy in 1995, and his LL. B from Sukhothai Thammathirat Open University in 1996. He served in the Royal Thai Army for 10 years before transferring to the Northern Petroleum Development Center, Chiang Mai, Thailand. After redeveloping his engineering background as a drilling engineer for two years, he joined the Geo-Exploration and Petroleum Geo-Engineering program and earned his M.Eng. (professional) from the School of Engineering and Technology, Asian Institute of Technology in 2008. He went back and served the Northern Petroleum Development Center as the Chief of Drilling Section for six more years. In 2014, he was accepted to be a doctorate student at Missouri University of Science and Technology. He completed his PhD in Petroleum Engineering in July 2017. After his graduation, he went back to serve the Defense Energy Department in Fang oil field, Chiang Mai, Thailand.